Volume 34. No. 4 October- December 2018

PHYSICS EDUCATION

ISSN 0970-5953

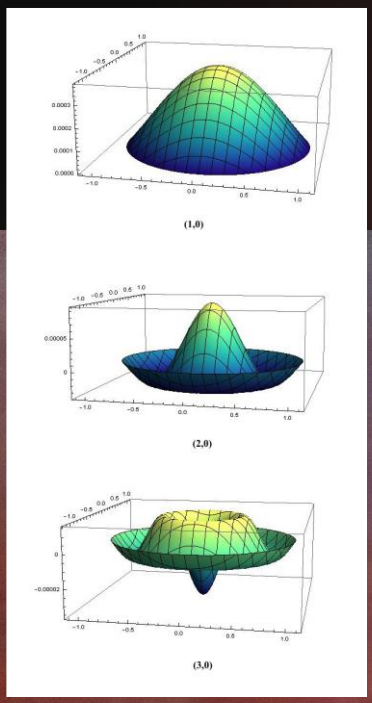

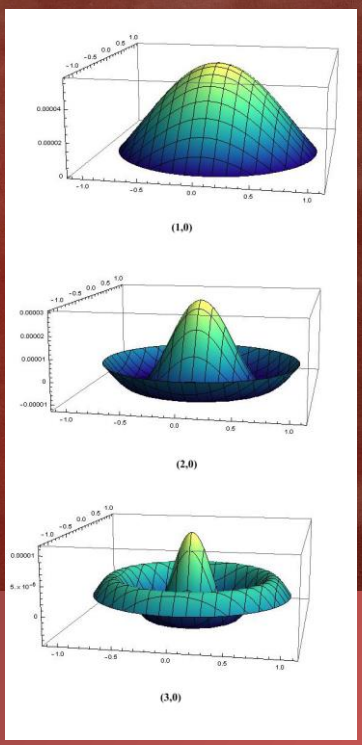

www.physedu.in

Volume 34, Number 4

In this Issue

EDITORIAL

Let me begin by wishing the readers of *Physics Education* a happy new year.

A little before the turn of the new year, we were informed that a physical quantity of both fundamental and practical interest, the weight of one kilogram, has been redefined in terms of fundamental constants such as the Planck's constant. There was also some sentimentality associated with this change. The block of metal that served as the International Prototype Kilogram and maintained in a laboratory vault in Paris has served for nearly a century. With this change, all such standards based on physical objects have been dispensed with in favour of definitions in terms of fundamental constants of nature. This should not surprise a physicist since it is known that these constants do not change over long timescales, for most part. The new standard for kilogram has become dependent on the definitions of second and meter through the Planck's constant. After nearly 130 years, the International Prototype Kilogram is set for retirement.

One more year is born and one more Indian Science Congress has taken place. This is an annual gathering of Indian scientists that started almost 106 years ago. Irrespective of its merits in the contemporary context, it has unfortunately attracted attention for all the wrong reasons. It is indeed sad that some academics have attempted to pass off ancient literature as proof of the existence of advanced scientific knowledge. There is a lot in ancient Indian science to be justifiably proud of, from the invention of zero to relatively recent Madhava-Gregory Series. On the other hand, the ancient Indian literature is undeniably a treasure trove of literary merit, stories of moral and practical value. Yet, we should avoid inventing non-existent achievements based on poetic interpretations. Even as we enjoy the best of ancient Indian literature, let us not forget to evaluate scientific claims through the rigorous process based on hard evidence.

M. S. Santhanam
Chief Editor
Physics Education

Newton's Method and Energy Eigenvalue Problems for the Schrödinger Equation

Kiyoto Hira

Sumiyoshi, Hatsukaichi,
Hiroshima 738-0014, Japan
da43827@pb4.so-net.ne.jp

Submitted on 31–01–2018

Abstract

For a pedagogical example, we take up Newton's method and energy eigenvalue problems for the Schrödinger equation. Newton's method is systematically used to obtain energy eigenvalues and energy eigenfunctions of the Schrödinger equation.

The Schrödinger equation with the Woods-Saxon potential is considered for an S-state. One solution is obtained analytically by means of the hypergeometric series. Another one is obtained numerically using the Runge-Kutta method.

Because our approach makes the most of Newton's method in this paper, our calculations would have pedagogical benefits for those undergraduate students beginning to learn practical computations actively in physics.

1 Introduction

As is well known, Newton's method is very celebrated in mathematical analysis. However, it is less well-known in practical learnings of physics and chemistry. Therefore attempts to apply it to some topics of them seem to be very interesting. In order to use Newton's method for exercises of Quantum mechanics, we take up an eigenvalue problem for the Schrödinger equation with the Woods-Saxon potential, which is very popular in the textbooks of nuclear physics, as a pedagogical example. We use two distict approaches to deal with this problem. One solution was obtained analytically with the help of the hypergeometric series by T. Ishidzu [5]. Another one is obtained numerically using the fourth-order Runge-Kutta method [1]. We would like to stress that in both approaches the Newton's method plays key roles.

Motivations of this paper consist of four viewpoints: to show how to solve a transcendental equation using Newton's method without recourse to the graphical method, to show that the solution to the transcendental equation is fully compatible with the numerical one obtained by the distinct method using the Runge-Kutta method, to explain explicitly that Newton's method plays key roles in obtaining these two solutions, and to show clearly, thanks to the transcendental equation, that when the diffuseness parameter of the Woods-Saxon potential gets closer and closer to zero, energy eigenvalues, as expected, converge to those of the 3-dimensional square-well potential.

Tools for our approaches are explained briefly in the following four sections after the introduction and section 6 is devoted to numerical calculations and results.

Newton's method explained in this paper has been applied to the complex energy eigenvalues problems of kaonic atoms for the first time in the work of M. Atarashi *et al.* [2] and the present paper originated from their work.

2 Startup

The radial Schödinger equation $u(r)$ of a neutron in a symmetrical Woods-Saxon potential $V(r)$ is given by

$$\frac{d^2u(E,r)}{dr^2} + \frac{2m}{\hbar^2}(E - V(r) - \frac{l(l+1)\hbar^2}{2mr^2})u(E,r) = 0, \quad (1)$$

where the total wave function $\psi(\mathbf{r})$ for the neutron is represented by $\psi(\mathbf{r}) = r^{-1}u(r)Y_{l,m}(\theta,\phi)$, and $V(r)$ is given by

$$V(r) = \frac{V_0}{1+e^{\frac{r-R}{d}}}. \quad (2)$$

In this paper we take the parameters in the Woods-Saxon potential for convenience as

$$\begin{array}{ll} A = 208, & Z = 82, \\ d = 0.67\,\text{fm}, & r_0 = 1.27\,\text{fm}, \\ V_0 = (-51 + 33\frac{(N-Z)}{A})\,\text{Mev}, & R = r_0A^{1/3}\,\text{fm}. \end{array} \quad (3)$$

These parameters are adopted from Blomqvist and Wahlborn [3] and give us

$$V_0 = -44.01923076923077\,\text{MeV},$$
$$R = 7.5247400137547205\,\text{fm}.$$

Besides, the mass of neutron $mc^2 = 940\,\text{Mev}$ and $\hbar c = 197.3\,\text{MeV}\cdot\text{fm}$ are taken.

We note that for $l \neq 0$, equation (1) is easy to solve numerically but impossible to solve analytically. However, as Ishidzu calculated, only for $l = 0$ can we solve the equation analytically. For this reason, in this paper, we restrict our considerations to an S-state ($l = 0$). When $E < 0$ we solve equation (1) numerically with condition that

$$u(E,r) = 0 \text{ at } r = 0 \text{ and } u(E,r) \to 0 \text{ for } r \to \infty. \quad (4)$$

With these boundary conditions we can determine the energy eigenvalues numerically.

3 Runge-Kutta method

In order to solve equation (1) numerically in case $l = 0$ we rewrite it as

$$\frac{d^2u(E,r)}{dr^2} = g(E,r)u(E,r), \quad (5)$$

where

$$g(E,r) = -\frac{2m}{\hbar^2}(E - \frac{V_0}{1+e^{\frac{r-R}{d}}}). \quad (6)$$

If we put $v(E,r) = du(E,r)/dr$, equation (5) is changed to a couple of the first-order differential equations as follows:

$$\begin{cases} \frac{du(E,r)}{dr} = v(E,r), & (7) \\ \frac{dv(E,r)}{dr} = g(E,r)u(E,r). & (8) \end{cases}$$

We apply the fourth-order Runge-Kutta method [1] for solving the differential equations (7) and (8) numerically. Let $[a,b]$ stand for the interval where the equations are solved and we divide it into N intervals of width h each such that $h = (b-a)/N$. Then we put $r_0 = a, r_1 = r_0 + h, \cdots, r_N = b$ and set $u_i(E) = u(E,r_i)$ and $v_i(E) = v(E,r_i)$.

If we solve the recurrence relations resulting from the Runge-Kutta method numerically with the initial values $u_0(E) = u(E,r_0)$ and $v_0(E) = u'(E,r_0)$, we can obtain every $\{r_i, u_i(E), v_i(E)\}(i = 0,1,\cdots,N)$.

4 Newton's method

We find a solution x of a differentiable function $f(x) = 0$ numerically. Suppose x_0 is an approximate solution to $f(x) = 0$ and let δx_0 be the correction to x_0 such that $f(x_0 + \delta x_0) = 0$, We expand $f(x_0 + \delta x_0)$ in powers of δx_0 as

$$f(x_0 + \delta x_0) = f(x_0) + \delta x_0 f'(x_0) + \cdots. \quad (9)$$

Keeping terms up to the first order in δx_0,

$$f(x_0 + \delta x_0) = f(x_0) + \delta x_0 f'(x_0) = 0. \quad (10)$$

Then we obtain

$$\delta x_0 = -\frac{f(x_0)}{f'(x_0)}. \quad (11)$$

Accordingly we obtain, by letting $x_1 = x_0 + \delta x_0$,

$$x_1 = x_0 - \frac{f(x_0)}{f'(x_0)}. \quad (12)$$

If we replace x_0 and x_1 with x_n and x_{n+1} respectively, we obtain the recurrence relations

$$x_{n+1} = x_n - \frac{f(x_n)}{f'(x_n)} \qquad (n = 0, 1, \cdots). \tag{13}$$

By iterating these recurrence relations, the sequence $\{x_n\}$ is expected to converge to an exact solution. When we use these relations, a choice of the starting value x_0 is important. If $f(x)$ has an analytic expression, we can calculate the derivative $f'(x)$ analytically. Usually, we can easily compute the derivatives numerically using the following relations:

$$f'(x_n) = \frac{f(x_n + h_n) - f(x_n - h_n)}{2h_n} \qquad (n = 0, 1, \cdots), \tag{14}$$

where h_n are taken sufficiently small, and $f(x_n + h_n)$ and $f(x_n - h_n)$ are numerically computed.

5 Ishidzu's analytical solution for S-state with the Woods-Saxon potential

In this section we explain briefly Ishidzu's theory along the lines of his paper [5]. Putting

$$\begin{aligned} r &= R\rho, & d &= \alpha R, \\ V_0 &= -v_0^2\hbar^2/2mR^2, & E &= -\kappa^2\hbar^2/2mR^2, \end{aligned} \tag{15}$$

where α, v_0, and κ are constants and furthermore changing the variables by

$$\begin{aligned} x &= -\exp\{(1-\rho)/\alpha\} = -\exp\{(R-r)/d\}, \\ u(E,r) &= e^{-\kappa\rho}\chi(E,x), \end{aligned} \tag{16}$$

equation (1) becomes in case of $l = 0$

$$\chi''(E,x) + \frac{1+2\kappa\alpha}{x}\chi'(E,x) + \frac{\alpha^2 v_0^2}{x(x-1)}\chi(E,x) = 0 \qquad (-e^{1/\alpha} < x < 0), \tag{17}$$

which can be solved by means of the hypergeometric series [1]. For the solution $\chi(E,x)$ to this equation to take a finite value at $x = 0$ $(r \to \infty)$, $\chi(E,x)$ must be

$$\chi(E,x) = F(\mu, \bar{\mu}; 1 + 2\kappa\alpha | x), \tag{18}$$

where F is the hypergeometric series [1], and we put

$$\mu = \alpha(\kappa + i\kappa'),\ \bar{\mu} = \alpha(\kappa - i\kappa'),\ \kappa' = \sqrt{v_0^2 - \kappa^2}. \tag{19}$$

The other boundary condition $u(E,r) = e^{-\kappa\rho}\chi(E,x) = 0$ at $r = 0$ $(x = -e^{1/\alpha})$ yields

$$F(\mu, \bar{\mu}; 1 + 2\kappa\alpha | -e^{1/\alpha}) = 0. \tag{20}$$

Since generally $|-e^{1/\alpha}| \gg 1$, the function F must be continued analytically. By use of the relation between the hypergeometric series [1]:

$$\begin{aligned} &F(a,b;c|z) \\ &= \frac{\Gamma(c)\Gamma(b-a)}{\Gamma(b)\Gamma(c-a)}(-z)^{-a}F(a, a-c+1; a-b+1|1/z) \\ &+ \frac{\Gamma(c)\Gamma(a-b)}{\Gamma(a)\Gamma(c-b)}(-z)^{-b}F(b, b-c+1; b-a+1|1/z), \end{aligned} \tag{21}$$

where Γ is the Gamma function, equation (20) is reduced to

$$\begin{aligned} &F(\mu, \bar{\mu}; 1 + 2\kappa\alpha | -e^{1/\alpha}) \\ &= \frac{\Gamma(1+2\kappa\alpha)\Gamma(\bar{\mu}-\mu)}{\Gamma(\bar{\mu})\Gamma(\bar{\mu}+1)} \\ &\times e^{-\mu/\alpha}F(\mu, \mu - 2\kappa\alpha; \mu - \bar{\mu} + 1 | -e^{-1/\alpha}) \\ &+ \frac{\Gamma(1+2\kappa\alpha)\Gamma(\mu-\bar{\mu})}{\Gamma(\mu)\Gamma(\mu+1)} \\ &\times e^{-\bar{\mu}/\alpha}F(\bar{\mu}, \bar{\mu} - 2\kappa\alpha; \bar{\mu} - \mu + 1 | -e^{-1/\alpha}) = 0. \end{aligned} \tag{22}$$

Since $d = 0.67\,\text{fm}, R = 7.52\,\text{fm}$, and $|-e^{-1/\alpha}| = 1.34E-5 \ll 1$, we keep only the first term of the expansion in powers of $(-e^{-1/\alpha})$ of the hypergeometric series F. Therfore, the function F on the right-side of equation (22) can be approximated as unity to fairly good approximation. Consequently equation (22) becomes

$$\begin{aligned} &e^{-\kappa}\Gamma(1+2\kappa\alpha) \\ &\times \{\frac{\Gamma(-2i\kappa'\alpha)}{\Gamma(\bar{\mu})\Gamma(\bar{\mu}+1)}e^{-i\kappa'} + \frac{\Gamma(2i\kappa'\alpha)}{\Gamma(\mu)\Gamma(\mu+1)}e^{i\kappa'}\} = 0, \end{aligned} \tag{23}$$

where we have used equation (19) and have replaced the function F on the right-side of equation (22) with unity.

If we set

$$\theta = arg\ \frac{\Gamma(-2i\kappa'\alpha)}{\Gamma(\bar{\mu})\Gamma(\bar{\mu}+1)}, \tag{24}$$

where the notation arg represents the argment of a complex number, equation (23) gives us significant relations

$$cos(\theta - \kappa') = 0,$$
$$\kappa' - \theta = (n - \frac{1}{2})\pi \quad (n = 0, \pm 1, \pm 2, \cdots). \tag{25}$$

With the help of equation (24), equations (25) become

$$\kappa' + arg\Gamma(2i\kappa'\alpha) + arg\Gamma(\bar{\mu}) + arg\Gamma(\bar{\mu} + 1)$$
$$= (n - \frac{1}{2})\pi \quad (n = 0, \pm 1, \pm 2, \cdots). \tag{26}$$

As κ, κ', and μ depend on E through equations (15) and (19), the solutions E_n to these transcendental equations (26) are energy eigenvalues.

6 Numerical calculations and the results

We consider Ishidzu's approximate analytical expressions (26) and rewrite them, thanks to the mathematical properties of the Gamma function [1], as

$$\kappa' + arg\Gamma(1 + 2i\kappa'\alpha) - 2arg\Gamma(\mu) - arg(\mu)$$
$$= n\pi \quad (n = 0, \pm 1, \pm 2, \cdots). \tag{27}$$

we decompose equations (27) into two functions $arg(E)$ and $h(n)$ $(n = 0, \pm 1, \pm 2, \cdots)$ such that

$$arg(E) = \kappa' + arg\Gamma(1 + 2i\kappa'\alpha)$$
$$- 2arg\Gamma(\mu) - arg(\mu), \tag{28}$$
$$h(n) = n\pi \quad (n = 0, \pm 1, \pm 2, \cdots). \tag{29}$$

We recognize that expression (28) is not yet well suited for our straightforward calculations. For that we deform it to a different form that is easy to calculate.
By use of the following equation [4]:

$$\frac{\Gamma(x + iy)}{\Gamma(x)}$$
$$= e^{-i\gamma y} x(x + iy)^{-1} \prod_{m=1}^{\infty} [\frac{1}{1 + iy/(x + m)}] e^{iy/m}, \tag{30}$$

where γ is the Euler's constant, the argument of $\Gamma(x + iy)$ is easily given by

$$arg\Gamma(x + iy)$$
$$= -\gamma y - \tan^{-1}(\frac{y}{x}) + \sum_{m=1}^{\infty} [\frac{y}{m} - \tan^{-1}(\frac{y}{x + m})]. \tag{31}$$

Thanks to this equation, equation (28) can be deformed to a tractable form

$$arg(E) = \kappa' + \tan^{-1}(\frac{\kappa'}{\kappa})$$
$$- \sum_{m=1}^{\infty} [\tan^{-1}(\frac{2\alpha\kappa'}{m}) - 2\tan^{-1}(\frac{\alpha\kappa'}{\alpha\kappa + m})]. \tag{32}$$

Keep in mind that for practical calculations of the values of the function $arg(E)$, equation (32) is used and its summation is carried out from $m = 1$ to $m = 100000$.

When α goes to zero in equation (32), equation (27) becomes

$$\kappa' + \tan^{-1}(\frac{\kappa'}{\kappa}) = n\pi \quad (n = 0, \pm 1, \pm 2, \cdots), \tag{33}$$

which is changed to

$$\kappa \tan \kappa' = -\kappa'. \tag{34}$$

This is the celebrated eigenvalue condition [6] of the 3-dimensional square-well potential (**SQWP**). From this it is shown explicitly that Ishidzu's expression is a mathematical extension from the 3-dimensional square well potential to the Woods-Saxon potential.

Now we can plot $arg(E)$ and $h(n)$ $(n = 1, 2, \cdots)$ against E as in **Figure 1**, which shows us that the intersection points satisfy equations (27) and give the energy eigenvalues. When we want to obtain the exact eigenvalues numerically, we need only to apply Newton's methods to the equation $f(E, n) = 0$, where $f(E, n)$ is defined by $f(E, n) = arg(E) - h(n)$. From **Figure 1** we see the energies E_n of the intersections for $n = 1, 2, 3$, and 4 are approximately equal to -40.0, -29.0, -15.0, and -1.0 MeV respectively. These values can be adopted as the starting values for Newton's method.

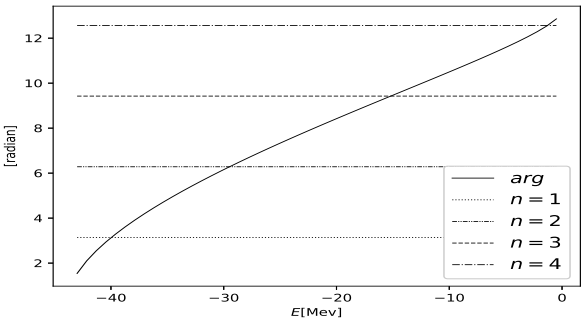

Figure 1: The increasing curve with respect to E represents $arg(E)$ and horizontal lines correspond to $h(n)$ for each integer $n = 1, 2, 3,$ and 4.

In what follows, using the Runge-Kutta method we solve equations (7) and (8) over an interval $[a, b]$ $(a < b)$, where a is very small and b is sufficiently greater than R (Nuclear radius). This time, at an intermediate point $r = c$ between $r = a$ and $r = b$ so that $a < c < b$, we split the interval $[a, b]$ into the two intervals $[a, c]$ and $[c, b]$. We solve numerically the equations over each interval using the Runge-Kutta method as stated in section 3. For the interval $[a, c]$ we solve forward from $r = a$ to $r = c$ with the initial conditions $u(E, a) \approx a^{l+1}$ and $v(E, a) \approx (l+1)a^l$ $(a \approx 0, l = 0)$. For the interval $[c, b]$ we solve backward from $r = b$ to $r = c$ with the initial conditions $u(E, b) \approx \exp(-\sqrt{\frac{2m}{\hbar^2}(-E)}\ b)$ and $v(E, b) \approx -\sqrt{\frac{2m}{\hbar^2}(-E)}\exp(-\sqrt{\frac{2m}{\hbar^2}(-E)}\ b)$. Then let $u_{in}(E, c)$ and $v_{in}(E, c)$ denote the numerical solutions at $r = c$ solved from $r = a$ to $r = c$ and let $u_{out}(E, c)$ and $v_{out}(E, c)$ denote the numerical solutions at $r = c$ solved from $r = b$ to $r = c$, and if we write the difference between their logarithmic derivatives as $f(E, c)$, then it is given by

$$f(E, c) = \frac{v_{out}(E, c)}{u_{out}(E, c)} - \frac{v_{in}(E, c)}{u_{in}(E, c)}. \tag{35}$$

Now we can obtain an energy eigenvalue if we can determine a solution E to $f(E, c) = 0$, the continuity of the logarithmic derivative of the wave function at $r = c$. This is an easy task for Newton's method. We need to verify that the solution E of $f(E, c) = 0$ is free of c.

Method	Ishidzu	Runge-Kutta
Approximate energy (MeV)	-40.0	-40.0
Convergence value(Mev)	-39.9600215	-39.9600216
.....	.....	.....
SquareWell (MeV)	-40.9937792	$-40.9937792^{\dagger}$
Approximate energy (MeV)	-29.0	-29.0
Convergence value(Mev)	-29.4847423	-29.4847313
.....	.....	.....
SquareWell (MeV)	-31.9986175	$-31.9986175^{\dagger}$
Approximate energy (Mev)	-15.0	-15.0
Convergence value(Mev)	-15.1906846	-15.1906682
.....	.....	.....
SquareWell (MeV)	-17.3887057	$-17.3887056^{\dagger}$
Approximate energy (MeV)	-1.0	-1.0
Convergence value(MeV)	-1.2770512	-1.2770569
.....	.....	.....
SquareWell (MeV)	no-solution	no-solution

Table 1: The comparisons between Ishidzu formula and the Runge-Kutta (**R-K**) method. For the **R-K** method we adopt the parameters of the intervals explained in this section as $a = 0.0$ fm, $b = 25.0$ fm, $c = 6.0$ fm, and $N = 500$ for convenience. Each of the approximate energies are estimated from **FIG. 1**. The eigenvalues for the 3-dimensional square-well potential are calculated using equation (33) and also calculated from the **R-K** method using equation (35). †When the **R-K** method is applied, to avoid the singularity of the square-well potential at $r = R$, the following recipes are taken: The endpoint c of the inner interval $[0, c]$ is shifted from $c = R$ to $c = R * 0.9999999$; the endpoint c of the outer interval $[c, b]$ is shifted from $c = R$ to $c = R * 1.0000001$.

r	E_1(MeV)	E_2(MeV)
1.0	-39.9600215	-29.4847423
0.1	-40.9795173	-31.9498045
0.01	-40.9936277	-31.9980921
0.001	-40.9937777	-31.9986123
0.0001	-40.9937792	-31.9986175
SQWP	-40.9937792	-31.9986175
r	E_3(MeV)	E_4(MeV)
1.0	-15.1906846	-1.2770512
0.1	-17.3145854	no-solution
0.01	-17.3878786	no-solution
0.001	-17.3886974	no-solution
0.0001	-17.3887056	no-solution
SQWP	-17.3887057	no-solution

Table 2: The energy eigenvalue dependence on the diffuseness parameter d. r is defined as the diffuseness parameter d divided by 0.67 fm ($d = r * 0.67$ fm). The subscript numbers of E correspond to the number n in equation (27). $E_n(n = 1, 2, 3, 4)$ are the calcuated values for r using equation (27).

Finally, we present **Table 1** to compare the results calculated using Ishizdu's approximate analytical expression with those calculated using the Runge-Kutta method. From these two results we can emphasize that the results obtained by these two distinct methods are in good agreement with each other. Understandably we use Newton's method in order to obtain the convergence value in each individual method.

Furthermore we calculate the energy eigenvalues of the 3-dimensional square-well potential with the same V_0 and R in equation (3) for the S-state ($l = 0$) using Newton's method. We include them in **Table 1** for comparison.

Besides, by using Ishidzu's expression we demonstrate explicitly in **Table 2** that when the diffuseness parameter d of the Woods-Saxon potential approaches zero, the energy eigenvalues, as expected, converge to those of the 3-dimensional square-well potential.

7 Concluding remarks

We have demonstrated that Newton's method is a clearly powerful technique for solving eigenvalue problems of quantum mechanics and also have endorsed the validity of Ishizu's analytical solution numerically using the Runge-Kutta method.

Although most of books on quantum mechanics are unfamiliar with Ishidzu' analytic approximate expression explained in this paper in contrast to the eigenvalue problem for the 3-dimensional square-well potential, it should be noted that Ishidzu' analytic approximate expression has a good accuracy and is very interesting from the viewpoint of mathematical physics.

In particular, we believe that most novice students beginning to learn practical uses of quantum mechanics can follow our calculations easily, which may have pedagogical merits for those students. Our approach may be of interest to those instructors who would like to introduce applications of Newton's method to various fields into their courses.

Acknowledgments

I would like to thank the editor for reading my manuscript carefully, pointing out errors and ambiguities, and giving me fruitful comments.

References

[1] M. Abramowitz and I. A. Stegun, Handbook of Mathematical Functions With Formulas, Graphs, and Mathematical Tables Dover Publications, Inc, New York, 1972.

[2] M. Atarashi, K. Hira, and H. Narumi, "On the kaon-nucleus optical potential at low energy", Prog. Theor. Phys, **60**, 209-219, 1978.

[3] J. Blomqvist and S.Wahlborn, "Shell model calculations in the lead region with a diffuse nuclear potential", Airkiv Fysik, **16**, 545, 1960.

[4] A. Erdelyi, W. Magnus, F. oberhettinger, and F. G.Tricomi, Higher Transcendental Functions volume 3, McGraw-Hill Book Co., New York, 1953.

[5] T. Ishidzu, "Analytical solution for S-state with the Woods-Saxon potentials", Prog. Theor. Phys, **40**, 796-807, 1968.

[6] L. Schiff, Quantum Mechanics 3rd. ed., McGrawHill, New York, 1968.

Vibrations of a Circular Membrane - Some Undergraduate Exercises

Nishanth P.[1] and Udayanandan K. M.[2]

[1]Department of Physics, Kannur University, Kannur, India.
mailnishanthp@yahoo.com

[2]Department of Physics, Nehru Arts and Science College, Kanhangad, India.
udayanandan@gmail.com

Submitted on 25-06-2018

Abstract

In this paper we revisit the vibrational modes of a circular membrane with different boundary conditions. This we hope will serve as an exercise to get more insight into the study of percussion instruments. The displacement for various modes are found for two initial velocities and two initial displacements. The first three modes are plotted for both cases. We found that the different initial velocities and initial displacements does not change the frequency or shape of different modes. Such an exercise, we believe, will help the students to understand the importance of the concept of modes associated with vibrations.

1 Introduction

The essential component in the sound production of percussion drums is the vibration of a circular membrane. When the drum head is struck, the circular membrane vibrates in different modes. The basic equation governing the vibration of a circular membrane is the wave equation, which is given by [1]

$$\frac{\partial^2 u}{\partial t^2} = c^2 \left(\frac{\partial^2 u}{\partial r^2} + \frac{1}{r}\frac{\partial u}{\partial r} + \frac{1}{r^2}\frac{\partial^2 u}{\partial \theta^2} \right) \quad (1)$$

where $u = u(r, \theta, t)$ is the displacement of the membrane and the velocity of sound wave $c = \sqrt{\frac{T}{\rho}}$ where T is the tension on the membrane and ρ is the uniform mass density. Using the separation of variable technique, the solution obtained is [2]

$$u(r, \theta, t) = \sum_{m=1}^{\infty} \sum_{n=0}^{\infty} J_n(k_{mn} r) \cos(n\theta) \left[a_{mn} \cos(c k_{mn} t) + b_{mn} \sin(c k_{mn} t) \right] \quad (2)$$

Here m and n are integers, where m represents the number of nodal circles and n represents the number of nodal lines. There are certain regions on the membrane where

there is no motion or vibration. When the non vibrating region is a circle it is called a nodal circle and when it is a line, the same is called a nodal line. $J_n(k_{mn}r)$ is the n^{th} order Bessel function where k_{mn} is the wave number and r is the radius. a_{mn} and b_{mn} are the constants to be determined. For an axis symmetric circular membrane the displacement $u(r,\theta,t)$ is independent of θ and then we modify our wave equation (1) as

$$\frac{\partial^2 u}{\partial t^2} = c^2\left(\frac{\partial^2 u}{\partial r^2} + \frac{1}{r}\frac{\partial u}{\partial r}\right) \tag{3}$$

For axis symmetric membrane no nodal lines are present and hence we fix our $n = 0$ and then equation (2) changes to

$$u(r,t) = \sum_{m=1}^{\infty} J_0(k_m r)$$

$$[a_m \cos(ck_m t) + b_m \sin(ck_m t)] \tag{4}$$

where a_{m0}, b_{m0} and k_{m0} are redefined as a_m, b_m and k_m.

2 Values of the coefficients a_m and b_m

At time $t = 0$, we get the displacement of the membrane from Eq (4) as

$$u(r,0) = \sum_{m=1}^{\infty} J_0(k_m r)a_m$$

Let

$$u(r,0) = f(r)$$

We have a theorem given in the book "*Fourier Series and Boundary Value Problems*" by James Brown and Ruel Churchill (pp 275, theorem 1) [3] which states that when F(q) is a continuous function in the interval $0 < q < p$ and if α_j are the positive roots of equation

$$J_0(\alpha_j p) = 0$$

then the function F(q) can be written as a Fourier-Bessel series

$$F(q) = \sum_{j=1}^{\infty} A_j J_0(\alpha_j q)$$

where

$$A_j = \frac{2}{p^2[J_1(\alpha_j p)]^2}\int_0^p qF(q)J_0(\alpha_j q)dq$$

Our drum has a radius R and we can define an interval $0 < r < R$. At R, the boundary is fixed and there is no vibration. The radial part of the solution in (4) at the boundary becomes

$$\sum_{m=1}^{\infty} J_0(k_m R) = 0 \tag{5}$$

Then for that region by the above theorem

$$a_m = \frac{2}{R^2[J_1(k_m R)]^2}\int_0^R rf(r)J_0(k_m r)dr$$

On differentiating $u(r,t)$ in (4) with respect to t we get

$$\frac{du(r,t)}{dt} = \sum_{m=1}^{\infty} J_0(k_m r)$$

$$[-ck_m a_m \sin(ck_m t) + ck_m b_m \cos(ck_m t)]$$

For $t = 0$, let $\frac{du}{dt} = g(r)$ and we get

$$g(r) = \sum_{m=1}^{\infty} J_0(k_m r)ck_m b_m$$

Using the theorem stated above, we get

$$b_m = \frac{2}{ck_m R^2[J_1(k_m R)]^2} \int_0^R rg(r)J_0(k_m r)dr$$

For the equation (5), let the positive roots be α_m, then

$$k_m R = \alpha_m$$
$$k_m = \frac{\alpha_m}{R} \quad (6)$$

Thus we get

$$a_m = \frac{2}{R^2[J_1(\alpha_m)]^2} \int_0^R rf(r)J_0\left(\frac{\alpha_m}{R}r\right) dr \quad (7)$$

$$b_m = \frac{2}{c\alpha_m R[J_1(\alpha_m)]^2} \int_0^R rg(r)J_0\left(\frac{\alpha_m}{R}r\right) dr \quad (8)$$

From the above equations (4), (7) and (8) we get

$$u(r,t) = \sum_{m=1}^{\infty} J_0\left(\frac{\alpha_m}{R}r\right) [\frac{2}{R^2[J_1(\alpha_m)]^2}$$

$$\int_0^R rf(r)J_0\left(\frac{\alpha_m}{R}r\right) dr \cos(ck_m t) + \frac{2}{c\alpha_m R[J_1(\alpha_m)]^2}$$

$$\int_0^R rg(r)J_0\left(\frac{\alpha_m}{R}r\right) dr \sin(ck_m t)]$$

3 Defining Cauchy conditions

For a circular membrane, the initial displacement indicates the shape of the drum at initial time. If the initial parameters are known, it is easy to find the parameters for the system at a later time. This is achieved by finding unknowns from the solutions describing the system using initial conditions [4]. Initial conditions are also known as Cauchy conditions. The value of particular unknown function and appropriate number of its derivatives are used to find the solution [5]. Since the wave equation is a second order partial differential equation, displacement and its derivative - velocity are considered as initial conditions. We had already defined the initial displacement of the membrane as f(r) and initial velocity as g(r) and we choose three cases of boundary conditions

3.1 Different choices of boundary conditions

1. **Case 1**

$$f(r) = 0$$
$$g(r) \neq 0$$

When our initial displacement is zero, the constants a_m are all zero. The complete solution for vibration of axis symmetric circular membrane from equation (4) is

$$u(r,t) = \sum_{m=1}^{\infty} J_0(k_m r)b_m \sin(ck_m t) \quad (9)$$

2. **Case 2**

$$f(r) \neq 0$$
$$g(r) = 0$$

When the initial velocity is zero all b_m values are zero then from equation (4)

$$u(r,t) = \sum_{m=1}^{\infty} J_0(k_m r)a_m \cos(ck_m t) \quad (10)$$

3. **Case 3**

$$f(r) \neq 0$$
$$g(r) \neq 0$$

In this case a_m and b_m values are non zero and hence the complete solution is equation (4) itself.

3.2 Different types of boundary conditions

In our study we choose two different forms of initial velocity functions

$$g_1(r) = AJ_0\left(\frac{\alpha_m r}{R}\right) \tag{11}$$

$$g_2(r) = B\,(R - r) \tag{12}$$

The 3D plot of two initial velocity functions are shown in figure 1. Initial displacement

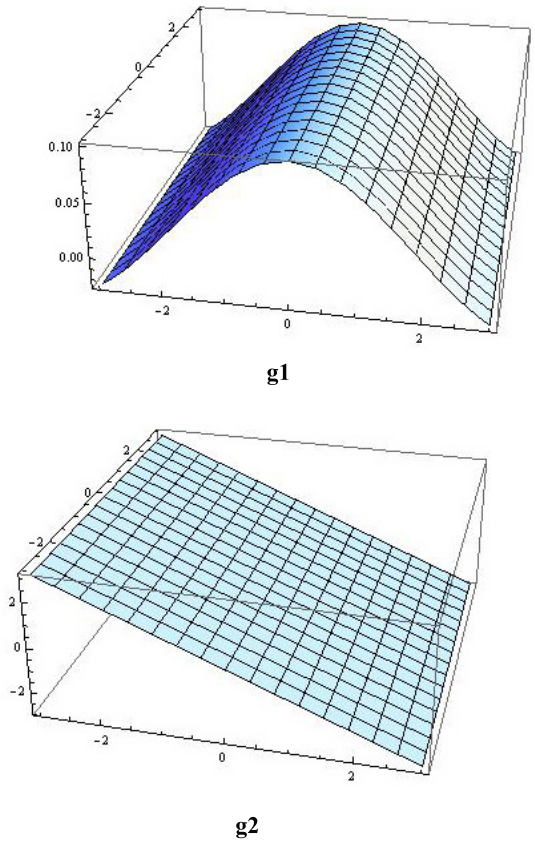

Figure 1: Initial velocity functions.

functions used in our study are [6]

$$f_1(r) = C(R^2 - r^2)^2 \tag{13}$$

$$f_2(r) = D(R - r)^2 \tag{14}$$

The constants A, B, C and D will be properly chosen to match the dimensionality. We have chosen $f_1(r)$ and $f_2(r)$ such that they satisfy boundary conditions, at r=R, $f_1(r) = f_2(r) = 0$. The initial displacement functions are plotted in figure 2.

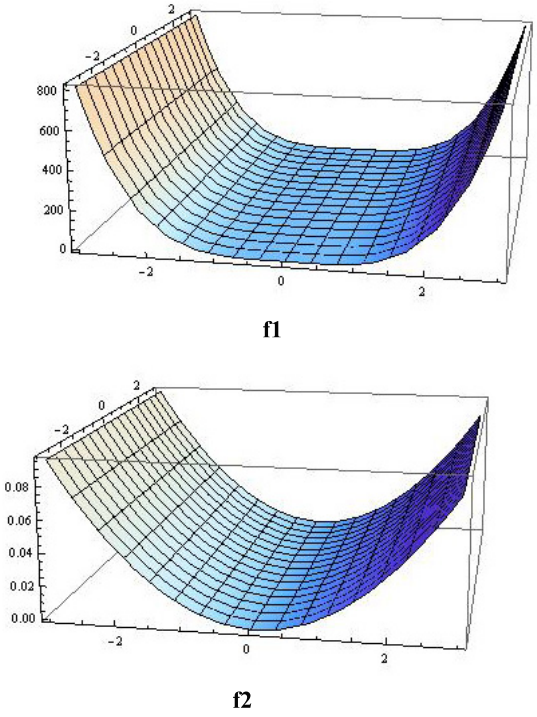

Figure 2: Initial displacement functions.

4 Mode determination using the different initial velocities

Example 1

Let us take the first initial velocity

$$g_1(r) = AJ_0\left(\frac{\alpha_m r}{R}\right)$$

On substituting the function in Eq (8) we get

$$b_m = \frac{2}{c\alpha_m R[J_1(\alpha_m)]^2}\int_0^R rAJ_0^2\left(\frac{\alpha_m r}{R}\right)dr$$

Let

$$\frac{\alpha_m r}{R} = x$$

So

$$\frac{\alpha_m dr}{R} = dx$$

when $r = 0$, $x = 0$ and when $r = R$, $x = \alpha_m$.

We have the standard integral

$$\int_0^a zJ_0^2(z)dz = \frac{1}{2}a^2\left(J_0^2(a) + J_1^2(a)\right)$$

On integration

$$b_m = \frac{A\,R}{c\alpha_m[J_1(\alpha_m)]^2}[J_0^2(\alpha_m) + J_1^2(\alpha_m)]$$

We have from boundary condition

$$J_0(\alpha_m) = 0$$

$$b_m = \frac{AR}{c\alpha_m} \tag{15}$$

$$u(r,t) = \sum_{m=1}^{\infty}\frac{AR}{c\alpha_m}J_0(k_m r)\sin(ck_m t)$$

Maximum displacement is produced when the drum is struck at centre. At $r = 0$ we have $J_0(0) = 1$ and hence our expression for deflection of the membrane becomes

$$u(r,t) = \sum_{m=1}^{\infty}\frac{AR}{c\alpha_m}\sin(ck_m t)$$

Using the equation (6) we have

$$u(r,t) = \sum_{m=1}^{\infty}\frac{AR}{c\alpha_m}\sin\left(\frac{c\alpha_m}{R}t\right) \tag{16}$$

We have from Eq (4)

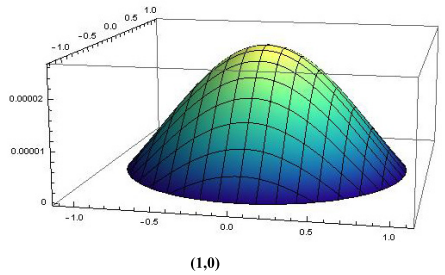

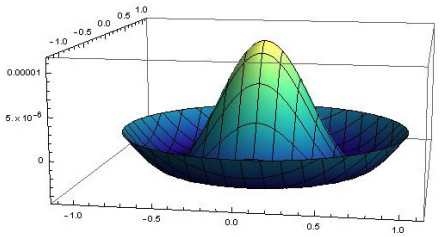

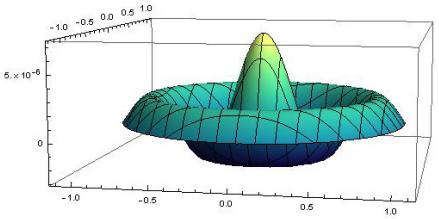

Figure 3: First three modes plotted for first initial velocity function.

$$ck_m = \omega_m$$

Multiplying numerator and denominator with R we get

$$ck_m\frac{R}{R} = \omega_m$$

and from Eq (6) we get

$$\frac{c\alpha_m}{R} = \omega_m$$

So frequency is

$$f_m = \frac{c\alpha_m}{2\pi R} \tag{17}$$

Here c, α_m and R are constants. From equation (17) it is clear that the frequency of different modes of vibration is independent of initial velocity and initial displacement.

5 Calculation of amplitudes for different modes of Timila

To verify the results obtained above, we will apply them to a percussion drum largely used in Kerala, called Timila[7]. Timila has a long resonator body which is made of jack wood. The instrument consists of circular membranes on both heads and are not loaded. The drum does not give a sense of pitch but is used as a rhythmic drum. The main strokes produced by the timila are 'tha' and 'thom'. The instrument is played with palms of both hands. The body of timila has a length of 20.5 in and the diameter of the drum is 6.5 in. When the drum is played, the head vibrates in different modes and these vibrations are transfered to the air molecules in the resonator and the sound is produced. The peculiar construction and playing style adds beauty to the instrument.

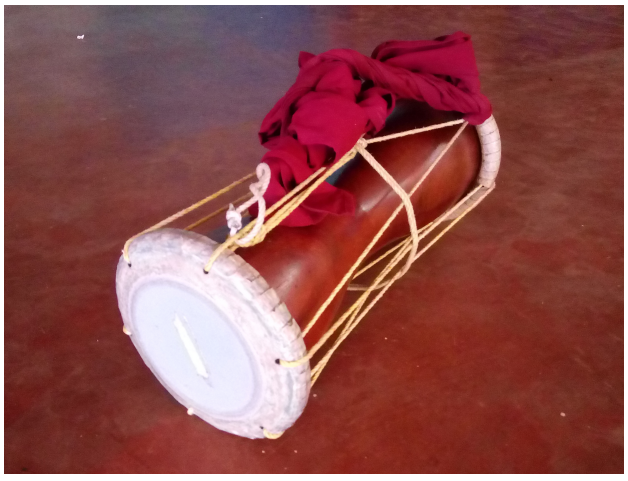

Figure 4: A typical timila used In Kerala.

We will find the frequency of modes of circular membrane with following parameters - R=0.082m (the radius of Indian rhythmic drum timila [7]) and c=130.31m/s. The values of α_m, the positive roots of Bessel function of order zero are taken from the book by Enrique A. Gonzalez-Velasco [6]. The conventional animal membrane of timila drum head is nowadays replaced by mylar membrane. The value of mass density of such a membrane is $0.26 kg/m^2$ [8] and assuming the value typical tension applied as 4415N/m, the c is obtained as 130.31m/s. From Eq (15) the amplitude depend on α_m and we had taken n=0 hence for various α_m we get various b_m. The values obtained for b_m are tabulated below. The numerical calculation of first mode is shown below with A=0.1m/s and $\alpha_1 = 2.4048$. We get

$$b_1 = \frac{0.1 \times 0.082}{130.31 \times 2.4048} = 2.6167 \times 10^{-5} m$$

Mode	$b_m(m)$
(1,0)	2.6167×10^{-5}
(2,0)	1.13995×10^{-5}
(3,0)	7.2717×10^{-6}
(4,0)	5.3366×10^{-6}
(5,0)	4.2145×10^{-6}
(6,0)	3.4822×10^{-6}

The displacements of first three modes are plotted and given in figure 3. For vibration of circular membrane with applied initial velocity, frequency of the modes remain same but the amplitude changes.

Example 2

For second velocity function

$$g_2(r) = B(R - r) \tag{18}$$

$$b_m = B\frac{2}{c\alpha_m R[J_1(\alpha_m)]^2}\int_0^R r(R-r)J_0\left(\frac{\alpha_m r}{R}\right)dr \tag{19}$$

We get b_m after integration and simplification as

$$b_m = B\frac{\pi R^2 H_0(\alpha_m)}{c\alpha_m^3 J_1(\alpha_m)}$$

where $H_0(\alpha_m)$ is the Struve function of order zero. Struve function is the solution of non homogeneous Bessel equation and usually found in integrals involving Bessel function. Then we get

$$u(r,t) = B\sum_{m=1}^{\infty}\frac{\pi R^2 H_0(\alpha_m)}{c\alpha_m^3 J_1(\alpha_m)}\sin\left(\frac{c\alpha_m}{R}t\right)$$

For the same parameters as in example 1 the values of b_m are tabulated. The b_1 value is calculated with $B = 1s^{-1}$, $J_1(\alpha_m) = 0.5192$ and $H_0(\alpha_1) = 0.7497$. The values of Bessel function and Struve function are obtained using online calculators. The other parameter values are same as example 1.

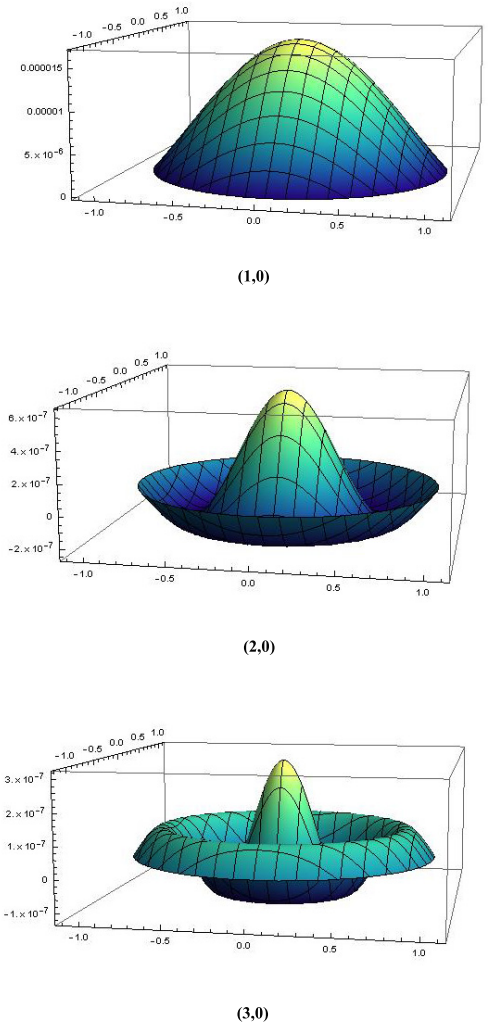

Figure 5: First three modes plotted for second initial velocity function.

$$b_1 = 1\frac{3.14 \times (0.082)^2 \times 0.7497}{130.31 \times (2.4048)^3 \times 0.5192}$$

$$= 1.6823 \times 10^{-5}m$$

Mode	$b_m(m)$
(1,0)	1.6823×10^{-5}
(2,0)	6.41695×10^{-7}
(3,0)	3.1662×10^{-7}
(4,0)	7.5916×10^{-8}
(5,0)	5.8671×10^{-8}
(6,0)	2.2306×10^{-8}

The first three modes plotted for second initial velocity function are given in figure 4.

6 Mode determination using the different initial displacements

Example 1

We have

$$a_m = \frac{2}{R^2[J_1(\alpha_m)]^2} \int_0^R r f(r) J_0\left(\frac{\alpha_m}{R} r\right) dr \tag{20}$$

We have our first displacement function $f_1 = C(R^2 - r^2)^2$. On substitution and integration we get

$$a_m = C\frac{128R^4 - 16R^4(\alpha_m)^2}{(\alpha_m)^5 J_1(\alpha_m)}$$

The deflection of the membrane struck at centre is

$$u(r,t) = \sum_{m=1}^{\infty} C\frac{128R^4 - 16R^4(\alpha_m)^2}{(\alpha_m)^5 J_1(\alpha_m)} \cos\left(\frac{c\alpha_m}{R} t\right)$$

We calculated the numerical value of a_1 with same parameter values as in example 1 and 2 in section 4 and the value of C is taken as $10m^{-3}$. So

$$a_1 = 10\frac{(0.082)^4[128 - 16 \times (2.4048)^2]}{(2.4048)^5 \times 0.5192}$$

$$= 3.8406 \times 10^{-4} m$$

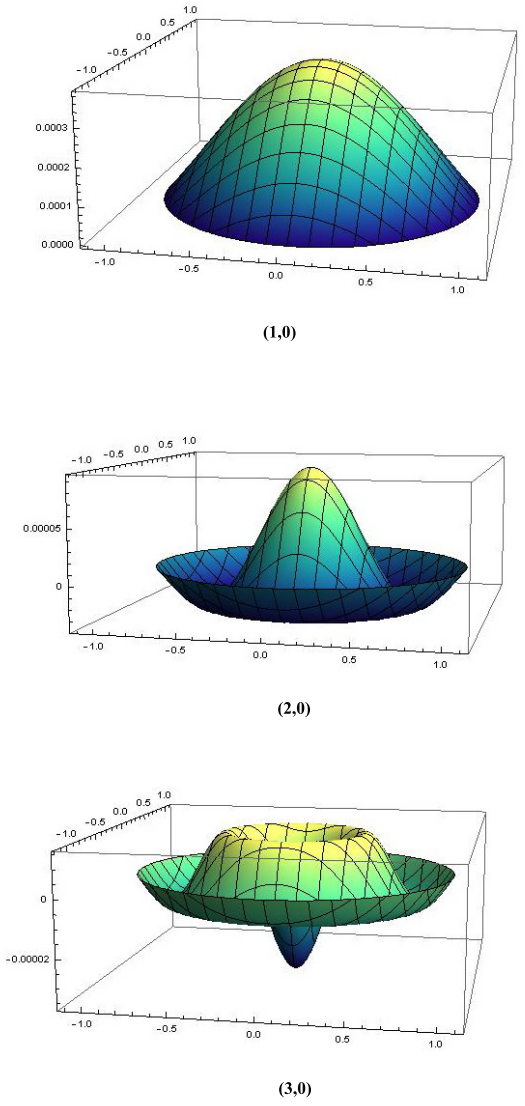

Figure 6: First three modes plotted for first initial displacement function.

Mode	$a_m(m)$
(1,0)	3.8406×10^{-4}
(2,0)	9.3199×10^{-5}
(3,0)	-3.6736×10^{-5}
(4,0)	1.7886×10^{-5}
(5,0)	-1.0147×10^{-5}
(6,0)	6.3707×10^{-6}

the first three modes are plotted in figure 5.

Example 2

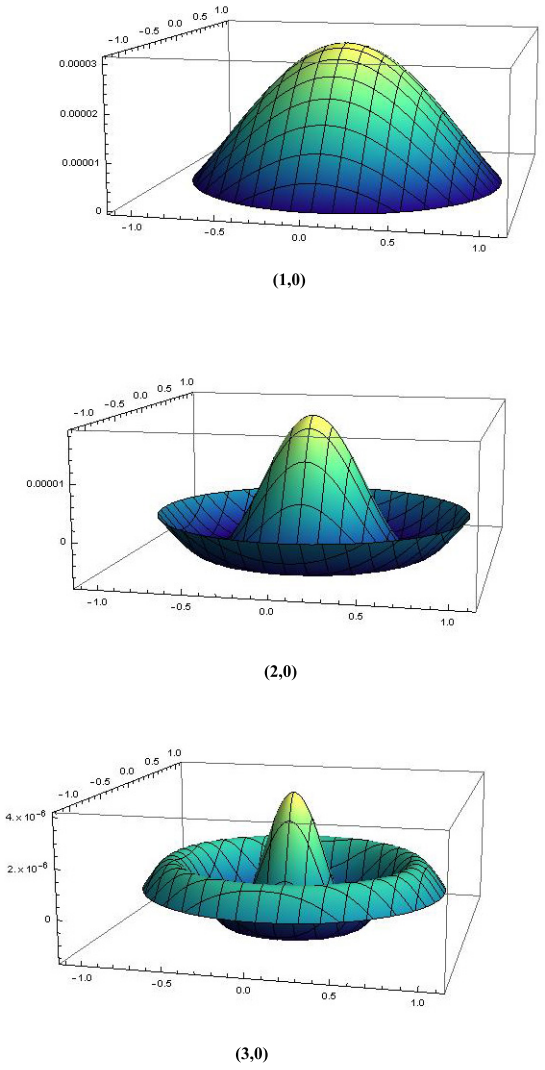

Figure 7: First three modes plotted for second initial displacement function.

Now consider the second displacement function $f_2 = D(R-r)^2$. On substitution in equation for a_m, we get

$$a_m = \frac{2D}{R^2[J_1(\alpha_m)]^2}\int_0^R r(R-r)^2 J_0\left(\frac{\alpha_m}{R}r\right)dr$$

On integration we get

$$a_m = D\left[\frac{2\pi R^2}{(\alpha_m)^2}\frac{H_0(\alpha_m)}{J_1(\alpha_m)} - \frac{8R^2}{(\alpha_m)^3 J_1(\alpha_m)}\right]$$

Here we get the complete solution

$$u(r,t) = D\sum_{m=1}^{\infty}\cos\left(\frac{c\alpha_m}{R}t\right)$$

$$\left[\frac{2\pi R^2}{(\alpha_m)^2}\frac{H_0(\alpha_m)}{J_1(\alpha_m)} - \frac{8R^2}{(\alpha_m)^3 J_1(\alpha_m)}\right] \quad (21)$$

We obtained the value of amplitude a_1 with same parameters as above and with $D = 0.01m^{-1}$

$$a_1 = 0.01\left[\frac{2\times 3.14\times(0.082)^2}{(2.4048)^2}\frac{0.7497}{0.5192}\right]$$

$$-0.01\left[\frac{8\times(0.082)^2}{(2.4048)^3\times 0.5192}\right] = 3.094\times 10^{-5}m$$

Mode	$a_m(m)$
(1,0)	3.094×10^{-5}
(2,0)	1.863×10^{-5}
(3,0)	4.082×10^{-6}
(4,0)	3.744×10^{-6}
(5,0)	1.500×10^{-6}
(6,0)	1.536×10^{-6}

The first three modes plotted are shown in figure 6.

7 Modes with both Initial displacement and initial velocity

In order to find the maximum displacement for case 3, we choose same initial velocity function and initial displacement function

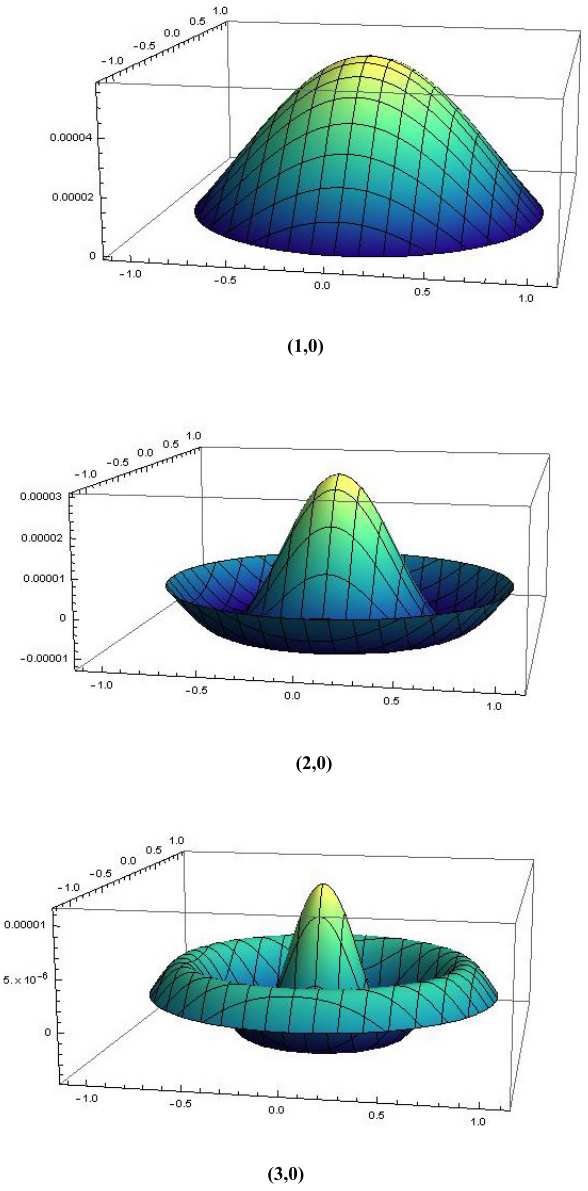

Figure 8: First three modes plotted for case 3.

as given in (11) and (14). For a circular membrane struck at centre the complete solution is arrived from equations (4), (16) and (21) as

$$u(r,t) = \sum_{m=1}^{\infty} D\cos\left(\frac{c\alpha_m}{R}t\right)$$

$$\left[\frac{2\pi R^2}{(\alpha_m)^2}\frac{H_0(\alpha_m)}{J_1(\alpha_m)} - \frac{8R^2}{(\alpha_m)^3 J_1(\alpha_m)}\right]$$

$$+ \sum_{m=1}^{\infty} \frac{AR}{c\alpha_m}\sin\left(\frac{c\alpha_m}{R}t\right)$$

In this case amplitude is the sum of a_m and b_m. The amplitudes of first six modes are given in the table below.

Mode	$a_m + b_m(m)$
(1,0)	5.7107×10^{-5}
(2,0)	3.00295×10^{-5}
(3,0)	1.1354×10^{-5}
(4,0)	9.0806×10^{-6}
(5,0)	5.7145×10^{-6}
(6,0)	5.0182×10^{-6}

The first three modes are plotted in figure 7.

8 Conclusion

The circular membrane vibration is studied for different initial velocities and initial displacements. The amplitudes of first six modes are found and the displacements of first three modes are plotted. It is seen that the mode shape remains invariant for any applied initial displacement and velocity. The parameter that changes with the application of initial displacement and velocity is the amplitude of vibration of modes. This study once again show the importance of modes in any vibration. We had assumed that the density of the membrane as uniform. In future we aim to solve vibration of membranes with non uniform densities.

References

[1] E. Kreyszig, H. Kreyszig and E. J. Norminton, Advanced Engineering Mathematics, (Wiley, 2010)

[2] Amir Javidinejad, J. Th. app. Mech. 43 (1), 19-26 (2013).

[3] J. W. Brown and R. V. Churchill, Fourier Series and Boundary Value Problems, (Mc Graw Hill, 2008)

[4] Nakhle H. Asmar, Partial Differential equations with Fourier Series and Boundary Value Problems, (Pearson, 2004)

[5] Prem K. Kythe, Pratap Puri and Michael R. Schaferkotter, Partial Differential equations and Mathematica, (CRC Press, 1997)

[6] Enrique A. Gonzalez-Velasco, Fourier Analysis and Boundary Value Problems, (Academic Press, 1996)

[7] L. S. Rajagopalan, A. Purushothaman and A. Harindranath, Temple Musical Instruments of Kerala, (D. K. Print World and Sangeet Nadak Akademi, 2010)

[8] V. E. Howle and L. N. Trefethen, Journal of Computational and Applied Mathematics 135, 23-40 (2001).

Examining the Decay Constants of Radioactive Dice Experiment

Bhakta Kunwar[1] and Pronita Chettri[2]

[1]Department of Physics, Sikkim Government College,
Tadong, Sikkim-737102, India.
bhaktakunwar@yahoo.co.in

[2]Department of Physics, Sikkim Manipal Institute of Technology,
Majitar, Rongpo, East Sikkim, Sikkim-737136
pronita.c@smit.smu.edu.in

Submitted on 16-07-2017

Abstract

Radioactive dice experiment is widely used as a pedagogical tool to demonstrate the phenomenology of radioactivity in classrooms. The decay constants obtained in such experiments are found to be consistently higher than the values predicted by the exponential nuclear decay law. It was suggested by some authors that the discrepancy could be minimized by using polyhedral dice having higher number of faces. In this article, some analytical attempts have been made to look for better numerical formulae which could minimize the discrepancy between the probabilistic prediction for dice experiment and the predictions based on exponential nuclear decay law. It was observed that the probabilistic prediction closely approaches the prediction based on exponential nuclear decay law under two different conditions: (i) when the data corresponding to a large number of throws are used, and (ii) when polyhedral dice having higher number of faces are used. Comparatively, the prediction based on the first condition yield better results than the second one.

1 Introduction

Radioactive decay of heavy nuclei is usually simulated in the laboratory or class room of higher secondary schools and undergraduate colleges by rolling dice [1–3]. The most common dice being a cube whose six faces are usually marked by numbers like 1 to 6. Rolling of one such dice would yield an outcome which has the probability of occurrence 1/6. Flipping a coin, which has two

faces, would yield an outcome which has the probability of occurrence 1/2. Polyhedral dice having 8,10,12 or more faces can also be used but these are relatively costlier and not readily available in the market. So, in general, cubic dice with six faces are the most widely used dice in the simulation of radioactive nuclei as these are relatively cheaper and readily available.

A large collection of six-faced dice is thrown simultaneously. The dice showing a particular number (say, for example a '3') are deemed to have decayed like radioactive nuclei and all the other dice showing the numbers other than three (i.e., 1,2,4,5 and 6) are taken as 'undecayed' nuclei. All the dice with outcome '3' are removed and the remaining 'undecayed' dice are counted. This number of 'undecayed' dice is recorded and represents the number of undecayed nuclei remaining after a certain interval of time. The 'undecayed' dice are then thrown and, again, those showing a '3' are removed and the remainder counted. This is repeated for many times and the number of 'undecayed' dice is counted every time. Such dice rolling experiment is meant to represent decay of a particular species of radioactive nuclei with a certain decay constant λ. It was pointed out by Murray and Hart [1] that the 'decay constant' obtained from dice rolling experiment was consistently higher, on average, than the value predicted by the theory of nuclear disintegration. They have quantitatively shown that the cause of discrepancy in the dice decay experiment is the choice of six faced cube. If, instead, dice having more number of faces are used, then the discrepancy would be minimized. Greater the number of faces of dice, lesser would be the discrepancy.

In this article, we attempt to obtain numerical formulae which are mathematically consistent with the exponential decay law representing the real nuclear decay. Through simple analytical steps we arrive at two different results corresponding to two different mathematical conditions. One of the conditions leads us to the same conclusion as suggested in [1] while the other condition leads us to a new formula. The values of decay constants yielded by this new formula are found to be more closer to those predicted by the exponential decay law, provided, one compiles enough data corresponding to those dice throws whose 'mass throw numbers' are equal to or greater than the number of faces of the dice. For this, we need to take a very large number of dice at the beginning so that we can repeat the dice throw for a large number of times without being exhausted of the dice within a few intervals of time.

2 Theory of decay of real nuclei

In the decay of real nuclei, the rate of disintegration at any instant of time is directly proportional to the number of nuclei available at that instant. If N be number of nuclei present at an instant of time t, ΔN be the decrease in the number of nuclei within a small

time interval Δt, then

$$\frac{\Delta N}{\Delta t} = \lambda N. \tag{1}$$

The decay constant λ represents the probability per unit time that a nucleus can undergo disintegration. It is evident from (1) that the decay rate depends not only on λ but also on N. If N_0 be the number of nuclei at the beginning and N_t be the number of nuclei remaining after a time t, then we have

$$N_t = N_0 e^{-\lambda t} \tag{2}$$

The half life period of the radioactive nuclei $t_{\frac{1}{2}}$ is defined as

$$t_{\frac{1}{2}} = \frac{ln2}{\lambda} \tag{3}$$

3 Theory of the decay of the radioactive dice

A large collection of dice, each having $'s'$ number of surfaces, is thrown simultaneously. The dice showing a particular face are deemed to have decayed like radioactive nuclei and all the other dice are taken as 'undecayed' nuclei. We choose a constant time interval Δt between any two successive throws. Let us throw N_0 dice simultaneously by the end of first time interval. Since we are taking polyhedral dice having s faces, the probability that a dice decays in time interval Δt is $1/s$. From the theory of probability, then, the number of remaining undecayed dice after the first throw is given by $N_1 = N_0(1 - 1/s)$ .After n simultaneous mass throws the number is

$$N_n = N_0(1 - \frac{1}{s})^n. \tag{4}$$

Now, the probability per unit time and hence, by definition, its decay constant λ is given by

$$\lambda = \frac{1}{s\Delta t}. \tag{5}$$

Since Δt is the time interval between two successive throws, the total time elapsed t after n mass throws is given by $t = n\Delta t$. Therefore, $n = s\lambda t$. Substituting this in (4) we obtain

$$N_n = N_0(1 - \frac{1}{s})^{s\lambda t}. \tag{6}$$

Now, we will make use of a well known formula of limits which goes as

$$\lim_{s\to\infty}(1 - \frac{x}{s})^s = e^{-x} \tag{7}$$

If we choose dice having large s, then we can employ (7) so as to express (6) in the approximate form

$$N_n = N_0\Big[\lim_{s\to\infty}(1 - \frac{1}{s})^s\Big]^{\lambda t} = N_0\big[e^{-1}\big]^{\lambda t} = N_0 e^{-\lambda t} \tag{8}$$

Thus, we find, for large value of s, that the prediction of (4) would be close to that of (2). Recall that (2) represents real decay of nuclei. In other words, the discrepancy can be reduced by using polyhedral dice having higher number of faces. This result is in agreement with the findings of [1]. Alternatively, we can use the relation $n = s\lambda t$ and express (4) as

$$N_n = N_0\Big(1 - \frac{\lambda t}{n}\Big)^n. \tag{9}$$

For large values of n, one can use Eq.(7) to write Eq.(9) approximately as

$$N_n = N_0 \lim_{s\to\infty} \left(1 - \frac{\lambda t}{n}\right)^n = N_0 e^{-\lambda t}. \quad (10)$$

This means that the decay constant measured from dice experiment approaches the value of decay constant predicted by the real nuclear decay law when n is large. In other words, we can say that the discrepancy can also be minimized by throwing the dice a large number of times instead of using dice having large s.

4 Numerical estimation of decay

In the large s approximation, the number of undecayed dice can be predicted by using (4). In the case of large n approximation, one cannot employ (9) directly to make numerical predictions as this equation involves λ and t . We make the following rearrangements in (10), again, by using (7) with $x = 1$:

$$N_n = N_0 e^{-\lambda t} = N_0 \left[e^{-1}\right]^{\lambda t} = N_0 \left[\lim_{n\to\infty} (1 - \frac{1}{-})^n\right]^{\lambda t}$$

On dropping the limit and using $\lambda t = n/s$ in the above result, we obtain the numerical formula for large n approximation as

$$N_n = N_0 \left(1 - \frac{1}{n}\right)^{\frac{n^2}{s}}. \quad (11)$$

Obviously, the formula given in (11) would be valid for large values of n. The values of λ obtained by using (11) are henceforth termed as those obtained under large n approximation (LnA). On the other hand, the results obtained by using (4) are termed large s approximation (LsA) results. On the same footing, decay constants given by the exponential nuclear decay law, that is (2), are called real nuclear decay (RnD) results. Note that (4) and (11) are expressed in terms of the variables n and s while (2) involves the variable t . So, for the sake of uniformity of variables used in (2), (4) and (11), the exponential law of (2) can be written in terms of n and s instead of t . Using in (2), we simply get

$$N_n = N_0 e^{-n/s}. \quad (12)$$

Now, we compare the numbers of undecayed dice or nuclei as predicted by Eq.(4) (LsA), Eq.(11) (LnA) and Eq.(12) (RnD) and obtain their respective decay constants.

Table 1: Numbers of undecayed dice/nuclei with $N_0 = 10000$ and $s = 6$

Throw number (n)	Numbers of undecayed dice/nuclei			Throw number (n)	Numbers of undecayed dice/nuclei		
	LsA	LnA	RnD		LsA	LnA	RnD
1	8333	*	8465	20	261	327	357
2	6944	6300	7165	21	217	277	302
3	5787	5443	6065	22	181	235	256
4	4019	3946	4346	24	126	168	183
6	3349	3349	3679	25	105	142	155
7	2791	2840	3114	26	87	120	131
8	2326	24077	2636	27	73	102	111
9	1938	2039	2231	28	61	86	94
10	1615	1727	1889	29	51	73	80

Table 1 shows the numbers of undecayed dice/nuclei after various throws for $N_0 = 10000$ and $s = 6$. A glance at table 1 reveals that (i) LnA predictions are closer to the RnD predictions than those predicted by LsA when , (ii) LnA cannot predict N_1, that is the number of undecayed dice after the first throw. But, this drawback is insignificant in the calculation of decay constant,

and (iii) the number of undecayed dice after every throw in both, LnA and LsA, are smaller than that in RnD. For $n > s$, the number of undecayed dice in LnA is more than that in LsA. We have plotted $ln\frac{N_0}{N}$ for three different ranges of n in figure 1. For uppermost graph n runs from 2 to 10, for middle graph n goes from 7 to 17 and for lowermost graph n is from 30 to 40. Note that for the last two graphs, we have $n > s$. These are straight lines whose slopes give the values of decay constants λ . The LsA values of λ for all the three ranges of n are consistently higher $(\lambda = 0.18)$ than the RnD values $(\lambda = 0.167)$ .The LnA yields relatively poor result $(\lambda = 0.163)$ in the uppermost graph while it gives better results in the middle $(\lambda = 0.166)$ and lowermost $(\lambda = 0.166)$ graphs. This is expected as the condition of validity of LnA is $n > s$. In order to check the validity of LsA (4) and LnA (11) for other values of n and s, we generated data similar to table 1 for $s = 10, 20$ and 40 and obtained the value of $\frac{ln(N_0/N)}{n}$ for each value of n and plotted them. The resulting graphs are presented in figure 2. Thus, we observe that the LnA-formula (11) appears to predict reasonably good results for $n > s$ while it is not reliable for $n < s$. The accuracy of LsA results increases with increasing values of s. For $s = 6$, the difference between LsA and RnD result is about 9% and this difference gradually decreases to 5%, 2.6% and 1.2% for s equal to 10, 20 and 40 respectively. Interestingly, LnA yield better results than the LsA for $n > s$.

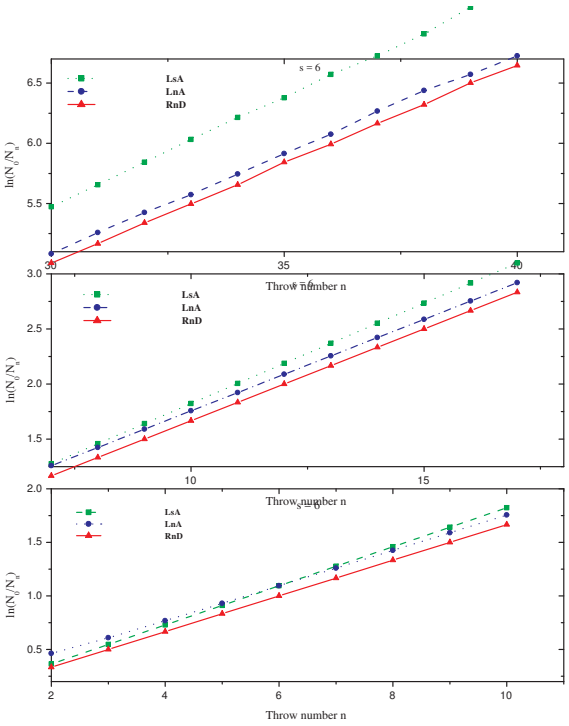

Figure 1: Plots of $ln(N_0/N)$ for three different ranges of mass throw number n. Here, $N_0 = 10000$ and $s = 6$. The throw number n runs from 2 to 10 in the uppermost panel, it goes from 7 to 17 in the middle panel and it runs from 30 to 40 in the lowermost panel. The red solid line represents the real nuclear decay (RnD), the blue dotted line denotes dice decay in large n approx.(LnA) and the green dashed line shows dice decay in large s approximation (LsA).

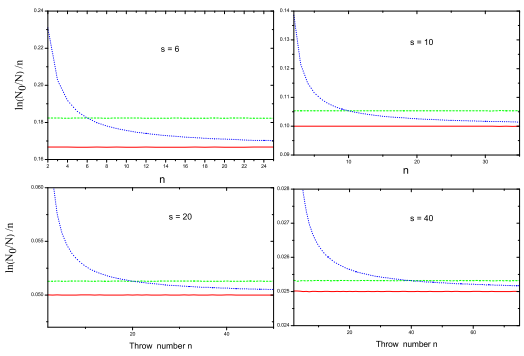

Figure 2: Variation of $\frac{ln(N_0/N)}{n}$ with throw number n for different values of s. The predictions of RND, LnA and LsA are represented by the red solid line, the blue dotted line and the green dashed line respectively.

5 Conclusion

The accuracy of predictions of the LsA-formula given in (4) is found to increase with increasing values of s. Thus, the discrepancy between the rolling dice experiment and the theoretical formula (4) can be minimized by using polyhedral dice having large number of faces.

But, polyhedral dice having 8,10,12 or more faces are relatively costlier and not readily available in the market. Therefore, cubic dice with six faces are the most widely used dice in the simulation of radioactive nuclei.

In the preceding sections, we have seen that the LnA-formula (11) predict reasonably good results for $n > s$. Therefore, it appears to be possible to perform rolling dice experiment even with six-faced cube and still obtain a better value of decay constant by using LnA-formula given in (11). This means that in the actual dice experiment one has to take a large number of data so that she is left with enough data even after discarding the data of the first s throws. In this scenario, one can use even cubic dice and obtain still better result. However, in order to consider only those data for which the throw numbers are greater than the number of faces of dice, i.e., data satisfying the condition $n > s$, one has to begin with a large number of dice and record a large number of data. This result (11) may be also extended to other simulation activities involving exponential decay.

References

[1] Arthur Murray and I. Hart. *Phys. Educ.* 47, 197, (2012).

[2] E. Schultz, *J. Chem. Educ.*, 74 (5), 505, (1997).

[3] S. Sahu, *Creative Education*, 3, 673, 2012.

Degeneracy of Fresnel Reflection Coefficients at Normal Incidence.

Luc Lévesque

Department of Physics
Royal Military College of Canada
Kingston, K7K 7B4, Canada.
luc.levesque@rmc.ca

Submitted on 16-12-2016

Abstract

The Fresnel reflection coefficients are revisited by choosing consistent directions for the relative electric field orientations normal and parallel to the plane of incidence. The boundary conditions are applied at the interface between two semi-infinite uniform media. This leads us to the conclusion that the reflection coefficients for both the *s* and *p* waves are equal at normal incidence, in agreement with the treatment presented in some textbooks. A different convention is also used in other textbooks and gives Fresnel reflection coefficients that are of opposite signs. These contradictory results have no implications on the reflectivity at an interface, which equals the square of each Fresnel coefficient, but is changing the phase of the electric field reflected at the interface. It is believed that the considerations being examined, which are based upon symmetry, will be useful to university or college teachers when introducing Fresnel's equations in the classroom.

1. Introduction

The amplitude reflection coefficient r is defined as the ratio of the reflected electric field strength E_r over the incident electric field strength E_i, i.e.,

$$r_{s,p} \equiv \left(\frac{E_r^{s,p}}{E_i^{s,p}} \right) \qquad (1)$$

where superscripts s and p correspond to the electric fields perpendicular and parallel to the plane of incidence, respectively, as shown in figure 1. Some authors [1-7] compute the amplitude Fresnel coefficients from the definitions of field vectors shown in figure 1, from which we can conclude that, at normal incidence (θ_i):

$$r_s = r_p\big|_{\theta_i=0} \qquad (2)$$

However, the $\boldsymbol{E}$ and $\boldsymbol{H}$ field conventions depicted in figure 2 are also used by some authors [8-13]. Yet, from this convention, we obtain a different result for the amplitude Fresnel coefficients at normal incidence, that is,

$$r_s = -r_p\big|_{\theta_i=0} \qquad (3)$$

This previous result means that r_s is shifted by 180º with respect to r_p even though the $\boldsymbol{E}$-field magnitudes (E_i^s and E_i^p) are parallel to the interface at $\theta_i = 0$º. These conclusions have no consequences when calculating the reflectance R, as it is given by the square of each amplitude Fresnel coefficient. Nevertheless, it could lead to errors when computing the quantity ρ defined as the ratio of r_p / r_s in the equations of ellipsometry [14-15] even for $\theta_i > 0$º. At normal incidence, the electric field vectors $\boldsymbol{E}$ for both the *s* and *p* waves are parallel to the interface bounded by the two semi-infinite

media and as a result they should behave in the same way. From this basic symmetry concept, the reflection coefficients r_s and r_p should be equal at normal incidence and this means that Eq. (2) would be correct.

Eq. (2) also implies that the phase of the reflected electric field vector E_r for both the *s* and *p* waves remains the same at normal incidence. This is so because at this given incident angle both E_r^s and E_r^p happen to be parallel to the interface. From figure 1, note that both the *s* and *p* waves are parallel to the plane of incidence as θ_i (= θ_r) approaches zero. Note this is no longer the case for $\theta_i > 0^o$. The result in Eq. (3) is predicting a phase change in the reflection coefficient at normal incidence, despite the symmetry of the electric field vector for $\theta_i = 0^o$. This contradictory result from equation (2) arises from the definitions of the directions of the electric vectors in the system used to represent each state of polarisation.

The definition of directions for the vector fields shown in figure 1 is often used by some authors [1-7] and leads to Eq. (2), as shown later in the next section.

The relative orientations of the field vectors shown in figure 1 are consistent because for the following reasons:

1) The ***E***-fields ($\boldsymbol{E}_i$, $\boldsymbol{E}_r$, $\boldsymbol{E}_t$) point in the same direction for both polarisations at normal incidence.
2) The relative directions of the reflected ***H***-field vectors reverse their direction for both polarisations at normal incidence. Note that the incident and transmitted ***H***-fields keep their direction for both polarisations at normal incidence.
3) The relative directions of the reflected ***H***-fields were chosen so as to ensure that the cross-product ***E x H***, for both independent polarisations will always point in the direction of the power flow. Also, each field vector can be found using

$$\mathbf{H}_{i,r,t} = \sqrt{\frac{\varepsilon}{\mu}}\hat{\mathbf{k}}_{i,r,t} \times \mathbf{E}_{i,r,t} \qquad (4)$$

where $\hat{\mathbf{k}}_{i,r,t}$ is a unit vector pointing in the direction of propagation of the incident (*i*), reflected (*r*) and transmitted (*t*) rays, respectively.

In Eq.*4*, ε and μ are the electric permittivity and the magnetic permeability of the material, respectively. Because of the above reasons, the Fresnel coefficients are expected to be equal (with the same sign) at normal incidence.

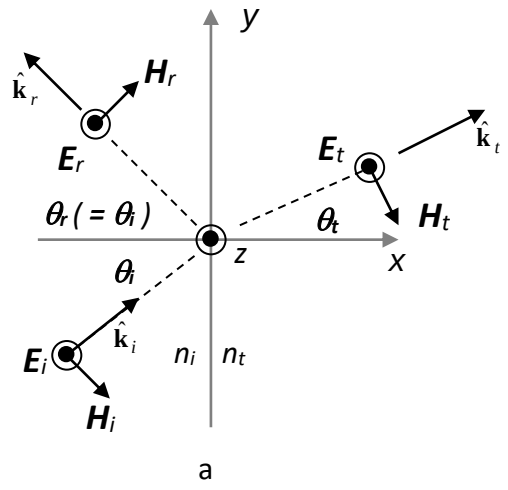

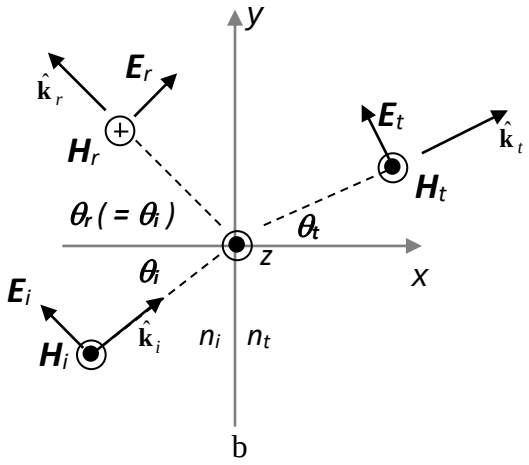

Figure 1: Reflection in the plane of incidence at the interface between two media. The electric field ***E*** is perpendicular to the plane of incidence (s-wave) in a) and parallel to it (p-wave) in b).

However, the ***E*** and ***H*** field conventions depicted in figure 2 are also used by some authors [8-13]. In this system, the defined directions for both the incident and the reflected ***E***-fields are the same at normal incidence for the *s*- wave, but they are reversed when treating the *p* -wave. For instance, the incident and reflected ***H***-field vectors are of opposite directions at normal incidence for the s-wave and yet they are assumed to be along the same directions at $\theta_i = 0^o$ for the *p*-wave. As θ_i reaches zero (normal incidence) the reflected vector fields should take the same direction for both the *s* and *p* waves. Therefore the convention used in figure 2 for the *s*-wave (*cf.fig. 2a*) is inconsistent with that of the *p*-wave (*cf.fig. 2b)*. If one decides to change the direction of the reflected ***H***-field ($\boldsymbol{H}_r$) for the *s*-wave, the change should also be made accordingly when treating the *p*-wave in order to be consistent. Based on the convention system in figure *2*, the Fresnel coefficients for r_s and r_p are expected to change sign upon reflection at normal incidence. This sign change has no physical meaning (such as a phase shift) and only occurs as a result of the contradictory choice of directions of each field when treating both independent polarisations. Note that the requirement on the power flow is fulfilled.

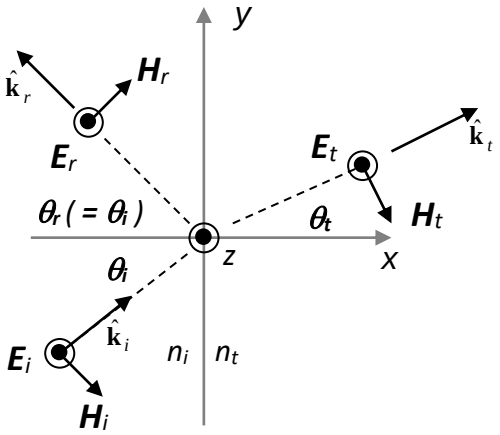

a

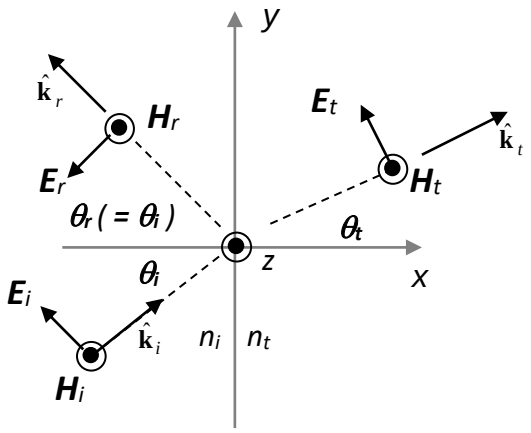

b

Figure 2: Reflection in the plane of incidence with the interface between two media. The electric field ***E*** is perpendicular to the plane of incidence (s-wave) in a) and parallel to it (p-wave) in b).

2. Calculations of r_s and r_p for both convention systems

In this section, boundary conditions are applied to both the consistent (*c.f. fig.1*) and inconsistent (*c.f. fig.2*) convention systems for the field vector directions. In accordance with Maxwell's boundary conditions the tangential component of both the ***E*** and ***H*** field vectors must be continuous at the interface bounded by the two media.

i) For the consistent convention system of field vector directions (*c.f. fig.1a*) — *s*-wave.

Tangential component of the ***E***-field is continuous at the interface. As each vector ***E***-field component is pointing along the z-axis in this case, we merely write

$$E_i + E_r = E_t \qquad (5)$$

where $E_i = |\boldsymbol{E}_i|$, $E_r = |\boldsymbol{E}_r|$ and $E_t = |\boldsymbol{E}_t|$.

Tangential component of the ***H***-field is continuous at the interface. Using Eq.(4), the y-component of $\boldsymbol{H_i}$, $\boldsymbol{H_r}$ and $\boldsymbol{H_t}$ can be found in terms of E_i, E_r, E_t, θ_i and θ_t, from where it can be found that:

$$\sqrt{\frac{\varepsilon_i}{\mu_i}}(E_i - E_r)\cos\theta_i = \sqrt{\frac{\varepsilon_t}{\mu_t}}E_t\cos\theta_t \qquad (6)$$

Multiplying each member of Eq. (6) by $\sqrt{\frac{\mu_o}{\varepsilon_o}}$ and using Eq. *5* we find that the reflection coefficient for the s wave (r_s) is given by

$$r_s = \frac{n_i\cos\theta_i - n_t\cos\theta_t}{n_i\cos\theta_i + n_t\cos\theta_t} \qquad (7)$$

In previous equations, μ_i and μ_t are the magnetic permeability of the incident and transmitted media respectively. ε_o and μ_o is the electric permittivity and magnetic permeability in the vacuum. It is assumed that $\mu_i = \mu_t = \mu_o$ and $\theta_i = \theta_r$. Note in Eq.*7*, that the relationship $\sqrt{\frac{\varepsilon_i}{\varepsilon_o}} = n_i$ and $\sqrt{\frac{\varepsilon_t}{\varepsilon_o}} = n_t$ were also used, where n_i and n_t are the refractive indices of the incident and transmitted media, respectively.

ii) For the consistent convention system of field vector directions (*c.f. fig.1b*) — *p*-wave.

From boundary conditions and Eq.*4*, one can write that,

$$(E_i + E_r)\cos\theta_i = E_t\cos\theta_t \qquad (8)$$

$$\sqrt{\frac{\varepsilon_i}{\mu_i}}(E_i - E_r) = \sqrt{\frac{\varepsilon_t}{\mu_t}}E_t \qquad (9)$$

Using Eqs (8) and (9), we find that r_p is given by

$$r_p = \frac{n_i\cos\theta_t - n_t\cos\theta_i}{n_t\cos\theta_i + n_i\cos\theta_t} \qquad (10)$$

Using Eqs (7) and (10), one finds that at normal incidence ($\theta_i = \theta_t = 0^o$),

$r_s = r_p\big|_{\theta_i=0}$, which is Eq. (2).

iii) For the inconsistent system of field vector directions (*c.f. fig.2a*) — *s*-wave.

As the system of figure 2a is similar to that of figure 1a, the reflection coefficient for the *s*-wave is given by Eq. (*7*).

iv) For the inconsistent system of field vector directions (*c.f. fig.2b*) — *p*-wave.

Again applying boundary conditions and Eq.*4* for the tangential components of both the ***E*** and ***H*** fields, one may write:

$$(E_i - E_r)\cos\theta_i = E_t\cos\theta_t \qquad (11)$$

$$\sqrt{\frac{\varepsilon_i}{\mu_i}}(E_i + E_r) = \sqrt{\frac{\varepsilon_t}{\mu_t}}E_t \qquad (12)$$

From the two previous equations, it can be shown that r_p is given by:

$$r_p = \frac{n_t\cos\theta_i - n_i\cos\theta_t}{n_t\cos\theta_i + n_i\cos\theta_t} \qquad (13)$$

Thus, using directions for the ***E*** and ***H*** field vectors shown in figure 2, one deduces that

$$r_s = -r_p\big|_{\theta_i=0} \qquad (14)$$

Reflection coefficients r_s and r_p are plotted in figure 3 as a function of the incident angle for both the consistent (*c.f .fig 3a*) and inconsistent (*c.f .fig 3b*) directions which were defined for the field vectors.

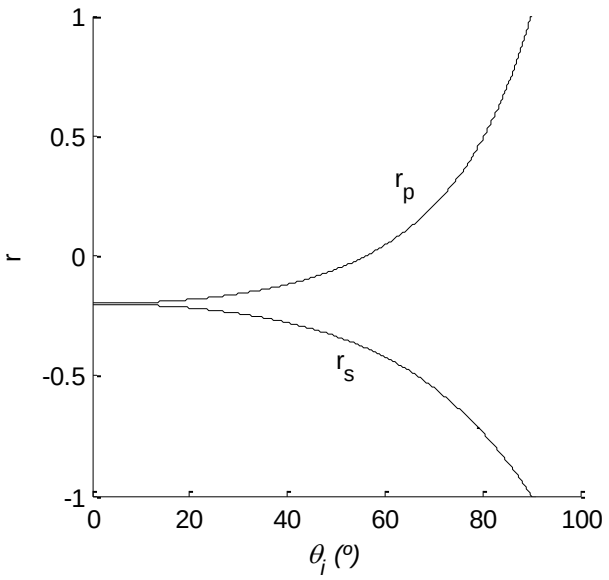

a

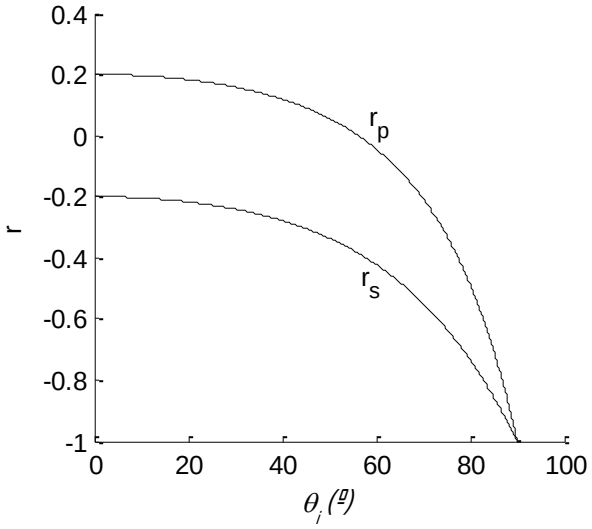

b

Figure 3: Reflection coefficients for each system defined. Data n_i = 1 and n_t = 1.5 were used to produce the plots for r_s and r_p . a) for the convention system shown in figure 1 b) for the convention system shown in figure 2.

3. Conclusion

Results obtained for the case of the inconsistent system are showing that the values for r_p and r_p are reversed at normal incidence. As the *E*-field vectors for both states of polarisation are parallel to the interface at normal incidence, the reflection coefficient are expected to be equal or degenerate at θ_i =0º. This change of sign for r_s and r_p at θ_i =0º (or splitting of degeneracy) does not correspond to a *180º* phase shift, but is rather a consequence of a choice in the direction definition for the electric fields $\boldsymbol{E_i}$ and $\boldsymbol{E_r}$ in figure *2b*. Note that a splitting in degeneracy often occurs in a lack of symmetry in physical systems, but it is not the case for a reflection at normal incidence for both states of polarisation. This sign change merely means that the direction of $\boldsymbol{E_r}$ was assumed incorrectly when treating the *p*-wave in figure *2b*. The same analogy can be made with electric circuits when the wrong direction of current is assumed in a loop when applying Kirchhoff's rules. The previous results do not have any implications on the reflectance *R* at the interface as it is given by the square of the amplitude reflection coefficients *r* for each polarisation.

4. Acknowledgement

This work is supported by the Academic Research Program (ARP) at Royal Military College of Canada. The author would like to thank Dr N. Gauthier for proofreading the manuscript and for his valuable suggestions.

References

[1] F.H. Read, Electromagnetic Radiation (John Wiley & Sons, Manchester physics series,1980), pp. 30-31.

[2] P. Yeh, Optical Waves in layered Media (John Wiley & Sons, N.Y., 1988), pp. 60-65.

[3] P. Lorrain, D. Corson, Electromagnetic fields and waves (W.H. Freeman and

Company, San Francisco, 1970), 2nd ed., pp. 509-515.

[4] J. Ph. Pérez, R. Carles, R. Fleckinger, Electromagnétisme: Vide et milieux matériels avec exercices et problèmes résolus (Masson, Paris, 1991), pp. 518-520.

[5] Dr.M. Fogiel, Editor, Problem Solvers, Electromagnetics (Research & Education

Association, N.J., 1995), pp. 682-683.

[6] H.A. Macleod, Thin-film Optical Fibers, 3rd Ed., Chapter 2, IOP, London, 2001.

[7] J.C. Palais, Fiber Optic Communications, 4th Ed. (Prentice-Hall, N.J.,1998), pp.69-70.

[8] E. Hecht, Optics (Addison-Wesley, Reading, Massachusetts, 1987), 2nd ed., pp. 94-96.

[9] E.C. Jordan, K.G. Balmain, Electromagnetic waves and radiating systems (Prentice-Hall, Englewood Cliffs, N.J., 1968), 2nd ed., pp. 139-147.

[10] J.D. Jackson, Classical Electrodynamics (John Wiley & Sons, N.Y., 1999), 3rd ed., pp. 305-306.

[11] M.Born, E. Wolf, Principles of Optics; Electromagnetic theory of propagation

interference and diffraction of light (Pergamon, N.Y., 1970), 4th ed., pp. 38-40.

[12] J. Vanderlinde, Classical Electromagnetic Theory (John Wiley & Sons, N.Y.,1993), pp. 212-215.

[13] F.L. Pedrotti, L.S. Pedrotti, Introduction to Optics, 2nd Ed. (Prentice-Hall, N.J., 1993), pp. 408-410.

[14] H.G. Tompkins, A User's Guide to Ellipsometry, Academic Press, Inc., pp. 16-17.

[15] A. Rahman, Z.Zaghloul and M.S.A. Yousef, Unified analysis and mathematical representation of film-thickness behavior of film-substrate systems, Appl. Opt. 45, 235-264, 2006.

An Indirect Analytical Method for Finding the Magnetic Field at any Point on the Azimuthal Plane of a Conducting Loop : A Filamentary Model Approach

Suman Aich[1,2] and Joydeep Ghosh[1,2]

[1]Institute for Plasma Research, Gandhinagar, Gujarat - 382428, India.
[2]Homi Bhabha National Institute, Anushaktinagar, Mumbai, Maharashtra - 400094, India.
suman.aich@ipr.res.in

Submitted on 13-07-2018

Abstract

Tokamak plasma characterisation is strongly correlated with the analysis of magnetic fields due to currents flowing in circular coils as well as in the plasma which forms a circular loop inside a toroidal chamber. The theoretical estimation of off-central magnetic induction on the azimuthal plane for a circular current carrying filamentary loop from Biot-Savart law comes up with a form that includes integral solution in terms of elliptic integrals, which requires numerical attempts for estimation. Here, we start from a result, obtained as a consequence of Biot-Savart law for a filamentary straight wire, and follow an approach for finding the same at any location on the plane of the circular conducting loop and end up with some interesting and useful outcomes, which avoid the computational attempts for evaluation of elliptic integrals.

1 Introduction

The tokamak is the most advanced concept for the realisation of controlled thermonuclear fusion towards energy production. In a tokamak, the plasma is confined in a toroidal chamber using magnetic fields and heated up to very high temperatures ($> 10^8$ K) in order to achieve fusion reactions to take place [1]. The magnetic fields are generated using electromagnets made up of conventional as well as superconductors. Several inherent forces, originating due to the toroidal geometry of the current carrying plasma column in a tokamak, lead to horizontal and vertical movements

of the plasma column. These movements of the current carrying plasma column are arrested by application of suitable magnetic fields in appropriate configuration. As the movement of plasma column depends on several dynamic parameters of the plasma, the magnitude of the controlling magnetic fields are required to be adjusted in real time during the plasma discharge. This requires fast and accurate measurements of the position of plasma column in a tokamak. One of the most common and widely used diagnostic of plasma column position in tokamaks is the magnetic pick up loops [2]. These pick up loops are placed around the poloidal periphery of the current carrying plasma column. The variations in the poloidal and radial magnetic fields due to the movement of current carrying plasma column are picked-up by these coils, which can be used to estimate the position of the column. Although the construction and installation of these pick-up probes are simple and the analysis for estimating the column position is straightforward, the accuracy of the plasma column position estimation strongly depends on the in-situ calibration of these probes.

It is quite well known that the poloidal magnetic field due to a toroidal current carrying plasma column varies along the poloidal periphery of the column at one toroidal location. The situation is schematically shown in Fig 1. It can be seen from the figure that even if the toroidal plasma column, without considering the Shafranov Shift [1, 3], sits perfectly at the center of two probes placed on poloidal periphery at the horizontal mid-plane, one on the inner circle of the torus and another on the outside of the torus, the inner probe is linked with more magnetic field lines than that placed on the outside of the torus. To calibrate these pick-up probes in ADITYA-U tokamak, a time-varying-current carrying conductor has been placed at the major axis of the torus and the poloidal magnetic field due to this current carrying conductor picked up by the probes placed in the inside ($R_0 - a$, where R_0 is the major axis and a is the distance of the probes from the R_0) and outside ($R + a$) has been measured.

To validate the measurements, the values of magnetic fields picked up by these two probes are calculated. The values of the poloidal magnetic fields around the poloidal periphery of a toroidal current carrying conductor can be estimated from the first principle, i.e., the Biot Savart law and it is quite well known [4]. However, using Biot Savart law to estimate the above mentioned magnetic fields involves elliptic integrals to be evaluated [5, 6]. The elliptical integrals are not very straightforward and have to be solved numerically to obtain the magnetic field values. In this paper, we propose an indirect, although simpler method to determine the magnetic field values at any location on the azimuthal plane of a toroidal current carrying conductor at one toroidal location. The simplified expression is much useful as well as very handy for the quick es-

timation of the above mentioned magnetic field values.

This paper is arranged as follows. After reviewing the well-known results in section II, we discuss thoroughly the proposed approach in section III. We then, justify the reliability of this approach and conclude how these results are satisfactory for a broad range of radial distance from the centre of the circular conductor, along with its limitations in section IV. Finally we summarize the important outcomes in section V.

2 Earlier Results involving Elliptical Integrals

If a circular filamentary conductor 'C', as shown in Fig 1, of radius 'a' carrying current 'I' follows a cylindrical coordinate system (r, ϕ, z) with its centre coinciding with the origin and its axis to be in z direction, the radial and vertical components of magnetic induction i.e., B_r and B_z, in the (r, z) plane are given by [5, 6]:

$$B_r = \frac{\mu_0 I}{2\pi} \frac{(z/r)}{\sqrt{(a+r)^2+z^2}} \Big(-K + \frac{a^2+r^2+z^2}{(a-r)^2+z^2} E \Big) \tag{1}$$

and

$$B_z = \frac{\mu_0 I}{2\pi} \frac{1}{\sqrt{(a+r)^2+z^2}} \Big(K + \frac{a^2-r^2-z^2}{(a-r)^2+z^2} E \Big), \tag{2}$$

where K and E are complete elliptic integrals of first and second kind, respectively, and defined by:

$$K(k) = \int_0^{\pi/2} \frac{d\theta}{\sqrt{1-k^2 sin^2\theta}},$$

$$E(k) = \int_0^{\pi/2} \sqrt{1-k^2 sin^2\theta}\, d\theta,$$

with $k = \sqrt{4ar/[(a+r)^2+z^2]}$.

The results obtained by this formulation are taken as the actual theoretical estimation of magnetic induction value and the values obtained from the proposed scheme is compared with the values obtained from the above mentioned formalism. It is to be noted here that we are interested in calculating the magnetic field values mainly at the probe positions, as shown in Fig 1, i.e. on the plane of the circular conducting coil. The total magnetic field at these locations has z-component only, i.e. $B = B_z$.

3 A Theoretical Approach Towards Simplified Consequences : A Filamentary Conductor Model

3.1 Derivation of magnetic field at a radial location, smaller than the conductor radius (inside the circumference of the loop)

In order to find the magnetic field due to a circular current (I) carrying filamentary conductor of radius R_0 at any arbitrary point, say E, in the plane of the conductor, within the circumference, let us imagine the conductor to be composed of infinitesimally small straight filamentary segments, which

are the parts of different infinite straight current (I) carrying conductors, as shown in Fig 2(a). One of the infinitesimal segments is shown by $\overrightarrow{dl}$ at A along with the dashed line, indicating the infinite straight conductor the part of which it is, schematically in Fig 2(b). Moreover, let the normal distance of E from the infinite straight conductor be 'd' (ED) and the nearest point (C) on the circular conductor is c unit apart from E. The angles $\angle AOC$ and $\angle AED$ are indicated by α and β respectively, as shown in Fig 2(b), O being the geometrical centre of the circular conductor.

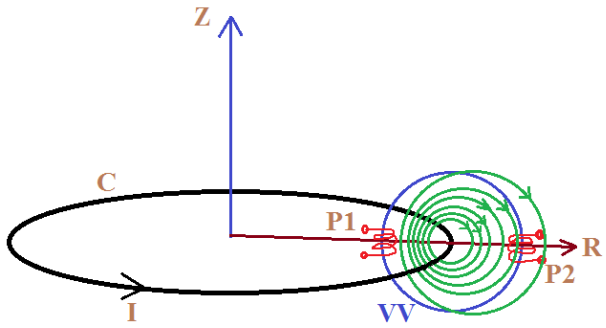

Figure 1: A circular conductor (C) within vacuum vessel (VV) carries current I and generates magnetic field profile, which is tried to show schematically by few magnetic field lines (green) in the vicinity of VV. P1 and P2 represent two magnetic probes, attached with VV, at inboard and outboard sides respectively. Z and R denote the vertical axis and horizontal radial axis of the tokamak respectively. (colored online)

If two end points of $\overrightarrow{dl}$ make angles β_1 and β_2 with DE as shown in Fig 3, the magnetic field, produced by $\overrightarrow{dl}$ due to I at E can be calculated using Biot Savart law and the

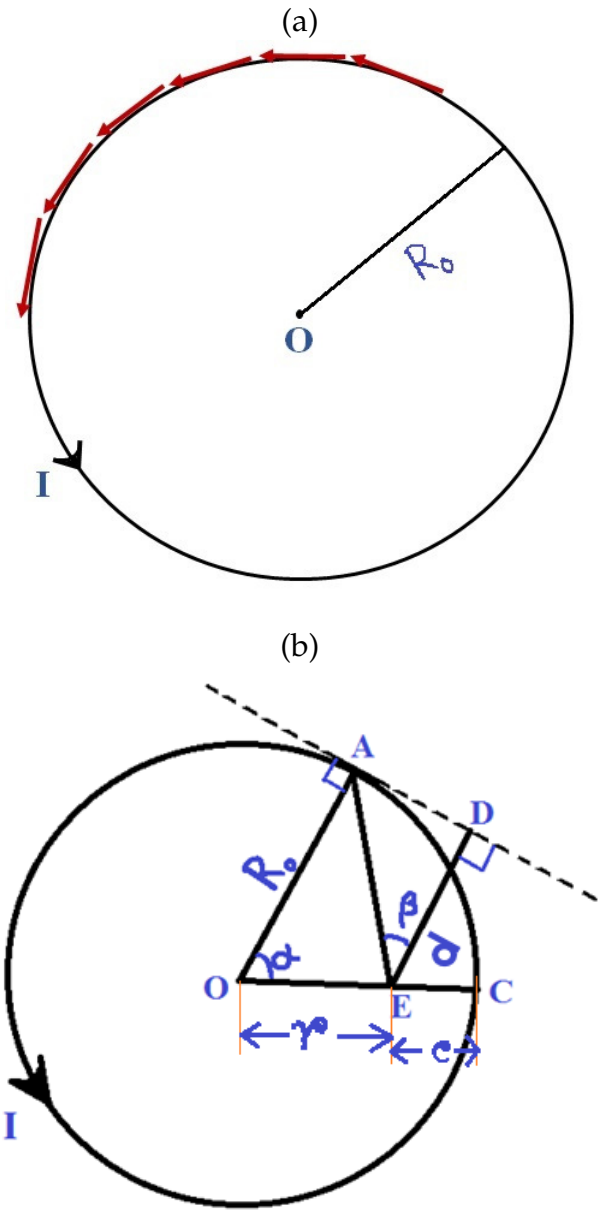

Figure 2: (a) A circular current carrying conductor (carrying I), of radius R_0 can be imagined to be composed of infinite number of current elements, as few of them shown schematically in red. (b) The circular conductor carrying current I and E is the field point where magnetic field needs to be estimated for the whole assembly. (colored online)

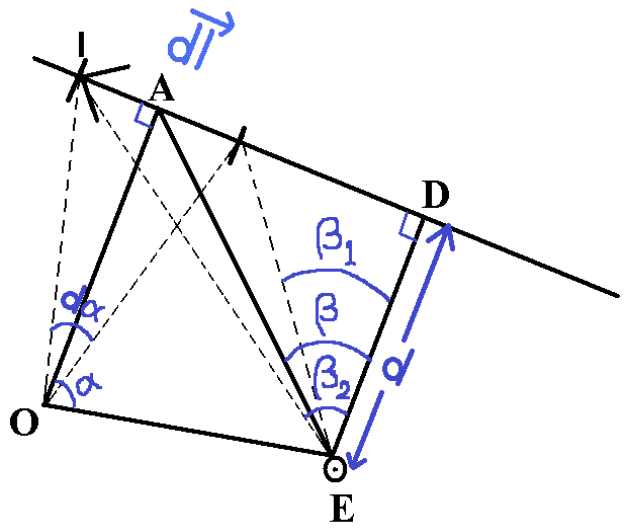

Figure 3: The current element, which is a part of an infinite current carrying conductor with current I, makes different angles at the centre O and object point E. (colored online)

simplified final expression comes up with the form [4]:

$$\triangle B = \frac{\mu_0 I}{4\pi d}(sin\beta_2 - sin\beta_1) \tag{3}$$

and from the geometry we can easily correlate d with α as:

$$d = 2R_0 sin^2(\frac{\alpha}{2}) + ccos\alpha. \tag{4}$$

Eq 3 can be simplified in the limit $\overrightarrow{dl} \to 0$ for which we can approximately write, $\beta_2 - \beta_1 = d\beta \to 0$, $d\alpha \to 0$, and hence $d\beta \simeq d\alpha$, $sin(\frac{d\alpha}{2}) \simeq \frac{d\alpha}{2}$, and $\beta_2 + \beta_1 = 2\beta$, where $d\alpha$ is the angle subtended by the two end points of $\overrightarrow{dl}$ at the centre O, as shown in Fig 3. So, Eq 3 simplifies as:

$$\triangle B = \frac{\mu_0 I}{4\pi d}.cos\beta.d\alpha. \tag{5}$$

In order to achieve a more simplified form of Eq 5 that will be a function of α only, we need to find the relation between β and α. Avoiding the complications of geometry we may find a subtle way to do so if we observe that at $\alpha = 90^0$, β is maximum and so one of the simplest ways we may express β in terms of α is $cos\beta = b_1 + a_1 sin\alpha$, where a_1 and b_1 are arbitrary constants. As at $\alpha = 0$, $\beta = 0$ and at $\alpha = 90^0$, $\beta = cos^{-1}\Big(\frac{R_0}{\sqrt{R_0^2+(R_0-c)^2}}\Big)$, we have $b_1 = 1$ and $a_1 = \Big[\Big(\frac{R_0}{\sqrt{R_0^2+(R_0-c)^2}}\Big) - 1\Big]$. Thus, Eq 5 reduces to

$$\triangle B = \frac{\mu_0 I}{4\pi d}(1 + a_1 sin\alpha)d\alpha. \tag{6}$$

To get the resultant magnetic field at E, we need to integrate the contributions from all such infinitesimal segments $\overrightarrow{dl}$ composing the entire conductor and so the total magnetic field at E can be found by integrating their individual's contributions, i. e.,

$$B_E = \frac{\mu_0 I}{4\pi}\int_0^{2\pi}\frac{d\alpha}{d} + \frac{\mu_0 I a_1}{4\pi}\int_0^{2\pi}\frac{sin\alpha d\alpha}{d},$$

or,

$$B_E = I_1 + I_2, \tag{7}$$

where $I_1 = \frac{\mu_0 I}{4\pi}\int_0^{2\pi}\frac{d\alpha}{d}$ and $I_2 = \frac{\mu_0 I a_1}{4\pi}\int_0^{2\pi}\frac{sin\alpha d\alpha}{d}$. By rigorous calculations we are left with

$$I_1 = \frac{\mu_0 I}{2\sqrt{c(2R_0 - c)}}, \tag{8}$$

$$I_2 = G'\Big[\frac{1}{\sqrt{1+(1-c/R_0)^2}} - 1\Big], \tag{9}$$

where $G' = \frac{\mu_0 I}{2\pi(R_0-c)} ln\left|1+2\left(\frac{R_0-c}{c}\right)\right|$.

Now, in the both limits of c i.e., $c \to R_0$ (near centre) and $R_0 \gg c$ (near circumference), we have $I_2 \to 0$. Moreover at $c = R_0/2$, I_2 has contribution of 6% in the total magnetic field. Thus, a crude way of writing the resultant magnetic field within the circumference is to take only the contribution from I_1 :

$$B_E \simeq \frac{\mu_0 I}{2\sqrt{c(2R_0-c)}}$$

or,

$$B'_{IN}(r) = \frac{\mu_0 I}{2\sqrt{R_0^2-r^2}}, \qquad (10)$$

where $r = R_0 - c$. The error, introduced by ignoring I_2, is taken care of by finding a proper correction factor and is discussed later.

3.2 Derivation of magnetic field at a radial location, greater than the conductor radius (outside the circumference of the loop)

The conservation of magnetic flux gives a clue for finding the planar (azimuthal) magnetic field outside the circumference of circular conductor. Let us consider a concentric annular region of radius r_{in} and width dr_{in} on the plane of the conductor inside its circumference ($r_{in} < R_0$). The magnetic field lines, which pass through the annular area $2\pi r_{in} dr_{in}$, come through another coplanner annular region of radius, say, r_{out} and width dr_{out}, outside the circular conductor. Due to conservation of magnetic flux, the flux through inner annular region, $d\phi_{in}$, must equal to that through outer annular region, i.e., $d\phi_{out}$ and so :

$$d\phi_{in} = d\phi_{out}$$

or,

$$2\pi r_{in} dr_{in} B(r_{in}) = 2\pi r_{out} dr_{out} B(r_{out}), \quad (11)$$

where B is the average magnetic induction value on the corresponding annular regions. Before we proceed further let us look into the fact that, as $r_{in} \to R_0$, $r_{out} \to R_0$ and when $r_{in} \ll R_0$ we have $r_{out} \to \infty$. These facts can be used to relate r_{in} with r_{out} and one of the simplest way is to take

$$r_{in} r_{out} \approx R_0^2 \qquad (12)$$

and hence

$$dr_{in} = -\left(\frac{R_0^2}{r_{out}^2}\right) dr_{out}.$$

With the help of these, Eq 11 reduces to

$$B(r_{out}) = -\left(\frac{R_0}{r_{out}}\right)^4 B(r_{in}). \qquad (13)$$

In the vicinity of the circular conductor, both inside and outside of circumference of the conductor, a more simplified and handy formula for $B(r_{out})$ can be derived using Eq 13. If $r_{out} = R_0 + c$ and $c \ll R_0$, we may write $r_{in} = R_0 - c$ and hence,

$$B(R_0+c) = -\left(\frac{R_0}{r_{out}}\right)^4 B(R_0-c), c \ll R_0. \qquad (14)$$

In order to check the accuracy of this formalism, we compare the ratio of the magnetic fields at r_{in} and r_{out} as calculated using Eq 14 in the vicinity of the conductor circumference with that obtained by the elliptical formulation of magnetic field i.e., Eq 2. For a circular filamentary conductor of radius $R_0 = 75$ cm carrying 1 kA of current, the maximum difference between both the formulations is of order of 9% for $c = 27$ cm, which seems to be due to the simplifications introduced in Eq 12. To overcome this discrepancy and to reduce the error, Eq. 14 is modified as

$$B(R_0 + c) = -\left(\frac{R_0}{R_0 + c}\right)^{4.3} B(R_0 - c), c \ll R_0. \quad (15)$$

The magnetic field values from two different formulations, i.e., from elliptic integral approach and from the proposed approach are compared in Table 1, which shows the ratios of $\left|\frac{B(R_0-c)}{B(R_0+c)}\right|$ for a circular filamentary conductor of radius $R_0 = 75$ cm carrying 1 kA of current. The improvement in Eq 15 from Eq 14 drops the inaccuracy in the percentage error from 9% to less than 0.1% in case of a circular filamentary conductor of radius $R_0 = 75$ cm carrying 1 kA of current at $c = 27$ cm and is also compared for different values of c in Table 1. Eq 15 is further verified for other values of R_0 and satisfactory results are obtained as discussed in the next section. It is to be emphasized here that, for $r \geq 2R_0$, Eq 15 can never be used, though sufficient error comes even at a distance shorter than $2R_0$.

Ratio of magnetic induction values for a circular filamentary conductor of radius $R_0 = 75$ cm carrying 1 kA of current. Here, B_i and B_o correspond to $B(r_{in})$ and $B(r_{out})$ respectively, and $|B_i/B_o|_{ell}$ stands for the ratio as obtained using elliptic formulation.

c in cm	$\lvert B_i/B_o\rvert_{ell}$	$\lvert B_i/B_o\rvert$ using Eq 14	$\lvert B_i/B_o\rvert$ using Eq 15
10	1.82	1.65	1.71
15	2.29	2.07	2.19
25	3.47	3.16	3.45
35	5.11	4.63	5.19

4 Correction in the Formulation

The approximations as well as the simplifications, used in the proposed indirect derivation of the magnetic fields at two radial locations, inside and outside of the circular conductor circumference at the horizontal mid-plane, lead to significant errors in magnetic field values, obtained from Eq 10 and Eq 14 as compared to those obtained from Eq 2. One of the major simplifications that is taken into account towards deriving

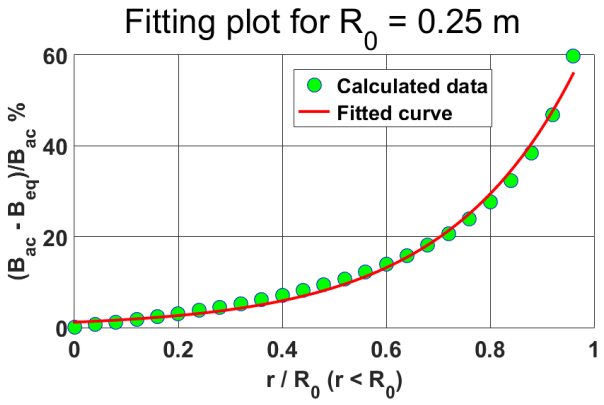

Figure 4: Plot of percentage error in $B_{eq}(r < R_0)$, found using Eq 10, with relative distance from centre of coil, x for $R_0 = 25$ cm as indicated by points. The solid line is the fitted curve following $a'e^{b'x}$ with $a' = 1.1860$, $b' = 4.014$. (colored online)

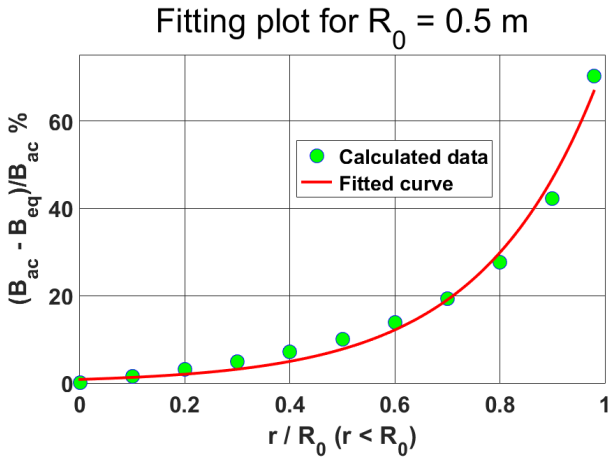

Figure 5: Plot of percentage error in $B_{eq}(r < R_0)$, found using Eq 10, with relative distance from centre of coil, x for $R_0 = 50$ cm as indicated by points. The solid line is the fitted curve following $a'e^{b'x}$ with $a' = 0.8202$, $b' = 4.494$. (colored online)

Eq 10 is corelating α and β through the relation $cos\beta = b_1 + a_1 sin\alpha$, which is explained in section 3.1 . Due to this a maximum error $\sim \pm 8 - 10\%$ occurred in the estimation of $cos\beta$ for a given α and this has the major contribution in the inaccuracy in estimated B'_{IN} that reaches upto 50% as we come at the vicinity of R_0. The details are discussed in the following sections. Further in case of magnetic field values at r_{out} obtained using Eq 15, an approximated relation defined in Eq 12 is taken into account. As described in section 4.2, the error due to assumption defined in Eq 12 is very small in the vicinity of the conductor, however, it drastically increases as one moves away from the conductor. To quantify the error in both the cases (at r_{in}, r_{out}), we define fractional error $(g) = (B_{ac} - B_{eq})/B_{ac}$, where B_{ac} and B_{eq} are magnetic flux densities calculated using Eq 2, and Eq 10 and 15 respectively. The correction in the formalism for removal of these errors are described in the following sub-sections.

4.1 For magnetic field at $r < R_0$

In the case of $r < R_0$, the percentage error is obtained for magnetic fields calculated at different normalized radial positions ($x = r/R_0$) and are shown in Fig 4 to 7. Interestingly, this percentage error g can be well-fitted using an exponential function of the form

$$g \times 100 = a'e^{b'x},$$

where a' and b' are arbitrary constants and can be found from chi-square fitting of the data. Table 2 enlists few of the a' and b'

values for different R_0 . Towards correcting Eq 10, we can proceed with the averaged a' and b' values that are $a = \langle a^{'} \rangle \sim 0.88885$ and $b = \langle b^{'} \rangle \sim 4.4095$, respectively.

Therefore, we may write

$$\frac{B_{ac} - B_{eq}}{B_{ac}} \times 100 = a e^{b\left(\frac{r}{R_0}\right)}. \qquad (16)$$

Finally, the corrected expression of magnetic induction at $r < R_0$ can be given by :

$$B_{ac}(r < R_0) = \frac{B_{eq}(r)}{1 - \left(\frac{a}{100}\right) e^{b(r/R_0)}}, \qquad (17)$$

where $B_{eq} = B^{'}_{IN}$, given by Eq 10.

Here we end up with the approximated formula that is justified to estimate the magnetic field at $r < R_0$ for the circular coil of randomly chosen radii and for few of the R_0 values we have the percentage error not exceeding 10%, as shown in Fig 9 and 10. Although we have restricted our choice to few randomly chosen radii, the similar procedure can be followed for other ranges of R_0 to have appropriate values of a and b. In this way, a huge numerical effort can easily be by-passed.

Fitting parameters, as obtained from Fig 5 to 8, due to the plots of $g \times 100$ vs. x.

R_0 in cm	a'	b'
25	1.1860	4.014
50	0.8202	4.494
75	0.7804	4.556
100	0.7688	4.574

4.2 For magnetic field at $2R_0 > r > R_0$

The error introduced in the values of B outside the circular conductor ($r > R_0$) is mainly due to the assumption made in Eq 12. To quantify the error, for a given r_{in}, r_{out} is found with the help of POISSON code [7, 8]. r_{out} from POISSON is estimated by following different magnetic field lines passing through r_{in} and r_{out}. The normalised error in r_{out}, calculated using

$$\delta r_{out} = (r^{ac}_{out} - r^{12}_{out})/r^{ac}_{out}$$

for a circular conductor of radius $R_0 = 77$ cm, is shown in Fig 8, where r^{12}_{out} is found using Eq 12, r^{ac}_{out} is found from POISSON. It can be clearly seen from the figure that although the relative difference is very small ($\sim 2.44\%$) in the vicinity of the conductor, it rises and reaches up to $\sim 25\%$ at $r_{out} \sim 2R_0$. The similar plots are obtained for a number circular conductors with different R_0 and the nature of the error is found to follow the similar trend both in magnitude and posi-

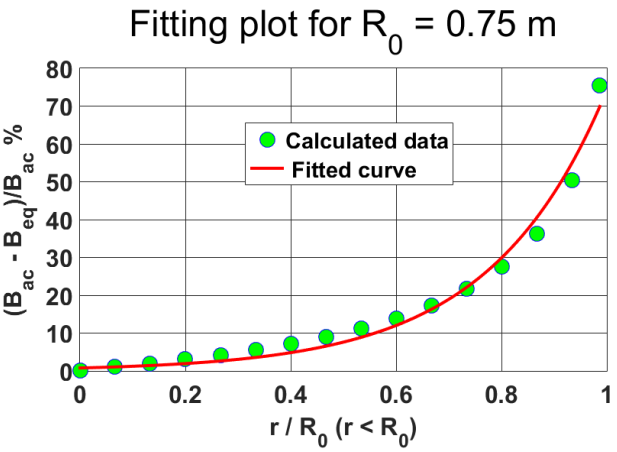

Figure 6: Plot of percentage error in $B_{eq}(r < R_0)$, found using Eq 10, with relative distance from centre of coil, x for $R_0 = 75$ cm as indicated by points. The solid line is the fitted curve following $a'e^{b'x}$ with $a' = 0.7804$, $b' = 4.556$. (colored online)

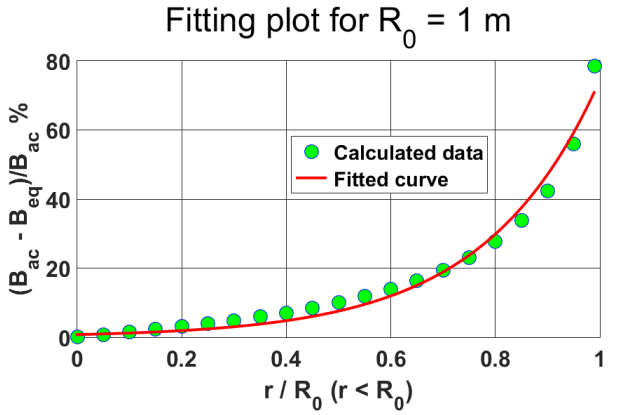

Figure 7: Plot of percentage error in $B_{eq}(r < R_0)$, found using Eq 10, with relative distance from centre of coil, x for $R_0 = 100$ cm as indicated by points. The solid line is the fitted curve following $a'e^{b'x}$ with $a' = 0.7688$, $b' = 4.574$. (colored online)

tional variation. This leads to a percentage error in B_{out} with relative distance from the coil centre i.e., $x = r/R_0$ as shown in Fig 9

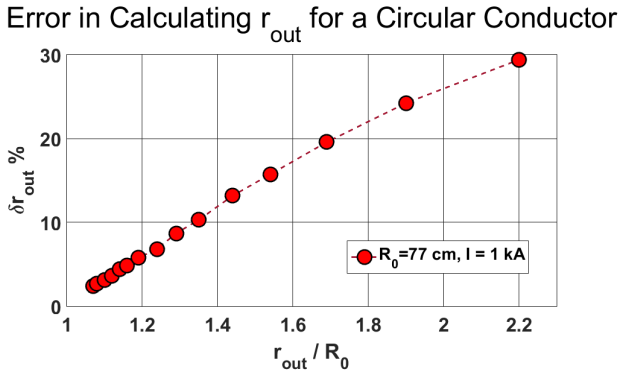

Figure 8: The variation of relative error in finding r_{out}, using Eq 12, with relative distance r_{out}/R_0 for a given circular conductor and given r_{in}. (colored online)

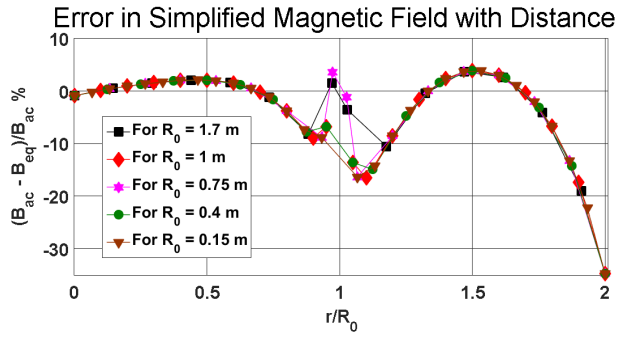

Figure 9: Plot of percentage error in B_{eq}, found using Eq 15 and 17, with relative distance x for five arbitrary circular coil radii, as provided in the legend box. (colored online)

for few arbitrary values of R_0 as indicated in the legend box. The error in B is found to be in the range of $\sim 4\%$ to -17%, in which the major contribution comes from the maximum error 25% in r_{out} in the vicinity of $2R_0$, up to a relative distance $r/R_0 = 1.88$, beyond of which this error grows significantly. Also, the graphs show a good overlap of plots for different R_0 in the range of x from 0.0 to 0.9 (inside the circumference)

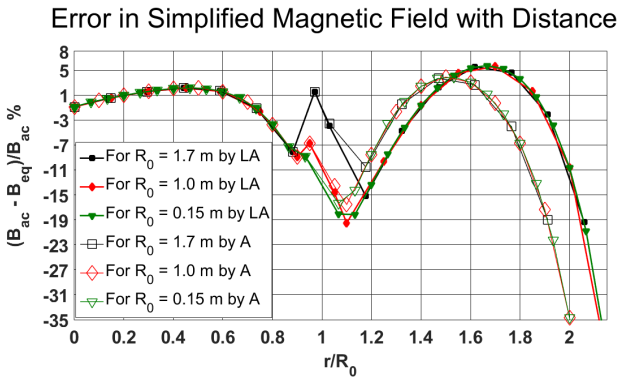

Figure 10: Plot of percentage error in B_{eq}, found using approximated Eq 15, 17 as indicated by A and using less approximated scenario in Eq 17, 18 as indicated by LA, with relative distance x for three arbitrary circular coil radii, provided in the legend box. (colored online)

and from 1.1 to 1.88 proving the universality of this formulation. Now, as we approach from $r = R_0$ to $r = 2R_0$, $c(= r - R_0)$ is no longer small i.e., $c \ll R_0$ no longer holds and so Eq 15 needs to be rectified as r approaches to $2R_0$. By chi-square fitting, as before, we find the modfied form of Eq 15 to be

$$B(r_{out}) = -(R_0/r_{out})^{4.9} B(r_{in}),$$

or,

$$B(r_{out}) = -(R_0/r_{out})^{4.9} B(R_0^2/r_{out}). \quad (18)$$

Fig 10 compares the results obtained from Eq 15 and 18, where the percentage error in B is obtained by Eq 17 for $r < R_0$ and by Eq 15 and 18 for $r > R_0$. The results are plotted with respect to relative distance x for three arbitrary coil radii covering a wide range of coil radii, as indicated in the legend box. The approximated formula as given by Eq 15 is indicated by **A** whereas, a less approximated formulation given by Eq 18 is described by **LA** in the figure. As per our expectation, a more accurate result is found using Eq 18 in the vicinity of $r = 2R_0$ and we can find a value of $x = r/R_0$ to be 1.765 from the plots, above which Eq 18 gives a better estimate and below to that, Eq 15 shall be taken into account for the calculations in the regime $r > R_0$.

5 Summary and Discussions

We can summarize the outcomes for the magnetic field on the azimuthal plane of a current carrying loop at a radial distance r as follows :

$$B_{IN}(r) = \frac{B'_{IN}(r)}{1 - \left(\frac{a}{100}\right) e^{b(r/R_0)}}, r < R_0,$$

$$B_{OUT}(r = R_0 + c) = -\left(\frac{R_0}{R_0 + c}\right)^{4.3} B_{IN}(R_0 - c),$$

for

$$R_0 < r \leq 1.765 R_0,$$

$$B_{OUT}(r) = -(R_0/r)^{4.9} B_{IN}(R_0^2/r),$$

for

$$r > 1.765 R_0,$$

where

$$B'_{IN}(r < R_0) = \frac{\mu_0 I}{2\sqrt{R_0^2 - r^2}},$$

$a \sim 0.88885$, $b \sim 4.4095$, and other symbols have their usual meanings.

It is very interesting to achieve the well-known expression for the central magnetic induction if we simply put $r = 0$ in the expression of B_{IN} as, then the limiting value goes as : $\left[1 - \left(\frac{a}{100}\right)\right] \rightarrow 1$. Due a drastic increase in the percentage error in B_{OUT} beyond $2R_0$, this method is never suggested to use in this limit of r.

In case of upgraded ADITYA tokamak (major radius, R = 75 cm), we needed the in-board to outboard ratio of magnetic induction at the location of Mirnov probes, for which the experimental values of this ratio was still unavailable, to find the positional shifts of plasma column and as the probe is at 27 cm apart from the centre of vacuum vessel, the corresponding ratio came up to be 3.42 using Eq 14. This helped to choose an appropriate value of the ratio from 3.1 and 3.7, found using POISSON [7, 8] and elliptic formulations, respectively, and finally achieved the temporal variation of plasma shifts in horizontal direction satisfactorily. Later on, these values experimentally are found to be 2.53 and 2.86 for two different Mirnov garlands, installed in ADITYA-U, and this discrepancy in the magnitude is found to come due to some other suspected source, induced in the nearby conducting structures.

As our analysis follows a general approach towards the estimations and is verified for the accuracy in case of a broad range of radii values of the circular coils, we conclude these results to be useful enough within the specified radial distance for quick and easy estimation of magnetic fields in the azimuthal plane of circular loop current-carrying conductor, as it does not require any numerical calculation.

References

[1] J. Wesson. Tokamaks, (Oxford, 1997)

[2] I. H. Hutchinson. Principles of Plasma Diagnostics, (Cambridge University Press, 1987)

[3] V. D. Shafranov (1960). JETP (No. 4) 10, 775

[4] D. J. Griffiths. Introduction to Electrodynamics, (Prentice Hall of India Pvt. Ltd., 1991)

[5] A Method for Measuring Plasma Position in TJ-I Tokamak, J. Qin and TJ-I Team, Asociacion Euratom/Ciemat-Fusion, 28040 Madrid, Spain.

[6] W. Feneberg, K. Lackner, P. Martin (1984). Computer Physics Communications 31, 143-148

[7] Los Alamos Accelerator Code Group (1987). Reference Manual for the Poisson/Superfish Group of Codes, New Mexico: Los Alamos National Laboratory LA-UR-87-126

[8] Los Alamos Accelerator Code Group (1987). Users Guide for the Poisson/Superfish Group of Codes, New Mexico: Los Alamos National Laboratory LA-UR-87-115

Relativistic Rocket, Its Equation of Motion and Solution for two Special Cases

Somnath Datta

Professor of Physics (Retired),
National Council of Educational Research and Training,
New Delhi-110016
Res: 656, "Snehalata", 13th Main, 4th Stage,T K Layout,
Mysore 570009, India
datta.som@gmail.com;
http://sites.google.com/site/physicsforpleasure

Submitted on 21-10-2018

Abstract

This article adopts 4-dimensional Minkowski formalism to obtain the equation of motion of a relativistic rocket, i.e., a vehicle in which the exhaust particles are ejected with a fixed relativistic velocity u opposite the direction of the motion of the rocket, which is taken to be the x direction. We obtained the equation of motion in the instantaneous rest frame of the rocket, labeled as S_o, and then converted this equation of motion into the ground frame S. As a prerequisite to this derivation we also reviewed the mass equation of the rocket, i.e., the relationship between the instantaneous rest mass M of the rocket and its velocity v. We subjected both equations, i.e., the mass equation and the equation of motion to the N.R. test, i.e., the requirement that the forms they assume when $v \ll c$ (where c is the velocity of light) converge to their Non Relativistic counterparts. We obtained the solution of the equation of motion in two special cases, namely (i) $u = c/3$, and (ii) $u = c$, and made a plot of the $v - t$ relationship for both cases. It is seen that the $v - t$ plot for the case (i) nearly follows the corresponding N.R. counterpart, i.e., $u \ll c$, up to $v \simeq 0.5c$.

1 Relativistic Rocket

A relativistic rocket, in principle and for all theoretical calculations, is the same familiar rocket the students have studied in their mechanics books[1, 2], with the difference that the exhaust gas is ejected with a "relativistic speed" u and, as a consequence, the

rocket accelerates to a relativistic speed in due time. What we call relativistic speed is roughly the range: $c/3 \lessapprox u \leqq c$, where c is the speed of light. Because of the relativistic velocities involved in this case Newtonian mechanics breaks down, and we have to use Minkowskian mechanics, in particular Minkowskian equation of motion.

A relativistic rocket, i.e., a space-ship propelled by ejected gas to a relativistic speed is hardly a reality. However, one can still think of matter-antimatter annihilation rockets, pion rockets, for intellectual entertainment[3]. The impracticability of operating such contrivances has been illustrated through actual calculations by some authors[4, 5], using the example of a *photon rocket* (i.e., a spaceship propelled by a beam of photons.) Even then the purpose behind our spending time on such an object is somewhat pedagogical. The exercises we are going to undertake are intended to sharpen ones understanding of Minkowskian Equations of Motion, employing 4-vectors.

The mass equation we have derived for a relativistic rocket (see Eq. 28), and the momentum-energy conservation principles used to arrive at it have been covered by several authors[6, 7, 8, 9]. Pomeranz wrote several papers on this subject[10, 11, 12]. We have written the Equation of Motion (EoM) for the rocket in two equivalent forms as Eqs.(46) and (47). The second form agrees with the 1969 paper (but not with the 1964 paper) of Pomeranz.

Some features of this article that may kindle a special interest in a student or a teacher of special relativity are the following.

1. We have subjected the two important equations derived in this article, namely, (a) the mass velocity equation (28), often referred to as the Ackeret equation[6], and (b) the EoM (49) to the *N.R. Test*, by which we mean that all relativistic equations that have a Non-Relativistic (N.R.) analog must converge to their N.R. counterparts when $v \ll c$.

2. Taking u as the ejection velocity of the emitted gas/radiation, we have obtained two special solutions of the EoM, corresponding to (i) $u = c/3$, and (ii) $u = c$. We have plotted the velocity-time relation for both the cases, and shown that the plot for the case (i) closely follows the the plot for the corresponding formula for $v = v(t)$ obtained using N.R. (Newtonian) mechanics, up to $v \simeq 0.5c$.

3. We have adopted a 4-dimensional Minkowskian approach to obtain the EoM of the rocket, using 4-vectors, e.g., 4-velocity, 4-momentum, 4-acceleration, 4-force. For this purpose we have adopted a mathematical formalism as outlined by Moller[13].

In a recent article Bruce[14] has demonstrated convergence of the Ackeret equation (28) to its N.R. counterpart Tsiolkovsky

equation[15] (1b), by writing the mass ratio as a product of an infinite series, and obtaining the result using a finite number of terms. In contrast we have demonstrated exact convergence of both the Ackeret equation and the EoM to their N.R. counterparts when $\beta \ll 1$.

2 Symbols and Conventions

All 4-vectors will be presented by a bold letter with a full arrow overhead. While writing its components, the *time component*, i.e., the t-component, will come first, to be followed by its *space components* in the x, y, z directions. For example, if $\overrightarrow{\mathbf{A}}$ is a 4-vector, we shall express it as $\overrightarrow{\mathbf{A}} = (A^t, A^x, A^y, A^z) = (A^0, \mathbf{A})$, where $\mathbf{A} = (A^x, A^y, A^z)$ constitutes a 3-vector. Since the motion of the rocket will be only one-dimensional, confined to the x-direction, the y, z components will be absent. The same 4-vector $\overrightarrow{\mathbf{A}}$ will have only t and x components, i.e., $\overrightarrow{\mathbf{A}} = (A^t, A^x)$.

The "ground frame" of reference, from which the motion of the rocket is observed will be denoted as S. The instantaneous rest frame (IRF) will be denoted by S_o.

Time and space components of a typical 4-vector $\overrightarrow{\mathbf{A}}$, corresponding to motion in the x-direction, will be written as (A^t, A^x) with respect to S, and as (A'^t, A'^x) with respect to S_o. Note the prime tag " $'$ " attached to the IRF S_o.

3 The Rocket, its Specifications

Let us now take a look at the rocket of our discussion. It is moving along the x-axis with velocity $\mathrm{v(t)}$ m/s with respect to an inertial frame S, which, for fixing the idea, we shall call the *Ground Frame* (GF). It is ejecting gas at a constant velocity $-u$ m/s and its *rest mass* at a constant rate $r = \frac{d\mu_0}{d\tau}$ kg/s, relative to its *Instantaneous Rest Frame* (IRF) $S_o(\Theta)$, thereby generating a Reaction force (in this case a Thrust force) $\overrightarrow{\boldsymbol{\mathcal{R}}}$. Our purpose is to find a formula for $\overrightarrow{\boldsymbol{\mathcal{R}}}$, and then the Equation of Motion (EoM), and then a solution of this EoM for two representative cases.

Note that we have labeled the IRF with with the extra tag (Θ) to stress that it coincides with the rocket frame R at the event "Θ", which, for fixing the idea can be taken as "Θ : "rocket passes a space station A"". Every IRF has to be associated with one, and only one, event "Θ". This association will be useful in the discussions to follow.

It may be worthwhile to stress at this point, even though the reader is aware of it, that S and S_o are both inertial frames and therefore, the components of any 4-vector w.r.t these two frames can be connected by a Lorentz Transformation. Such connection is not possible between the rest frame R of the rocket in which the rocket is permanently at rest and either S or S_o, because R is an accelerating frame.

Three quantities are specified for the assessing the performance of the rocket: u, r

and $M_i \equiv$ initial *rest* mass of the rocket at the instant $t = 0$, when it starts with zero velocity. In this article $M = M(\Theta)$ will stand for the *instantaneous rest mass* of the rocket at the event Θ. When written as a function of the "ground time" t, it will be appear as $M(t)$.

Let us consider two infinitely close events Θ_A and Θ_B (corresponding to the rocket passing two infinitely close space stations A and B on its path), the time-space coordinate differentials between them being $(c\,\delta t, \delta x)$ w.r.t S, and $(c\,\delta\tau, 0)$ w.r.t S_o. Between these events the rocket ejects a quantity of gas of *rest mass* $\delta\mu_0$. Consequently its own velocity changes (i) from v(t) to v(t) + δv w.r.t the GF S, (ii) from 0 to dv$'$ w.r.t S_o, and (iii) its *rest mass* changes from $M(t)$ to $M(t) + \delta M$. Note that the time differential between the events being infinitesimally small, $\delta\tau$ is the *proper time* between the events. Also, note that, the rate of emission of the *rest gas mass* w.r.t. the rocket frame is $r = \frac{d\mu_0}{d\tau} = \lim_{\delta\to 0}\frac{\delta\mu_0}{\delta\tau}$, which is taken as a constant.

In summary, the performance of the rocket is decided by three specifications: (i) its initial mass M_i, (ii) the rate $r = \frac{d\mu_0}{d\tau}$ at which *rest mass* is ejected from the rear end w.r.t the IRF, (iii) the speed $-u$, w.r.t the IRF, with which this rest mass is ejected. These quantities, being in the specification book supplied by the manufacturer, are frame independent and are to be taken as constants.

In Eq. (36) (to follow) we have defined another constant $\varrho \equiv gr$ = the rate of emission of the *relativistic gas mass* w.r.t. the rocket frame, where $g = g(u)$, defined in Eq. (2), is the Lorentz factor associated with the ejection velocity $-u$, and is therefore a constant. Finally in Eq. (49) we have combined all the above constants into a single constant k, while writing the Equation of Motion.

4 Review of the Non-Relativistic (N.R.) results

We shall briefly review the N.R rocket formulas so that we can compare the relativistic results with their N.R. counterparts. We shall drop the subscript "$_o$" from $d\mu_0$, because in the N.R. zone there is no such thing as proper mass. The N.R. formulas can be found in standard books on Mechanics. We shall quote the following formulas[1, 2].

$$
\begin{aligned}
\delta\mathrm{v} &= -u\frac{\delta M}{M}. && \text{(a)}\\
\mathrm{v} &= u\ln\left(\frac{M_i}{M(\mathrm{v})}\right)\\
\frac{M(\mathrm{v})}{M_i} &= e^{-\frac{\mathrm{v}}{u}}. && \text{(b)}\\
T &= \text{thrust force}\\
&= ru. && \text{(c)}\\
r &= \frac{d\mu}{dt} = -\frac{dM}{dt} && \text{(d)}\\
M(\mathrm{v})\frac{\mathrm{dv}}{\mathrm{dt}} &= T = ru,\\
M_i e^{-\frac{\mathrm{v}}{u}}\frac{dv}{dt} &= ru. && \text{(e)}\\
\text{Hence, v} &= -u\,\ln\left(1-\frac{rt}{M_i}\right). && \text{(f)}
\end{aligned}
\qquad (1)
$$

In line (b) $M(\mathrm{v})$ is the same as $M(t)$, since $\mathrm{v} = \mathrm{v(t)}$. Line (d) in which $d\mu$ is the mass of

the gas ejected in time dt, is a re-statement of conservation of mass. The relationship between the velocity differential and mass differential shown in line (a) is a consequence of *(i)* conservation of mass, and *(ii)* conservation of linear momentum. The mass ratio equation (b), known as Tsiolkovsky rocket equation[15], is obtained by integrating the differentials in line (a). Line (e) represents the EoM of the rocket. Line (f) gives the solution of the EoM, subject to the initial condition: $\mathrm{v} = 0$ when $t = 0$.

5 Review of the formulas to be used

Let us be specific about the frames of reference, the symbols for velocity, and the Lorentz factors associated with the velocities. All motions are in the X direction. As already mentioned, the ground frame is S, the IRF of the rocket (at Θ) is S_o. The velocity of the rocket, and hence that of S_o, is $\mathrm{v}(\mathrm{t})$ w.r.t S. The velocity of the ejected gas is constant w.r.t. S_o and equal to $-u$. Let $\mathbf{v}(t)$ represent the velocity 3-vector of an arbitrary particle having components (v_x, v_y, v_z) w.r.t S and (v'_x, v'_y, v'_z) w.r.t S_o.

In order to avoid future confusion let us remind the reader that v and v are two different velocities. The former, i.e, "roman v" stands for rocket velocity. The latter i.e. "italicized v" stands for the velocity of any arbitrary particle, and will be needed for defining the space and time components of 4-velocity, 4-acceleration, 4-momentum and 4-force in general.

This distinction between v and v will be removed from Sec. 6 downwards, when the particle in question becomes the same as the rocket itself, momentarily at rest in the IRF S_o, and moving with the velocity v w.r.t. S.

We now have the following Lorentz-factors (to be abbreviated as L-factors), corresponding to the velocities to be used .

$$\begin{aligned} g(u) &= \frac{1}{\sqrt{1-\frac{u^2}{c^2}}}; \quad \gamma(\mathrm{v}) = \frac{1}{\sqrt{1-\frac{\mathrm{v}^2}{c^2}}} \\ \Gamma(v) &= \frac{1}{\sqrt{1-\frac{v^2}{c^2}}}; \quad \Gamma'(v') = \frac{1}{\sqrt{1-\frac{v'^2}{c^2}}}. \end{aligned} \tag{2}$$

It has been our *usual* practice[16] to write the L-factor associated with the Lorentz transformation with the lower case symbol γ and the L-factor associated with the velocity of a particle with the upper case symbol Γ. We call them by two different names, viz., Boost Lorentz factor and Kinematic Lorentz factor, respectively. In this particular case γ is a boost L-factor (corresponding to the boost $S \to S_o$), and Γ, Γ', as well as g, are Kinematic L-factors.

Note that the other specifications (namely, u and r) remaining the same, introduction of the L-factors makes the difference between the N.R. case and the relativistic one.

We shall now start a relativistic approach to the motion of the rocket. We shall begin by a review of the 4-vectors to be used in our discussions, and the basic equations of motion.

The kinematic and dynamical 4-vectors

We shall write velocity, momentum, acceleration, force, as 4-vectors, so that (1) we can write the equations of motion covariantly, and make them valid in all inertial frames; and (2) we are able to transform the time and space components using Lorentz Transformation.

Let us introduce two dimensionless velocities

$$\beta \equiv \mathrm{v}(t)/c; \quad \nu \equiv v/c. \tag{3}$$

The transition $S \rightarrow S_o$, will be called boost $S(c\beta, 0, 0)S_o$, and the inverse transition $S_o \rightarrow S$ boost $S_o(-c\beta, 0, 0)S$. For our purpose the inverse transition is more important.

Suppose $\overrightarrow{\mathbf{A}}$ is a *contravariant* 4-vector, having components (A'^t, A'^x) in the IRF S_o, and (A^t, A^x) in the GF S. Then by Lorentz transformation the above components transform as follows:

$$\begin{aligned} A^t &= \gamma(A'^t + \beta A'^x). \quad (a) \\ A^x &= \gamma(A'^x + \beta A'^t). \quad (b) \end{aligned} \tag{4}$$

We shall now write the (t, x)-components of 4-velocity $\overrightarrow{\mathbf{V}}$, 4-momentum $\overrightarrow{\boldsymbol{\mathcal{P}}}$, 4-acceleration $\overrightarrow{\boldsymbol{\mathcal{A}}}$, 4-force $\overrightarrow{\boldsymbol{\mathcal{F}}}$ and obtain their transformation equations corresponding to $S_o \rightarrow S$. The arrows "$\rightarrow$" in some of the formulas below will imply narrowing down of the (t, x, y, z) components to (t, x) components.

4-velocity

Consider a particle moving with arbitrary velocity $\mathbf{v}(t)$. The Lorentz factor for this velocity is Γ, as defined in (2). Between two infinitely close events Θ_A and Θ_B on the world line of the particle, it undergoes a 4-displacement $\delta\overrightarrow{\mathbf{r}}$, as its own clock records a time lapse of $\delta\tau$, and the clock in any inertial frame S a time lapse of δt. Since $\delta\tau$ is *proper time*, it is related to the time δt by the equation[17]

$$\delta\tau = \frac{\delta t}{\Gamma}. \tag{5}$$

The displacement 4-vector $\delta\overrightarrow{\mathbf{r}} \equiv (c\,\delta t, \delta\mathbf{r})$ is the primordial contravariant 4-vector from which other contravariant 4-vectors are derived by multiplication or division with 4-scalars, namely m_o, the rest mass (or proper mass of the particle) and $\delta\tau$, the proper time between the events Θ_A and Θ_B. By this property all the 4-vectors to follow are contravariant 4-vectors.

The 4-velocity of the particle is defined as

$$\begin{aligned} \overrightarrow{\mathbf{V}} &\equiv \lim_{\delta\tau\rightarrow 0} \frac{\delta\overrightarrow{\mathbf{r}}}{\delta\tau} = \frac{d\overrightarrow{\mathbf{r}}}{d\tau} = \Gamma\frac{d\overrightarrow{\mathbf{r}}}{dt} \\ &= \Gamma\left(\frac{c\,dt}{dt}, \frac{d\mathbf{r}}{dt}\right) = \Gamma(c, \mathbf{v}) \;\rightarrow\; \Gamma(c, v). \end{aligned} \tag{6}$$

Note that $\mathbf{v} = \frac{d\mathbf{r}}{dt}$ is the velocity 3-vector. Let us apply the Lorentz transformation (4) to the components of $\overrightarrow{\mathbf{V}}$.

$$\begin{aligned} \Gamma c &= \gamma(\Gamma' c + \beta\Gamma' v'). \quad (a) \\ \Gamma v &= \gamma(\Gamma' v' + \beta\Gamma' c). \quad (b) \end{aligned} \tag{7}$$

Setting $v = c\,\nu$, and simplifying, we get the following two important relations.

$$\begin{aligned} \Gamma &= \gamma\Gamma'(1+\beta\nu'). \quad (a) \\ \nu &= \frac{\nu'+\beta}{1+\nu'\beta}. \quad (b) \end{aligned} \tag{8}$$

Equation (b) is known by the popular name *velocity addition formula*.

4-acceleration

The 4-acceleration $\overrightarrow{\mathcal{A}}$ is defined, from which its components are obtained[17, 18], as follows.

$$\begin{aligned} \overrightarrow{\mathcal{A}} &\equiv \frac{d\overrightarrow{\mathbf{V}}}{d\tau} \\ &= \left(\frac{\Gamma^4}{c}(\boldsymbol{a}\cdot\mathbf{v}),\ \frac{\Gamma^4}{c^2}(\boldsymbol{a}\cdot\mathbf{v})\mathbf{v}+\Gamma^2\boldsymbol{a}\right) \\ &\to \Gamma^4 a\left(\frac{v}{c},\ 1\right) = \Gamma^4 a\,(\nu,\ 1)\,. \end{aligned} \tag{9}$$

Here

$$\boldsymbol{a} \equiv \frac{d\mathbf{v}}{dt} \quad \to \quad a = \frac{dv}{dt} \tag{10}$$

is the acceleration 3-vector.

Let us now apply LT (4) to the x-component of $\overrightarrow{\mathcal{A}}$.

$$\begin{aligned} &\mathcal{A}^x = \gamma(\mathcal{A}'^x + \beta\mathcal{A}'^t). \\ \text{or,}\quad &\Gamma^4 a = \gamma\Gamma'^4 a'(1+\beta\nu'). \end{aligned} \tag{11}$$

Let us now suppose that the moving particle, being observed from S and S_o, is the rocket itself. In other words the particle is at rest in S_o, so that $\nu' = 0$, $\Gamma' = 1$, $\gamma = \Gamma$. In this case the boost L-factor is identical with the kinematic L-factor w.r.t. S. Also, we shall set $a' = a_o$ = acceleration of the rocket in its rest frame, which can be constant or variable. Then the above equation takes an important form[17]

$$a = \frac{a_o}{\Gamma^3}. \tag{12}$$

For a particle subjected to a finite acceleration a_o in its rest frame (due to some external force , e.g., an external electric field), its acceleration w.r.t. any inertial frame vanishes as $v \to c$, and consequently $\Gamma \to \infty$. The above equation protects the rocket from reaching or exceeding the speed of light, even under an ever-continuing acceleration in its rest frame.

4-momentum

Let us consider a particle of *rest mass* m_o moving with 4-velocity $\overrightarrow{\mathbf{V}}$. The *4-momentum* $\overrightarrow{\mathcal{P}}$ of the particle is then defined as[18]:

$$\overrightarrow{\mathcal{P}} \equiv m_o\overrightarrow{\mathbf{V}} = m_o\Gamma(c,\mathbf{v}) \to m_o\Gamma(c,v). \tag{13}$$

If we write

$$\begin{aligned} m &= \text{relativistic mass} \\ &= \Gamma m_o, \quad (a) \\ \mathbf{p} &= \text{relativistic momentum} \\ &= \Gamma m_o\mathbf{v} = m\mathbf{v}, \quad (b) \\ E &= \text{total energy} \\ &= \Gamma m_o c^2 = mc^2, \quad (c) \end{aligned} \tag{14}$$

then

$$\overrightarrow{\mathcal{P}} = \left(\frac{E}{c},\ \mathbf{p}\right). \tag{15}$$

For a mass-less particle, e.g., photon,

$$E = |\mathbf{p}|\,c. \tag{16}$$

Hence,

$$\overrightarrow{\mathcal{P}} = \left(\frac{E}{c},\ \frac{E}{c}\mathbf{n}\right) \quad \text{for a photon,} \tag{17}$$

where $\mathbf{n}$ is the direction of propagation of the photon.

4-force

The 4-force $\overrightarrow{\mathcal{F}}$, termed *Minkowski 4-force* is defined in such a way that it will satisfy *Minkowski's Equation of Motion*[18]:

$$\overrightarrow{\mathcal{F}} = \frac{d\overrightarrow{\mathcal{P}}}{d\tau} = \Gamma \frac{d\overrightarrow{\mathcal{P}}}{dt}. \tag{18}$$

It follows from (15) that

$$\overrightarrow{\mathcal{F}} = \Gamma \left(\frac{1}{c}\frac{dE}{dt}, \frac{d\mathbf{p}}{dt} \right) = \Gamma \left(\frac{\Pi}{c}, \mathbf{F} \right) \rightarrow \quad \Gamma \left(\frac{\Pi}{c}, F \right) \tag{19}$$

where $\mathbf{F} = \frac{d\mathbf{p}}{dt}$ is the 3-force as in Newtonian Mechanics, and Π (Capital-pi) stands for the *power* received by the particle (same as energy received by the particle per unit time), due to (i) work done on it by external forces, and/or (ii) by absorption of radiation or heat (thereby changing its rest mass). In the case of a particle whose rest mass does not change, Π is the same as the power delivered by the force $\mathbf{F}$, as shown in Eq. (22) below.

Consider a point particle with a constant rest mass m_o. Due to (13), the equation of motion (18) becomes

$$\overrightarrow{\mathcal{F}} = m_o \overrightarrow{\mathcal{A}} = m_o \frac{d\overrightarrow{\mathbf{V}}}{d\tau}. \tag{20}$$

In this case the 4-force $\overrightarrow{\mathcal{F}}$ is orthogonal to the 4-velocity $\overrightarrow{\mathbf{V}}$,

$$\overrightarrow{\mathcal{F}} \cdot \overrightarrow{\mathbf{V}} = 0, \tag{21}$$

and the 4-force takes the form[18]:

$$\overrightarrow{\mathcal{F}} = \Gamma \left(\frac{\mathbf{F}\cdot\mathbf{v}}{c}, \mathbf{F} \right) \rightarrow \overrightarrow{\mathcal{F}} = \Gamma \left(\frac{Fv}{c}, F \right). \tag{22}$$

Let us note here that the time-space components of the 4-force written in the form (22) is a consequence of the orthogonality between $\overrightarrow{\mathcal{F}}$ and $\overrightarrow{\mathbf{V}}$, which in turn is due to the 4-force written in the form (20). In the sequel we shall write the EoM in the form (20), in which $\overrightarrow{\mathcal{F}}$ will be replaced by the reaction 4-force $\overrightarrow{\mathcal{R}}$, and m_o by the instantaneous rest mass M of the rocket, which is variable. See Eq. (43). Therefore $\overrightarrow{\mathcal{R}}$ will have time-space components as in (22).

6 Relativistic mass equation

Even though the relativistic mass formula is well known (known as Ackeret[6] equation), we shall make a brief review with two purposes: (1) some of the formulas developed in the process will be required in the sequel; (2) we shall demonstrate that the mass equation and the EoM (to be derived soon) converge to the corresponding formulas (1 b) and (1 e) in the N.R. limit.

At this point we shall change the velocity symbol for the rocket from v to v w.r.t. S, and from v′ to v' w.r.t. S_o. Also we shall set $\beta = \frac{v}{c}$.

As noted in paragraph 5 of Sec. 3 the rocket velocity changes from 0 to $\delta v'$, and it ejects a quantity of gas of *rest mass* $\delta\mu_0$ from the event Θ_A to the event Θ_B in the IRF S_o. We shall write the components of the 4-momentum of the rocket at Θ_A and Θ_B, and of the gas ejected between these events - all of them in S_o.

At this point we draw the attention of

the reader to what we wrote in paragraph 4 of Sec. 3. We emphasize once again that $M = M(\Theta) = M(t) = M(\tau)$ is the instantaneous rest mass of the rocket at the event Θ and hence, is a 4-scalar.

The (t, x) components of the momentum 4-vectors we shall write below will follow from (13), in which we shall set $m_o = M(t)$. Also, note that the kinetic L-factors are: g for the ejected gas, and $\Gamma' = 1$ for the rocket, since $v' = 0$, i.e., the rocket is momentarily at rest in S_o. The 4-vectors written below have only (t, x) components, and are valid in the IRF S_o.

$$\begin{aligned}
\text{At } \Theta_A: \quad \overrightarrow{\mathcal{P}} &= M(c,0) && \text{(a)}\\
\text{At } \Theta_B: \quad \overrightarrow{\mathcal{P}} + \delta\overrightarrow{\mathcal{P}} &= (M+\delta M)(c,\delta v') && \text{(b)}\\
\text{Change in 4-momentum}: \quad \delta\overrightarrow{\mathcal{P}} &= (\delta M c, M\delta v') && \text{(c)}\\
\text{4-momentum of the ejected gas}: \quad \delta\overrightarrow{\mathbf{p}} &= \delta\mu_0\, g(c,-u). && \text{(d)}
\end{aligned} \tag{23}$$

We shall apply the conservation of 4-momentum in S_o, using the data in Eqs. (23 c,d).

$$\begin{aligned}
\delta\overrightarrow{\mathcal{P}} &= -\delta\overrightarrow{\mathbf{p}}. && \text{(a)}\\
\text{t-comp}: \quad \delta M &= -\delta\mu_0\, g. && \text{(b)}\\
\text{x-comp}: \quad M\delta v' &= \delta\mu_0\, g\, u. && \text{(c)}\\
\text{Hence,} \quad M\delta v' &= -\delta M\, u. && \text{(d)}
\end{aligned} \tag{24}$$

Note that (i) The *rest mass* lost by the rocket equals the *relativistic mass* gained by the ejected gas, according to (b), (ii) Eq. (d) is valid in S_o. To validate it in S, we have to apply the velocity addition formula (8 b).

$$\begin{aligned}
v + dv &= \frac{dv' + v}{1 + \frac{dv'\,v}{c^2}}\\
&\approx (dv' + v)\left(1 - \frac{dv'\,v}{c^2}\right) \approx v + \left(1 - \frac{v^2}{c^2}\right) dv'.
\end{aligned} \tag{25}$$

Hence, (in the limit $dv' \to 0$),

$$dv = \left(1 - \frac{v^2}{c^2}\right) dv'. \tag{26}$$

This transforms Eq. (24 d) to

$$\frac{dv}{\left(1 - \frac{v^2}{c^2}\right)} = -u\frac{dM}{M}. \tag{27}$$

Integrating (27) from $t = 0$ to $t = t$, setting $M = M_i$ (i for "initial"), and $v = 0$ at $t = 0$, we get[17]

$$\begin{aligned}
&\frac{c}{2}\ln\frac{c+v}{c-v} = -u\ln\frac{M}{M_i}\\
\text{Or,}\quad &\frac{M}{M_i} = \left(\frac{c-v}{c+v}\right)^{\frac{c}{2u}} = \left(\frac{1-\beta}{1+\beta}\right)^{\frac{c}{2u}}.
\end{aligned} \tag{28}$$

The above equation is referred to as the Ackeret equation[6].

One of the requirements of all Relativistic formulas is that they must converge to the corresponding N.R. counterparts (if such counterparts exist) in the N.R. limit $v/c \to$

0. In this case the N.R. mass formula is (1 b). We shall show that this requirement is satisfied by the formula (28).

Proof: We set $\beta = v/c$. Then in the limit $\beta \to 0$

$\frac{1}{1-\beta} \overset{\beta\to 0}{\longrightarrow} (1+\beta)$. Hence, $(1-\beta) \overset{\beta\to 0}{\longrightarrow} \frac{1}{1+\beta}$.
$\left(\frac{c-v}{c+v}\right)^{\frac{c}{2u}} = \left(\frac{1-\beta}{1+\beta}\right)^{\frac{c}{2u}} \overset{\beta\to 0}{\longrightarrow} [(1+\beta)^{-2}]^{(\frac{c}{2v})(\frac{v}{u})}$
$= [(1+\beta)^{\frac{1}{\beta}}]^{-(v/u)}$.
By definition $e \equiv$ Euler's number[19]
$= \lim_{x\to 0}(1+x)^{1/x}$.
Hence, $\left(\frac{c-v}{c+v}\right)^{\frac{c}{2u}} \overset{\beta\to 0}{\longrightarrow} e^{-(v/u)}$.
Or, $\frac{M}{M_i} \overset{\beta\to 0}{\longrightarrow} e^{-(v/u)}$, (29)

Is the formula (28) valid when $u = c$? To make sure, we shall retrace the steps from Eq. (23) downward, specializing them to $u = c$. Instead of assuming that the gas is ejected with velocity $-u$ w.r.t. IRF S_o, we shall assume that, between the events Θ_A and Θ_B, a beam of photons is emitted in the $-x$-direction with energy δE_o w.r.t the IRF S_o. In this case we use Eq. (17) for photon momentum.

$$\begin{array}{rrcll}
\text{At } \Theta_A: & \overrightarrow{\mathcal{P}} & = & M(c,0) & \text{(a)} \\
\text{At } \Theta_B: & \overrightarrow{\mathcal{P}} + \delta\overrightarrow{\mathcal{P}} & = & (M+\delta M)(c,\delta v') & \text{(b)} \\
\text{Change in 4-momentum} & \delta\overrightarrow{\mathcal{P}} & = & (\delta M c, M\delta v') & \text{(c)} \\
\text{4-mom. of the emitted photons}: & \delta\overrightarrow{\mathbf{p}} & = & (\frac{\delta E_o}{c}, -\frac{\delta E_o}{c}). & \text{(d)}
\end{array} \tag{30}$$

We shall apply the conservation of 4-momentum in S_o, using the data in Eqs. (30 c,d).

$$\begin{array}{rrcll}
 & \delta\overrightarrow{\mathcal{P}} & = & -\delta\overrightarrow{\mathbf{p}}. & \text{(a)} \\
\text{t-comp} & \delta M & = & -\frac{\delta E_o}{c^2}. & \text{(b)} \\
\text{x-comp} & M\delta v' & = & \frac{\delta E_o}{c} & \text{(c)} \\
\text{Hence,} & M\delta v' & = & -\delta M\, c. & \text{(d)}
\end{array} \tag{31}$$

It follows that Eq. (24 d) will be valid for $u = c$. As a consequence (28) is also valid for $u = c$. We shall rewrite this for this special case same as the N.R. formula (1 b)

Q.E.D.

of a for a photon driven rocket[17].

$$\frac{M}{M_i} = \sqrt{\frac{c-v}{c+v}} = \sqrt{\frac{1-\beta}{1+\beta}}. \tag{32}$$

7 The Thrust 4-Force

The 4-momentum of the rocket at the event Θ_A can be written as $\overrightarrow{\mathcal{P}}(\Theta_A) = M(\Theta_A)\overrightarrow{\mathbf{V}}(\Theta_A)$. We have used Eq. (13), replaced m_o with $M(\Theta_A)$. The time difference between the events Θ_A and Θ_B is δt w.r.t. S, and $\delta\tau$ w.r.t. the IRF S_o. Differentiating $\overrightarrow{\mathcal{P}}$ w.r.t. τ we get

$$\frac{d\vec{\mathcal{P}}}{d\tau} = \frac{d}{d\tau}(M\vec{\mathbf{V}}) = M\frac{d\vec{\mathbf{V}}}{d\tau} + \frac{dM}{d\tau}\vec{\mathbf{V}}. \quad (33)$$

To evaluate $\frac{dM}{d\tau}$, we use (24 b)

$$\begin{aligned} &\frac{dM}{d\tau} = -g\frac{d\mu_0}{d\tau} = -gr, \\ \text{where} \quad &r = \frac{d\mu_0}{d\tau} \end{aligned} \quad (34)$$

as defined in paragraph 1 of Sec.3

To get a parallel formula for the photon-driven rocket we refer to (31 b), and get

$$\frac{dM}{d\tau} = -\frac{1}{c^2}\frac{dE_o}{d\tau}. \quad (35)$$

We can combine the two equations into one, *assuming* that the rocket is ejecting *relativistic mass*, either in the form of *matter* or in the form of *radiation* (we shall use the term radiation to mean photons), at the *constant rate* of ϱ kg/s in its *rest frame*.

$$\begin{aligned} &\text{For matter emission :} \\ &\varrho = \lim_{\delta\tau\to 0}\frac{g\,\delta\mu_0}{\delta\tau} = g\frac{d\mu_0}{d\tau} = gr. \quad \text{(a)} \\ &\text{For photon emission :} \\ &\varrho = \lim_{\delta\tau\to 0}\frac{\delta E_0/c^2}{\delta\tau} = \frac{1}{c^2}\frac{dE_o}{d\tau}. \quad \text{(b)} \end{aligned} \quad (36)$$

Note that r is constant by assumption, and g is constant because u is so. Hence ϱ is constant in line (a). We now *assume* that if photons are ejected to generate the reaction force, then $\frac{dE_o}{d\tau}$ is also constant in line (b). Then by (34) - (36)

$$\frac{dM}{d\tau} = -\varrho = \text{constant} \quad (37)$$

for both matter and radiation.

We now go back to (33), and rewrite it as follows.

$$\begin{aligned} M\frac{d\vec{\mathbf{V}}}{d\tau} &= \frac{d\vec{\mathcal{P}}}{d\tau} - \frac{dM}{d\tau}\vec{\mathbf{V}} \\ &= \frac{d\vec{\mathcal{P}}}{d\tau} + \varrho\vec{\mathbf{V}} \equiv \vec{\mathcal{R}} \qquad (a) \\ \text{where} \quad \vec{\mathcal{R}} &\stackrel{\text{def}}{=} \frac{d\vec{\mathcal{P}}}{d\tau} + \varrho\vec{\mathbf{V}} \qquad (b) \end{aligned} \quad (38)$$

is the "Reaction 4-Force", or better still the *Thrust 4-Force*[18]. However, we are using the symbol R instead of T, because the latter symbol can be confused with time.

In the following equations we write the (t, x) components of the 4-vectors in S_o. Using (24 a), (23 d), (36 a):

$$\begin{aligned} &\frac{d\vec{\mathcal{P}}}{dt} = -\frac{d\vec{\mathbf{p}}}{d\tau} = -g\frac{d\mu_0}{d\tau}(c, -u) \\ &= -\varrho(c, -u). \\ \text{from (6)} : \quad &\vec{\mathbf{V}} = (c, 0), \\ &\text{since } v' = 0,\ \Gamma' = 1. \\ \text{from (38 b)} : \quad &\vec{\mathcal{R}} = -\varrho(c, -u) + \varrho(c, 0) \\ &= \varrho(0, u) = (0, R). \end{aligned} \quad (39)$$

In other words, the Reaction 4-vector has the following components w.r.t S_o:

$$\begin{aligned} \vec{\mathcal{R}} &= (\mathcal{R}'^t, \mathcal{R}'^x) = (0, R) \\ \text{where } R &= \varrho u = gru \\ &= \text{Reaction 3-force, w.r.t.} S_o. \end{aligned} \quad (40)$$

Note that the (t, x)-components of the Reaction 4-force $\vec{\mathcal{R}}$ in S_o are in agreement with (22).

We shall now find the (t, x) components of the Reaction 4-force: $\vec{\mathcal{R}} = (\mathcal{R}^0, \mathcal{R}^x)$, in the ground frame S, applying Lorentz

transformation Eq.(4), corresponding to the boost: $S_o(-c\beta,0,0)S$, to the (t,x) components of $\overrightarrow{\mathcal{R}}$ in the IRF S_o, shown in (40).

$$\begin{aligned} \mathcal{R}^t &= \Gamma(\mathcal{R}'^t + \beta\mathcal{R}'^x) = \Gamma\beta R. \quad \text{(a)} \\ \mathcal{R}^x &= \Gamma(\mathcal{R}'^x + \beta\mathcal{R}'^t) = \Gamma R. \quad \text{(b)} \end{aligned} \tag{41}$$

Note that the (t,x)-components of the Reaction 4-force $\overrightarrow{\mathcal{R}}$ in S are in agreement with (22), which we rewrite in the present context as

$$\overrightarrow{\mathcal{R}} = (\mathcal{R}^t, \mathcal{R}^x) = \Gamma\left(\frac{Rv}{c}, R\right). \tag{42}$$

Referring back to Eq. (36)

- For radiation emission $R = \varrho c = \frac{1}{c}\frac{dE_o}{d\tau}$.
- For matter emission $R = \varrho u = gru = gT$, where $T = ru$ is the same thrust force of non-relativistic mechanics. See Eq. (1 c). It changes to $R = gT$ as it enters the relativistic domain.

8 The Equation of Motion

We return to Eq. (38 a) and write the equation of motion[18]

$$M\frac{d\overrightarrow{\mathbf{V}}}{d\tau} = \overrightarrow{\mathcal{R}}, \tag{43}$$

where $M = M(\Theta)$ is the instantaneous rest mass of the rocket at the event Θ, and is a 4-scalar. All we now have to do is to write the x-component of the 4-vectors on either side of the equation, and simplify the same to obtain the acceleration $a = \frac{dv}{dt}$ of the rocket in the GF S. We shall, however, find it convenient to work out the acceleration $a_o = \frac{dv'}{d\tau}$ in the IRF S_o, and convert this acceleration to a usng Eq (12).

Consider the x-component of $\overrightarrow{\mathbf{V}}$ using (6). The kinematic quantities in S_o will be identified with "prime". Then,

$$\frac{dV'^x}{d\tau} = \frac{d(\Gamma' v')}{d\tau} = \Gamma'\frac{dv'}{d\tau} + \frac{d\Gamma'}{d\tau}v' = \frac{dv'}{d\tau} = a_o, \tag{44}$$

since v'= instantaneous velocity of the rocket in $S_o = 0$. Consequently $\Gamma' = 1$.

From (40), the x-component of $\overrightarrow{\mathcal{R}}$ is $R'^x = R = \varrho u$. We thus get a simple looking equation of motion, which is valid in S_o.

$$M(\Theta)a_o = \varrho u = \text{constant}. \tag{45}$$

Mass $\times$ acceleration is constant. But mass is not constant. Hence the acceleration in IRF S_o is not constant.

We shall write the EoM in the ground frame S, by converting $a_o \to a$, the acceleration in the ground frame S, using (12), which gives $a_o = \Gamma^3 a$.

$$\begin{aligned} M(\Theta)\,\Gamma^3 a &= \varrho u = \text{constant}. \quad (a) \\ \text{Or,}\quad M(\Theta)\,\Gamma^3\frac{dv}{dt} &= \varrho u = \text{constant}. \quad (b) \end{aligned} \tag{46}$$

An alternative version of Eq. (46 b) is

$$\begin{aligned} M(\Theta)\,\frac{d(\Gamma v)}{dt} = \varrho u &= -\frac{dM}{d\tau}u \\ &= -\Gamma\frac{dM}{dt}u = \text{constant}, \end{aligned} \tag{47}$$

in which Pomeranz wrote the EoM in his 1969 paper[12]. To see the equivalence between the two forms one has to show that $\frac{d\Gamma}{dt} = \Gamma^3\frac{v}{c^2}\frac{dv}{dt}$.

Now we rewrite Eq. (46 b), using the mass equation (28).

$$\left(\frac{c-v}{c+v}\right)^{\frac{c}{2u}} \Gamma^3 \frac{dv}{dt} = \frac{\varrho u}{M_i} = \text{constant}, \quad (48)$$

where M_i is the initial (rest) mass of the rocket.

We shall set $\beta = v/c$, and $c/u = n$ in the index of the leftmost factor in Eq. (48). Here $n \geq 1$ is a positive real number greater than or equal to 1. $n = 1$ corresponds to $u = c$. On the other extreme $n \to \infty$ would converge to the N.R. EoM shown in (1 e). We now simplify the left side:

$$\Gamma^3 = \frac{1}{(1-\beta^2)^{3/2}} = [(1+\beta)(1-\beta)]^{-3/2}$$
$$\left(\frac{c-v}{c+v}\right)^{\frac{c}{2u}} = \left(\frac{1-\beta}{1+\beta}\right)^{\frac{n}{2}}$$
$$\left(\frac{c-v}{c+v}\right)^{\frac{c}{2u}} \Gamma^3 \frac{dv}{dt} = c\left[\frac{(1-\beta)^{\frac{n-3}{2}}}{(1+\beta)^{\frac{n+3}{2}}}\right]\frac{d\beta}{dt}.$$

The EoM (48) now takes a simpler form

$$\left[\frac{(1-\beta)^{\frac{n-3}{2}}}{(1+\beta)^{\frac{n+3}{2}}}\right]\frac{d\beta}{dt} = \frac{\varrho u}{cM_i} = k = \text{const.} \quad (49)$$

Let us rewrite the mass equation (28), setting $v = c\beta$; $c/u = n$.

$$\frac{M}{M_i} = \left(\frac{1-\beta}{1+\beta}\right)^{\frac{n}{2}}. \quad (50)$$

We assume that the rocket has no payload, all its mass will ultimately be ejected out to provide the thrust. In other words, the rocket operates until $M \to 0$, which happens when $\beta \to 1$.

We shall now show that the above EoM (49) will converge to the Non Relativistic EoM as given in (1 e). We shall set $\varrho = gr$ as per (36 a), $\beta \to 0$ and use the definition of Euler's number e, as in (29).

Proof:

$$\left[\frac{(1-\beta)^{\frac{n-3}{2}}}{(1+\beta)^{\frac{n+3}{2}}}\right] \overset{\beta\to 0}{\longrightarrow} \left[\frac{1}{(1+\beta)^{\frac{n-3}{2}}}\right]\left[\frac{1}{(1+\beta)^{\frac{n+3}{2}}}\right]$$
$$= \frac{1}{(1+\beta)^n} = \frac{1}{(1+\beta)^{c/u}}$$
$$= \frac{1}{[(1+\beta)^{1/\beta}]^{v/u}} = \frac{1}{e^{v/u}}.$$

Substituting this in (49) we get:

$$M_i e^{-v/u}\frac{dv}{dt} = \varrho u = gru = ru, \text{ since } g \to 1. \quad (51)$$

Thus we get back (1 e).

Q.E.D.

9 Solution of the EoM in special cases

Example 1. Set $n = 3$, implying $u = c/3$.

The reason for choosing $n = 3$ is two fold: (1) The EoM shown in (49) will assume the simplest form, the numerator within the square brackets becoming 1; (2) We are now at the threshold of transition from the non-relativistic (N.R.) to the relativistic domain, the L-factor is very close to 1, in fact $g = \frac{3}{2\sqrt{2}} = 1.06$. Our results obtained here should be close to the N.R. results, so that we may feel comfortable that we are on right track.

We specialize the EoM (49) for this special case:

$$\left[\frac{1}{(1+\beta)^3}\right]\frac{d\beta}{dt} = \frac{\varrho}{3M_i} \equiv k_3 = \text{constant}. \tag{52}$$

Integration, subject to the initial condition: $\beta = 0$ when $t = 0$ leads to the following solution:

$$\beta = \left[\frac{1}{\sqrt{1-2k_3t}} - 1\right]; \quad 0 \le t \le t_c. \tag{53}$$

The reader can verify the answer by differentiating β w.r.t t.

We have written t_c to mean "critical time" when $M \to 0$ as explained below Eq. (50). In other words, t_c is the time at "burn out", assuming that the rocket has no payload, all its mass has ultimately been ejected out to provide the thrust. This happens when $\beta \to 1$. From Eq.(53):

$$\left[\frac{1}{\sqrt{1-2k_3t_c}} - 1\right] = 1$$
Or,
$$1 - 2k_3t_c = \tfrac{1}{4}. \quad \Rightarrow \quad k_3t_c = \tfrac{3}{8}$$
Or,
$$\frac{\varrho t_c}{M_i} = \frac{9}{8}. \tag{54}$$
for the N.R. case :
$$\frac{\varrho t_c}{M_i} = 1.$$

We have plotted the velocity-time relation (rather the β-t relation) in Fig.1 (a), using Gnuplot. On the same graph we have also plotted the N.R. equation (1 f).

We have set M_i = 1 kg, r = 1 kg/s (see specifications in Sec. 3). Setting $u/c = 1/3$ in the first of the equations in (2) we get $g = 3/\sqrt{8} = 1.06$. Hence ϱ (defined in Eq. 36a) $= g\,r$ = 1.06 kg/m. Therefore $k_3 = \frac{\varrho}{3M_i} = 0.3535$. From Eq (54) the critical time is $t_c = \frac{3}{8\times 0.3535} = 1.06$ s which has been set as the upper limit on the t axis.

The two plots, *Relativistic* and *Non-relativistic* almost coincide up to $t \approx 0.8$ s, $\beta \approx 0.5$.

In Fig.1 (b) we have plotted $\frac{d\beta}{dt} = k_3(1+\beta)^3 = 0.3535(1+\beta)^3$. However, in this case we set the vertical axis to represent the independent variable β, aligning it (tic-wise) with the vertical β axis of Fig.(a). The horizontal axis, pointing to the left, represents the dependent variable $\frac{d\beta}{dt}$. We achieved this configuration by first plotting $\frac{d\beta}{dt}$ versus β the usual way, then turning the plot anti-clockwise by 90^o. Our objective here has been to check whether the slope of the $\beta - t$ curve in Fig (a) is corroborated by the measure of $d\beta/dt$ in Fig (b). In order to judge the correspondence, we marked four selected points on the curve (a) and their corresponding points on (b), wrote the values of $\frac{d\beta}{dt}$ for these points on the upper horizontal axis of the plot box. Fair correspondence between these values in Fig(b) and the corresponding slopes in Fig (a) is discernible, suggesting that Eq.(53) is the solution of the EoM (52)

Example 2. Set $n = 1$, implying $u = c$.

This is the photon rocket mentioned in the Introduction. In this case a jet of photons flowing out from the tail end of the rocket is serving as the propellant. We specialize the

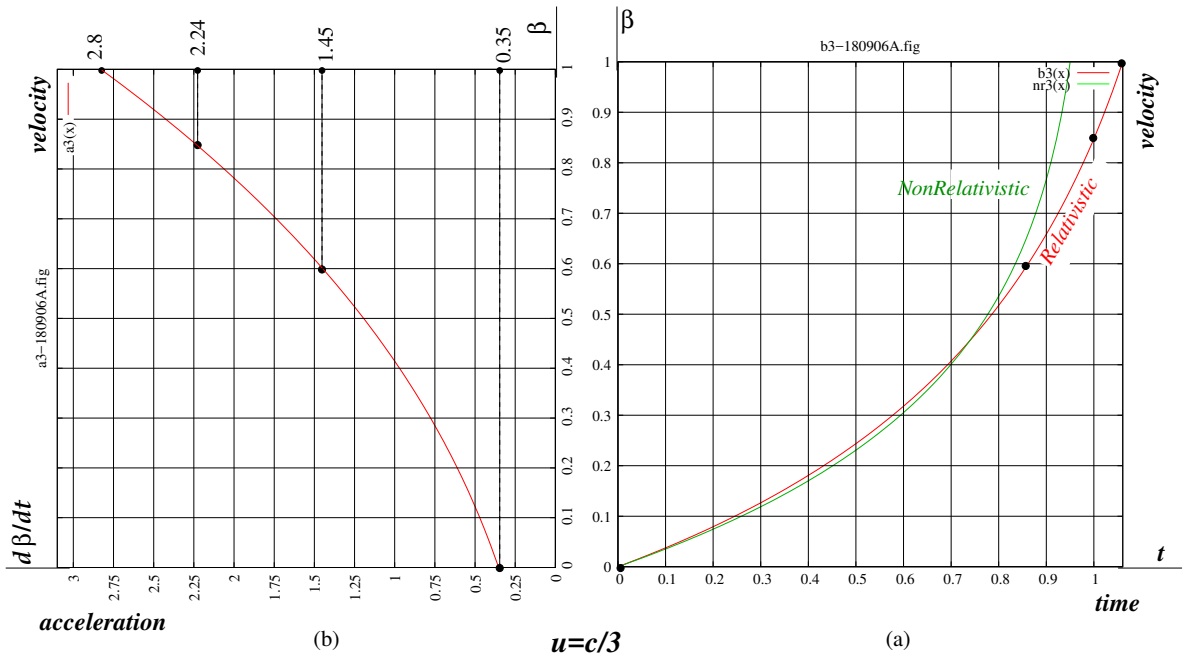

Figure 1: *Case I, n=3. Plots for (a) velocity vs time, (b) acceleration vs velocity*

EoM (49) for this special case:

$$\left[\frac{1}{(1-\beta)(1+\beta)^2}\right]\frac{d\beta}{dt} = \frac{\varrho}{M_i} \equiv k_o = \text{constant}. \tag{55}$$

Integrating from $t = 0$ when $\beta = 0$ to $t = t$; $\beta = \beta$

$$\int_0^\beta \frac{d\beta}{((1-\beta)(1+\beta)^2} = k_o t, \tag{56}$$

we get

$$\frac{\beta}{2(1+\beta)} + \ln\sqrt{\frac{1+\beta}{1-\beta}} = k_o t = \left(\frac{\varrho}{M_i}\right) t.$$

Or,

$$t = \left(\frac{M_i}{\varrho}\right)\left[\frac{\beta}{2(1+\beta)} + \ln\sqrt{\frac{1+\beta}{1-\beta}}\right] \tag{57}$$

The reader can verify the solution by differentiating t w.r.t β.

We have plotted the velocity-time relation (rather the β-t relation) in Fig.2 (a). However in Eq.(57) t is a function of β. Hence, using Gnuplot we first got β as the horizontal axis and t as the vertical axis. In order to reverse their roles we transformed the plot by (i) a rotation through 90^o in the anticlockwise direction, followed by (ii) a reflection about the vertical axis (i.e. about the new β axis).

In Fig.2 (b) we have plotted $\frac{d\beta}{dt}$ (its axis pointing left) versus β (its axis pointing upward). The procedure, objective, and explanations are the same as in Example 1.

It should be noted that in this case ϱ is given by (36 b), which we rewrite and interpret as follows.

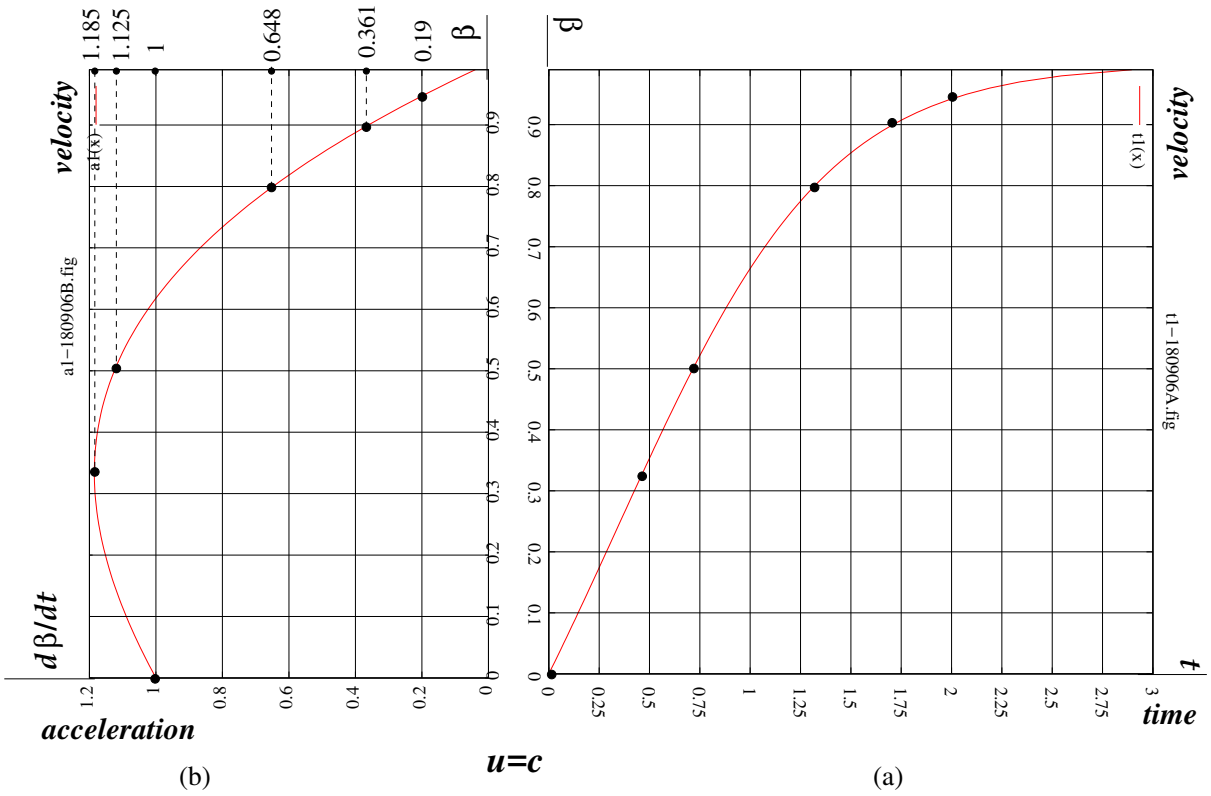

Figure 2: *Case II, n=1. Plots for (a) velocity vs time, (b) acceleration vs velocity*

$$\varrho = \frac{1}{c^2}\frac{dE_o}{d\tau} = \frac{1}{c^2} \times \text{radiative power emitted from the tail end of the rocket} \quad (58)$$

For the plottings we have taken $M_i = 1$ kg, $\varrho = 1$ kg/s.

How long does the rocket operate? Until $\beta \to 1$, as mentioned below Eq. (50), and therefore, by (57), until $t \to \infty$.

It is seen from the plot in Fig.2 (a) that β approaches unity or, v approaches c asymptotically.

10 Summary

1. It has been assumed that the rocket is emitting *relativistic mass* (in the form of gas/photons) with a *constant* speed u, opposite to the direction of the motion of the rocket.

2. The rate of ejection of relativistic mass (for both matter and photons) is a *constant*, represented by ϱ, and defined in Eq. (36).

3. The mass-velocity relation (Ackeret formula) (28) was rederived, and its validity for both matter and radiation was established. See Eq. (31).

4. The mass-velocity formula (28) has been shown to converge to the corresponding N.R. formula (1 b). See steps in (29).

5. The 4-dimensional (Minkowskian) equation of motion (EoM), shown in the frame-independent form (43), involves instantaneous mass of the rocket M (which is a 4-scalar), instantaneous 4-velocity $\overrightarrow{\mathbf{V}}$ and the Reaction (Thrust) 4-vector $\overrightarrow{\boldsymbol{\mathcal{R}}}$.

6. The same EoM takes the form (45) in the instantaneous rest frame S_o, and, upon Lorentz transformation, the form (46) in the ground frame S.

7. With simple manipulations, the EoM in S changes to a simpler looking equation (49), where $n = c/u$.

8. The same EoM (49) has been shown to converge to the corresponding N.R. formula (1 e).

9. The EoM (49) was specialized for two cases, namely, (i) $n = 3$, corresponding to $u = c/3$, and written as (53), and (ii) $n = 1$ corresponding to $u = c$ written as (57).

10. The corresponding EoMs were solved to obtain the relationship betweem v and t, written as Eq (53) for the case (i); and Eq. (57) for the case (ii). The velocity-time relations have been plotted for both cases, as shown in Figs.1 and 2 respectively. For the case (i) we have set $M_i = 1$ kg; $r = 1$ kg/s. For the case (ii) we have set $M_i = 1$ kg; $\varrho = 1$ kg/s. The following features can be easily noticed. For the case (i) the plot of the relativistic formula (53) follows the corresponding N.R. formula (1 f) closely, upto $t \approx 0.5$ s, or $\beta \approx 0.8$. For the case (ii), $\beta \to 1$ asympmtotically.

Acknowledgments

The author is grateful to American Association of Physics Teachers, in particular, Prof Rogers Fuller, Associate Director of Membership, *American Association of Physics Teachers*, and to Harold Q and Charolette Mae Fuller for granting him *Fuller Fund Membership of the American Association of Physics Teachers*. As a privilege of this membership, which has been continuing since 2001, the author could get online access to all the past issues of the American Journal of Physics, which made it possible to write this article.

References

[1] A.P.French, *Newtonian Mechanics, The M.I.T. introductory Physics Series* (W.W.Norton & Co, 1971), p.329.

[2] Somnath Datta, *Mechanics* (Pearson Education, New Delhi, 2013), pp. 86, 144.

[3] Wikipedia, *Relativistic Rocket*, https://en.wikipedia.org/wiki /Relativistic_rocket.

[4] A.P.French, *Special Relativity, The M.I.T. Introductory Physics Course* (W.W,Norton & Co, 1968), pp. 183-184.

[5] Edwin F. Taylor and John Archibald Wheeler, *Spacetime Physics, 2nd Ed.* (W.H.Freeman & Co, 1992). p.274.

[6] Ackeret, J. Helvetica Physica Acta, **19,** p.103 ff (1946) (quoted from Ref[14])

[7] W.L.Bade, "Relativistic Rocket Theory" Am. J. of Phys **21** , 310 (1953)

[8] John W. Rhee, "Relativistic Rocket Motion," Am. J. of Phys **33** (10), 587 (1965)

[9] Wolfgang Rindler, *Relativity, 2nd Ed* (Oxford), p. 126, Ex.6.6. (2006)

[10] K.B.Pomeranz, "The Equation of Motion for Relativistic Particles and Systems with a Variable Rest Mass," Am. J. of Phys **32**, 955 (1964)

[11] K.B.Pomeranz, "The Relativistic Rocket," Am. J. of Phys **34**, 565 (1966)

[12] K.B.Pomeranz, "Some Relativistic Effects in Systems with a Variable Rest Mass," Am. J. of Phys **37**, 741 (1969).

[13] C.Moller, *The Theory of Relativity, 2nd Ed* (Oxford London), Chapter 3 (1972).

[14] Adam L. Bruce, "A General Quadrature Solution for Relativistic, Non-relativistic, and Weakly Relativistic Rocket Equations", *Preprint submitted to Acta Astronautica*, April 28, 2015.

[15] Wikipedia, *Tsiolkovsky rocket equation*, https://en.wikipedia.org/wiki/Tsiolkovsky_rock

[16] Somnath Datta, *Inroduction to Special Theory of Relativity* (Allied Publishers, New Delhi) (1998), Chapter 4.

[17] Wolfgang Rindler, as cited above, p.64, Eq.(3,2); p.70, Eq.(3.16); p.101; p. 127, Ex.6.13.

[18] C.Moller, as cited above, p.101, Eq. (4.42); p. 102, Eq.(4.50); p.103, Eqs. (4.55) (4.54); p.105, Eqs. (4.61), (4.64) .

[19] Wikipedia, *e(mathematical constant)*, https://en.wikipedia.org/wiki /E_(mathematical_constant).

Physics and the Youth

Vishwamittar*

Department of Physics, Panjab University,
Chandigarh – 160014, India.
vm121@hotmail.com

Submitted on 28-05-2018

Abstract

With a view to bring out the fact that some cornerstone researches in physics were carried out by scientists in their youth, we have dwelt upon the major contributions of more than a dozen such illustrious physicists emphasizing the works done by them during the age 18 to 32 years.

*Retired: *The article is dedicated with affectionate regards to my dear Ribhu, Kusum and Suresh Ji.*

1. Introduction

It is generally believed that scientists are eccentric people with long grey hair implying that science is created by the people who are old enough to have vast knowledge as well as experience. This impression stands in contrast with the statement "almost everything that is great has been done by youth" by Benjamin Disraeli, the famous British politician and writer of the 19th century. No doubt, experience and professional maturity are important, but it is equally true that the youth can take risks to follow the roads less travelled rather than being conventional and they are passionate to pursue intellectually challenging work. In fact, a good number of path-breaking discoveries have been made by the scientists when they were young, say, in the age group 18 to 32 years. This article briefly describes achievements of some such celebrated physicists highlighting the seminal contributions these stalwarts made in their youth and decisively influenced the course of development in physics.

2. Galileo Galilei (1564 - 1642)

Galileo, who is known by his first name rather than by the conventional family name, was the Italian physicist and astronomer. He is usually referred to as the 'father of scientific method' and 'founder of the experiments - based physics', because of his revolutionary approach to seek the truth in Nature that led to recognition of science as distinctly different from philosophy, introducing the usage of mathematics in physics, emphasizing the importance of experimental verification of ideas and repeatability of the experiments, and giving impressive demonstrations in his classes.

He is credited for experimentally establishing the laws of the pendulum, of the bodies moving under the action of gravity (vertical fall and, also, along the sloping surfaces) and of the parabolic ballistics. He also proposed the basic principle of relativity, according to which the laws of physics are the same in all the frames of reference moving with respect to one another at a constant speed in a straight line (the inertial frames). This principle provided the basic framework for Newtonian mechanics and was used

as a postulate in Einstein's special theory of relativity. He also performed experiments on sound and put forward a theory of tides. He developed a hydrostatic balance to measure the pressure in a fluid and weigh small objects, a gas bulb and attached water containing tube based thermoscope (a precursor of thermometer), a lightweight military compass, improved techniques for grinding of lenses, set - up for finding strength of materials, and a pendulum based pulsimeter to measure the pulse rate. He used microscope to study the organs of the insects.

It was he who for the first time used the newly invented refracting telescope, having a magnification of about 1000, for conducting pioneering astronomical researches and observed the four large satellites of Jupiter (now called Galilean moons), phases of Venus, the ring of Saturn, mountains on the Moon, dark spots on the Sun and the nature of the Milky Way. His marvelous works on astronomy, first part of which was brought out in the form of a booklet in 1610, upheld the Copernican views favouring heliocentric system over the geocentric system of Aristotle and Ptolmey. Since the Roman Catholic church accepted the geocentric system, Galileo was summoned to face the Inquisition in Rome and was warned in 1616 not to support the Copernican system. However, he published his arguments in the form of dialogues in a book in 1632 for which he was called for Inquisition again in 1633. As a punishment, his book was banned, and he was essentially put in isolation under house arrest till his death.

His first important experiment in physics was performed when he was less than 20 years old. While in a cathedral he noticed the oscillations of a chandelier hanging from the ceiling and, comparing these with his own pulse rate, concluded that the time - period of oscillations of the chandelier is independent of the amplitude. Then he confirmed this aspect by performing an experiment at home in which he used two identical pendulums subjected to oscillations with significantly different amplitudes and varying lengths as well as weights suspended. The time - period changed only when the length of the pendulum was altered. And this is what we find in the case of a simple or a compound pendulum as long as its oscillations are simple harmonic. It is worth noting that, later, this observation formed the basis of the design of the clocks. The detailed description of the hydrostatic balance was published in the form of a small book in 1586 and this invention made him prominent in the scholarly world for the first time. Furthermore, the studies pertaining to falling bodies and projectiles were carried out when he was 25 years old or so.

3. Isaac Newton (1642 – 1727)

Newton, one of the founding fathers of physics, was a great British physicist and mathematician, who contributed immensely to the scientific revolution in the 17^{th} century by nurturing physical science (then referred to as natural philosophy) in its infancy. His prodigious contributions include the law of universal gravitation, three laws of motion, the scientific concept of force, principles of calculus (developed independently of his contemporary Leibnitz and called this 'fluxions'), generalised binomial theorem, techniques for studying properties of polynomials and finding their zeros, methods for using and reverting power series, the theory of finite differences, classification of cubic plane curves (the polynomials of degree three in two variables), and so on.

He used his theory of gravitation to derive the Kepler's laws of planetary motion, describe the trajectory of the comets, explain the precession of the equinoxes, predict the oblate spheroidal shape of the earth, determine the mass of the planets, and many other phenomena. This pioneering work showed that the same law is applicable to the description of the

motion of bodies on the earth and, also, of the celestial objects, making this a universal law. It was in contradiction with the Aristotlean view that the earth and the heavenly bodies were governed by two different sets of laws. Besides, the results of these derivations helped in establishing the heliocentric model of the solar system. His researches in mechanics are summarized in the highly acclaimed three volumes treatise 'Principia' written in Latin, which was published in 1687 and led to his recognition as a great physicist. This book laid the foundation of Classical Mechanics.

He carried out exhaustive experiments on dispersion of light, chromatic aberration of lenses and the formation of Newton's rings. He presented a theory of colours and the corpuscular theory of light. He made the first 20 cm long reflecting telescope in 1668, which brought him to the attention of the Royal Society and made him famous in Europe. He compiled his contributions to optics in the book 'Opticks' in 1704. In this book, written in English, he also described the use of multiple prism arrays; this idea has been now used in the development of narrow beam tuneable lasers.

Newton also put forward an empirical law of cooling and developed an analytic expression for the speed of sound in air. He spent nearly a decade on experiments pertaining to Alchemy, which was essentially the chemistry of that time. In 1696, he was appointed a Warden of the Royal Mint where he worked with full devotion leading to great efficiency in the operations of the mint and successful prosecution of the counterfeiters and other miscreants. As a reward, he was promoted as the Master of the Mint after about three years.

He conducted fascinating researches on theory of gravitation and its varied applications, the basics of calculus and dispersion of light, during August 1665 and April 1667 (i.e. between the ages 23 to 25 years) when the University of Cambridge was closed because of plague and he was forced to stay at his home. Most of the work on optics (including his theory of light and colour) and making of the reflecting telescope were accomplished by the age of 26. The studies pertaining to the power series were carried out before turning 27.

4. James Clerk Maxwell (1831 – 1879)

The Scottish theoretical physicist Maxwell is renowned for his stupendous contributions to development of the kinetic theory of gases (which he did independently of his contemporary physicist Ludwig Boltzmann), works on thermodynamics and formulation of the theory of electromagnetism including the set of differential equations describing the electromagnetic fields. These equations, now reduced to four and called the Maxwell equations, were obtained after modifying the Ampere's law by introducing the concept of displacement current, provided mathematical form to Faraday's physical ideas on electric and magnetic fields, brought out the fact that these two fields are inseparably connected with each other (the first incidence of unifying two then known fundamental forces of nature) and that all the electromagnetic fields are attributable to electric charges and currents. These fields are radiated outward as waves from the source with a constant speed, which numerically turned out to be close to the speed of light in that medium. This made him assert that light is an electromagnetic radiation produced by an oscillating charge and that it is one of a large family of such radiations travelling through a supporting medium called luminiferous ether. This, in turn, brought together the electromagnetism and optics. He presented his revolutionary views in the form of a mathematical theory of electromagnetism in the book 'A Treatise on Electricity and Magnetism', and this work established him as one of the greatest classical physicists. We now know that

the existence of electromagnetic waves was experimentally established by Hertz in 1888, that the electromagnetic spectrum ranges from about 10^{-13} m to 10^{5} m and that ether is a non-existent entity.

In the kinetic theory of gases, Maxwell obtained an expression for the velocity distribution of gas in a container in thermal equilibrium at temperature T using statistical ideas and investigated many associated aspects including the transport properties like viscosity, thermal conductivity and diffusion of the gases. He also introduced the concept of an intelligent tiny creature, now known as the Maxwell's demon, to bring out a possible violation of the second law of thermodynamics and thereby the statistical nature of entropy and derived the famous thermodynamic relations now named after him. These works constitute the content of his book 'Theory of Heat' (1871).

He mathematically showed that Saturn's rings are composed of numerous small particles each independently orbiting the Saturn, which was proved to be correct in 1980s by the first Voyager space probe. In addition to these, he studied the colour vision and coloured photography theoretically as well as experimentally, designing his own experimental set ups; investigated the effect of stresses on the polarized light passing through blocks of gelatin leading to the discovery of photoelasticity; developed the method of dimensional analysis; investigated the rigidity of rod-and-joint frameworks as used in the construction of many bridges; and brought into focus the contributions of Henry Cavendish by painstakingly editing his original notes.

Maxwell's genius came to the fore when (i) at the tender age of 15 he submitted an original paper on the drawing of oval curves to the Royal Society of Edinburgh, (ii) contributed research papers on 'equilibrium of elastic solids' and on 'rolling curves' to Transactions of the Royal Society of Edinburgh three years later, (ii) presented the work on 'Faraday's lines of force' when he was 24, (iii) explained the probable nature of Saturn's rings as a young man of 26, (iv) developed the kinetic theory of gases in 1859 – 60, and (v) showed equality of the speed of propagation of an electromagnetic field with that of light at the age of 31. Interestingly, in the first two instances the executives of the society considered him to be too young to address the members and the papers were read by other persons. Nonetheless, he did get recognition as an accomplished mathematician.

5. Ernest Rutherford (1871 – 1937)

Rutherford, who was born in New Zealand and carried out his researches in Britain and Canada, is remembered as an extremely skilled and accomplished experimental physicist and father of nuclear physics not only because he developed the nuclear model of the atom but also made numerous important contributions that laid the foundation of the subject.

He established that radioactive decay involves spontaneous transformation of one chemical element to another and is a completely random process governed by a decay equation (now known as Rutherford – Soddy disintegration formula) involving half – life or mean life which is characteristic of the element and used this for radiometric dating; investigated various properties of the charged constituents of the radiation emitted by natural radioactive substances, named these α and β particles and identified these as helium nuclei and electrons, respectively (later, he gave the name γ radiation to the third electrically neutral component discovered by Villard); developed the scintillation detectors and ionization chambers for counting the α particles in his studies; discovered a number of new radioactive materials; performed with Geiger and Marsden the illustrious experiment on scattering of α particles from gold foil and interpreted its surprising result that a very small fraction (about 10^{-4}) of incident particles got deflected by more than 90^{0} as an evidence that the atoms have positive charge and most of the atomic mass is concentrated in a very small central region, later called the nucleus, which gave rise to the Rutherford's nuclear model of the atom where the

negative charge was assumed to be uniformly distributed over a sphere having radius equal to that of the atom; carried out experiments of bombarding the ^{14}N atoms with α particles which yielded ^{16}O and another particle which he named the proton (this was the first nuclear reaction). He also argued that some neutral particle must be present in the nucleus to check the strong Coulombic repulsion effect of the positively charged protons and called this hypothetical particle the neutron (it was discovered by his student Chadwick in 1932). He presented an authoritative exposition of radioactive properties of materials in his book "Radioactivity'.

Before embarking upon the researches in radioactivity he had studied the effect of electromagnetic waves on magnetic materials; invented a detector for radio waves; investigated the conductive effects of x – rays on various gases that helped Thomson in concretizing the discovery of electron in 1897; worked on the effect of electric field on mobility of ions; etc. He along with Moseley carried out experiments by bombarding different elements with cathode rays and concluded that each element could be assigned an atomic number which determines its properties. During the Second World War he contributed to problems pertaining to the submarine detection.

Rutherford was around 23 years when he performed many experiments on the effect of electromagnetic waves on magnetization and did some work on the Tesla coil resulting into two publications. The following year he extended these efforts towards detection of electromagnetic waves and developed a detector for radio waves. The studies on conductive effects of x – rays on gases were carried out when he was 26. Naming and differentiating the α and β rays and investigation of some of their properties and the discovery of some new radioactive elements were mainly carried out during the age 27 - 29 years. The concept of half – life of the radioactive substances and the theory of radioactive decay were presented when he was 31years old.

6. **Albert Einstein (1879 – 1955)**

The exceptionally gifted German by birth and Swiss and American citizen by choice, the philosopher and theoretical physicist Einstein had superb ability to grasp precisely a specific simple situation and analyze this to arrive at a general principle. He created the revolutionary theories of special and general relativity almost single handedly, presented novel theories for the photoelectric effect as well as the Brownian motion, contributed a lot to the development of quantum mechanics particularly its philosophy (his discussions with Bohr and the famous publication with Podolsky and Rosen referred to as EPR paradox are typical examples), gave the mathematical formulation of stimulated emission that forms the basis of working of much later invented MASER as well as LASER, and tried to unify the gravitational and electromagnetic fields. He used the concept of quantization of lattice vibrations in solids to theoretically account for the general aspect of temperature dependence of their specific heat and, also, employed the idea of density fluctuations to explain the phenomenon of critical opalescence. He published research papers on what came to be known as Bose-Einstein statistics for the ideal or noninteracting gases and investigated the concept of Bose – Einstein condensation (which was initially used to explain the superfluidity in ^{4}He and has been now properly observed in atomic gases like ^{7}Li, ^{23}Na, ^{87}Rb, ^{133}Cs, etc cooled down to temperatures of few nanokelvin).

Assuming that light is not only emitted in energy packets as conceived by Planck but also travels and interacts in quanta he expounded the empirical laws of photoelectric effect by asserting that the electrons are ejected from the metals due to the collision of light quanta (now called photons) with these. This put Planck's work on the quanta of electromagnetic radiation on firm footing. The phenomenon of Brownian movement was explained by considering the effect of random bombardment of a particle by its surrounding molecules in the fluid yielding experimentally verifiable formulae and thereby it

made the molecular theory of matter to be acceptable beyond doubt.

In the most important of his early contributions namely the special theory of relativity, he reconciled Maxwell's equations for electricity and magnetism with the laws of mechanics by assuming the principle of relativity as well as the constancy of speed of light in all the inertial frames (thus, making the measurement of time and length velocity dependent). This marvelous theory rendered the idea of luminiferous ether to be redundant; showed that no material object can have speed greater than that of light in vacuum; brought in radical changes in the classical concepts of space and time as separate entities leading to the 4-dimensional space-time world; made length, time, the resultant of addition of two velocities, and mass to be variable with velocity (wherein the changes brought in these quantities become significant when their speeds are a substantial fraction of the speed of light, the so called relativistic speeds) and led to the famous relationship giving equivalence of energy and mass. The last result is the principal concept used in explaining the binding energy in the atomic nuclei, the energy produced in the nuclear reactions, working of nuclear reactors as well as the nuclear bomb, creation and annihilation of electron – positron pair, etc.

According to the general theory of relativity, gravity is a consequence of the distortion produced in the shape of space-time continuum by the masses; the light rays from distant stars passing close to a heavy body like sun would bend as these move through the space-time distorted by this object; the motion of the planets would be affected (precession of the perihelion of Mercury is the most conspicuous); spectral lines of the atoms originating from the stars would show gravitational red shift, and so on. The equations of the general theory of relativity demanded that the Universe should not be static - it should be either expanding or contracting. Later, Hubble's experiments supported the expanding condition. As such this theory is the key ingredient of the theories for big bang and, also, the black holes. Einstein also applied the general theory of relativity to model the large-scale structure of the universe and to predict the existence of gravitational waves. It is important to note that almost all his theoretical results have been found to be in conformity with the findings of the relevant experiments.

In 1905, when Einstein was a young man of 26, he published his groundbreaking research papers on the photoelectric effect, the Brownian motion and the special theory of relativity in the German journal Annalen der Physik, making this year to be referred to as the miracle year of physics. Prior to this, in 1902 and 1903, he had used the ideas from statistics to study the effect of finite atomic size on diffusion. He was 28 when he employed the concept of quantum vibrations to present the Einstein model of solids that partially explained the temperature dependence of their specific heat. Also, the principle of equivalence hypothesizing that a homogeneous gravitational field must be equivalent to the field arising in a suitably accelerated frame of reference was developed in 1911.

7. Niels Henrik David Bohr (1885 - 1962)

The Danish theoretical physicist Bohr is essentially revered for his remarkable works on the structure of hydrogen and other atoms and the explanation of the radiation emanating from these; the correspondence principle; the principle of complementarity; the compound model of nucleus; and enormous contribution to the epistemological aspects, including the Copenhagen interpretation, of quantum mechanics as a host (at Institute of Theoretical Physics, Copenhagen, where he was director) and mentor to many talented young minds involved in the creation of this subject besides being active participant in these developments and their chief defender.

He worked on problems of nature of nuclear transformations, theory of energy loss of α - particles on passing through matter and recognized the basis for the existence of nuclear isotopes. He also worked on electron theory of metals, explanation of optical spectra of helium, problem of consistency in applying

the principles of quantization to the electromagnetic fields and applied his complementarity principle to biology. He used his correspondence principle with prudence to elucidate the structure of complex atoms and their spectra, and the structure of the periodic table even before enunciation of Pauli's exclusion principle and the Dirac's theory of electron spin. He predicted the existence of a new zirconium-like element, which was called hafnium after the Latin name for Copenhagen.

He was deeply involved in the execution of Manhattan project, establishment of CERN as well as Research Establishment Risø of the Danish Atomic Energy Commission.

In his model of the atom, he postulated that the electrons revolve in stable orbits (around the atomic nucleus), characterized by a discrete angular momentum value which is integer multiple of $\hbar$ and that these can jump from one permitted energy level (or orbit) to another emitting or absorbing electromagnetic radiation of energy equal to the difference of energy of the two levels involved.

According to the principle of complementarity, items in the quantum world could be separately analyzed in terms of contradictory properties, like behaving as a wave or a stream of particles. The correspondence principle asserts that in the limit of large quantum numbers the quantum aspects of a system described by quantum mechanics become irrelevant and the results reduce to that of classical physics.

In the framework of compound nucleus model, the nuclear reactions occur in two stages: (i) the incoming particle is completely absorbed by the target nucleus leading to a new, highly excited and unstable intermediate nucleus called the compound nucleus; (ii) the compound nucleus, which has a lifetime of the order of 10^{-16} s or so, disintegrates into the product nuclei and particles in one or more ways depending on its excitation energy.

Bohr was 28 when he put forward the highly acclaimed model of hydrogen atom (which accounted for most of the then available experimental data on hydrogen spectra) and the principle of correspondence and 21 when as an undergraduate student he completed a brilliant gold medal winning project on measurement of surface tension by studying vibrating fluid jets covering its experimental as well as theoretical aspects and competed with the established scientists and engineers.

8. Arthur Holly Compton (1892 – 1962)

The American physicist Compton won the international recognition for the notable experiments on scattering of x – rays from materials, the studies of cosmic rays and the leading role in the Manhattan project on the development of atomic bomb.

His most important contribution to the field of x – rays is the finding that the spectrum of the radiation scattered from materials where electrons could be taken to be almost free has two peaks – one corresponding to the incident wavelength and the other at a higher wavelength with a shift increasing with increase in the angle of scattering and its explanation using Planck's quantum theory, together with the laws for conservation of energy and linear momentum, which made the concept of photon completely acceptable (this scattering is known as Compton effect). The other works on x – rays are observation that ferromagnetism arises from the alignment of electron spins in materials; proving that the radiations scattered from elements with atomic number Z = 1 through 16 are polarized; using ruled diffraction gratings for measurement of x – ray wavelength; discovering the total reflection of x - rays; and the accurate determination of number of electrons in atoms. He wrote few detailed books on importance and studies pertaining to x- rays.

His extensive investigations on cosmic rays at different altitudes and latitudes, incorporating the seasonal or temperature effect, established the geomagnetic latitude effect and that these radiations mainly consist of charged particles circulating in the space. During the execution of Manhattan project, he was director of the Metallurgical Laboratory at the

University of Chicago, where the first nuclear reactor was built. In addition to these, he carried out some work on absorption and scattering of γ - rays; development of sodium vapour lamp and aircraft instrumentation.

The work on Compton effect or Compton scattering was carried out when he was around 31 years old. As a young man of 21, he performed an experiment which demonstrated the rotation of earth by studying the motion of water in a circular tube.

9. Wolfgang Ernst Friedrich Pauli (1900 – 1958)

The Austria born theoretical physicist Pauli, who later became the citizen of Switzerland and USA, became immortal for his celebrated exclusion principle, idea of spin (to overcome the lack of agreement between the findings of the quantum theory and the experimental data on atomic and molecular spectra) and its theory in the framework of nonrelativistic quantum mechanics, immense contributions to quantum mechanics particularly as a key figure in the development of its Copenhagen interpretation, predicting the emission of an electrically neutral and almost massless particle in the beta decay of radioactive nuclei in order to explain the continuous energy spectrum of beta decay (these were called neutrino by Fermi), explanation of the hydrogen spectra using matrix mechanics, quantum theory of ionized diatomic hydrogen, introducing grand canonical ensemble in quantum statistics, theory of temperature independent paramagnetic behavior arising from the interaction of electron spins in metals with the magnetic field (known as Pauli paramagnetism), works in quantum field theory as well as quantum electrodynamics, formulation of the spin - statistics theorem establishing connection between the spin of a particle and its statistical properties, and meson theory.

Interestingly, when after some shocking happenings in the family he went into depression and was under the treatment of a psychiatrist and psychotherapist, he made significant contributions to psychiatry through his criticism of its epistemology. Besides he was a strong critic of modern synthesis of evolutionary biology. He was genius as well as perfectionist who used to have many new ideas, analyzed a problem in detail and went deep into this with full earnestness. His ruthless rigour applied not only to his own work, but to the work of others as well. This made him to be referred to in the physics community as the "conscience of physics".

Pauli published his first research paper on general theory of relativity at the age of 18 and contributed a superb 237 pages master exposition of special and general theories of relativity to the Encyclopedia of Mathematical Sciences when he was 21; this was later published as a well - received monograph and was highly admired by Einstein himself for its insight, systematic presentation and profoundness of treatment. The proposals for the two – valued quantum number for atomic electrons (which was later identified as spin) besides principal quantum number, orbital quantum number and magnetic quantum number and the famous exclusion principle were put forward at the age of 25 or so, while that for the emission of neutrino together with the β particles in radioactivity was given at the age of 30. He used Heisenberg's matrix mechanics to explain the hydrogen spectra in 1926 making this more acceptable and worked on the grand canonical ensemble in the framework of quantum statistics in 1927.

10. Enrico Fermi (1901 – 1954)

Fermi, who was native of Italy and later became an American citizen, was a rare example of an excellent theoretical as well as experimental physicist. On the theoretical side, he investigated the behavior of degenerate electron gas leading to the Fermi – Dirac statistics which soon formed the basis of electron theory of metals and the theory of thermodynamic equilibrium in white dwarfs, and is applicable to a system consisting of particles having half - integer spin; introduced the concept of weak interactions and used it together with the newly suggested massless particles (naming these neutrinos) to develop a

mathematical theory of β emission by unstable nuclei accounting for their continuous energy spectrum and the decay rate (this, in turn, helped in establishing β spectroscopy as an important technique for the determination of nuclear structure); presented the so called Thomas - Fermi model for the heavy atoms which was later extended to molecules, solids and even nuclei and can be viewed as a forerunner of the modern density function theory; obtained the Fermi age equation for the diffusion of neutrons slowing down in a medium like graphite, heavy water, etc; interpreted the latitude effect of cosmic rays and also gave a theory of origin of these rays; put forward the idea that the pion could be a composite particle (laying basis for the study of quarks); worked on the Fermi – Pasta – Ulam - Tsingou problem which laid the foundation of the nonlinear dynamics and brought out the importance of computer simulations in physics.

His major experimental contributions include nuclear reactions in heavy elements bombarded by slow neutrons and the production of new radionuclides; design and commissioning of the first nuclear reactor (the Chicago pile I) using the controlled nuclear chain reaction as a part of the atomic bomb programme of USA, which made him to be recognized as architect of the nuclear age; determination of mean life of neutron using the so called Fermi bottle; effect of magnetic field on mercury vapours; investigation of pion – nucleon interaction. His caliber to get good approximate results with little or no actual data has led to such an estimation being called Fermi estimate.

He published his first three research papers on some aspects of electrodynamics, special as well as general theories of relativity in 1921 - 22 which bore a mark of his mathematical talent. The work on Fermi – Dirac statistics was carried out at the age of 25, while the Thomas – Fermi model of atoms was presented in 1928. The theory of β transformation incorporating the weak interactions was developed at the age of 32 years.

11. Werner Karl Heisenberg (1901 – 1976)

The brilliant German theoretical physicist and philosopher Heisenberg was one of the pioneers who used the principles of abstract mathematics and depth in the understanding of physics to develop the revolutionary subject of quantum mechanics. Among his many research works the two outstanding ones, which brought him recognition as a genius, are the treatment of quantum transitions in terms of matrices leading to the matrix mechanics formalism of quantum mechanics and enunciation of the amazing uncertainty principle. His matrix mechanics (finalized in collaboration with Born, Jordan and Kramers) correctly explained the frequencies and relative intensities of hydrogen spectra.

He also made important contributions to the theories of the hydrodynamics of laminar and turbulent flows, theoretical explanation of the Helium spectrum and the anomalous Zeeman effect, modeling of ferromagnetism, the relativistic quantum field theory, the neutron – proton model of the atomic nucleus, theory of cosmic rays, unified field theory of elementary particles, theory of positron, the S-matrix theory for particle interactions, and problems of plasma physics as well as thermonuclear processes.

He played the key role in planning the nuclear reactors in West Germany. In fact, he showed as early as December 1939 that nuclear energy could be obtained from ^{238}U by slowing down the energetic neutrons by passing through heavy water or graphite and that enriched ^{235}U would be needed to get an explosive. In addition to these, he wrote philosophical essays and articles for the general audiences.

Heisenberg was a young man of 24 when he brought out his first landmark research paper on matrix mechanics, which was followed by the development of the uncertainty principle after 2 years. Prior to this at the age of about 22, he modified Bohr's theory of atoms by introducing the idea of half - integer quantum numbers to explain the then perplexing helium spectrum and the anomalous Zeeman effect.

The model for ferromagnetism was put forward when he was 27; this was later simplified by Ising to understand various features of the ferromagnetic materials. The papers on relativistic quantum field theory with Pauli appeared in 1929 and 1930, while his work on the nuclear model was published in 1932 – 33.

12. Paul Adrien Maurice Dirac (1902 – 1984)

A bachelor's degree holder in electrical engineering and a master's degree in mathematics, the great British theoretical physicist Dirac earned his place in the history of physics as one of the creators of quantum mechanics and the primary versions of quantum field theory as well as quantum electrodynamics (the modern theory of interaction of electromagnetic radiation or photons with charged matter).

He developed a transformation theory based formalism of quantum mechanics, introduced the idea of q numbers and of bra – ket vectors; showed relationship between the commutator and the Poisson brackets; proved that the matrix mechanics put forward by Heisenberg and wave mechanics of Schrodinger differ only in the sense that the former lays emphasis on the dynamical variables while the latter on the state functions; successfully unified the concepts of special theory of relativity and of quantum mechanics to present his monumental relativistic quantum theory of electron giving correct explanation of its spin as well as the magnetic moment, accounting for the fine structure of the hydrogen spectrum, predicting the existence of positively charged anti-electrons or positrons (which were experimentally detected after about 4 years in the cosmic rays and now find applications in positron emission tomography of human body and positron annihilation spectroscopy of materials) and of creation as well as annihilation of electron – positron pair. The interpretation leading to the idea of positron is referred to as hole theory and this gave rise to the speculation on the existence of antimatter.

Dirac also published research papers on special and general relativity, old quantum theory, thermodynamics, classical as well as quantum statistical mechanics including the theory of the particles that obey Pauli exclusion principle (now known as Fermi – Dirac statistics), and generalized Hamiltonian dynamics and theory of gravitation.

With a view to have greater symmetry in the Maxwell's equations of electromagnetism, he put forward the concept of a magnetic monopole and its theory though this has not yet been found. As a mathematical tool to handle the problems he introduced an improper function, which has been named Dirac δ - function.

In addition to the above mentioned researches, he worked with Kapitza on an experiment on not much successful separation of isotopes and explored the possibility of diffraction of electrons from grating of standing light waves (the Kapitza – Dirac effect, which was experimentally observed much later in 1980s using laser).

Dirac was a solitary quester whose researches displayed his mathematical prowess as he earnestly believed that the physical laws should have mathematical beauty and that a theoretical physicist should place more trust in mathematical formalism and follow its lead even if physical interpretation of the formulae temporarily lags behind.

It may be mentioned that the originality of ideas in the works published by Dirac in his youth is superb. His series of innovative research papers pertaining to the formulation of quantum mechanics started appearing when he was nearly 23 years of age and the glorious relativistic quantum theory of electron in the form of Dirac wave equation and the associated predictions was published at the age of 26 or so. The derivation for statistical distribution of particles with half integer spin appeared in 1926 while the quantum theory of emission and absorption of radiation leading to the birth of quantum field theory and quantum electrodynamics was presented in 1927. His masterpiece monograph 'The Principles of Quantum

Mechanics' was published at the age of 28 when he also put forward the hole theory. The prediction regarding the existence of magnetic monopoles was made about a year later. In 1933, he examined the possibility of developing quantum mechanics from the Lagrangian and this idea was later used by Feynman to develop the beautiful path integral version of quantum mechanics.

13. Carl David Anderson (1905 – 1991)

Anderson was an American experimental physicist who is best known for discovering two new particles positron and muon. With a view to investigate the composition of the cosmic rays, he placed his cloud chamber in a specially designed powerful magnet and observed tracks in some of the photographs that could be explained only by assuming the presence of particles having the same mass as electrons and equal but opposite charge. This was in conformity with the particle predicted by Dirac. He confirmed the existence of positron by passing highly energetic γ - rays emitted by the natural radioactive nuclide ^{208}Tl into other materials, resulting in the creation of positron - electron pairs. Later, Anderson and his student used the same set - up in the well - planned experiment involving lot of hard work that led to the discovery of negatively charged muons in the cosmic rays, whose rest mass was finally found to be 207 times that of the electron; magnitudes of its charge and spin are the same as for an electron.

During the second world war he carried out research in solid-propellant artillery rocketry. Before embarking on the study of cosmic radiations which was continued after the war also and was supplemented with studies in particle physics, he investigated the space distribution of photoelectrons emitted from various gases by the x-rays.

The experiments leading to discovery of the positron and the muon were performed when Anderson was 27 and 31 years old, respectively.

14. Lev Davidovich Landau (1908 – 1968)

The prominent Russian theoretical physicist and excellent teacher Landau made a mark for a wide range of his research activities covering different areas of physics and the set of 10 extremely well written books constituting essential course for theoretical physics with Lifshitz as coauthor.

His important contributions include empirical considerations based pioneering theory of liquid He II that explained reasonably well the hydrodynamic behavior and other experimental observations below 2 K of superfluid helium and also led to criterion for the existence of super flow; introduction of the concept of density matrices as a mathematical tool in quantum mechanics and its use in quantum statistical mechanics; studying the magnetism arising from the quantization of orbital motion of charged particles in the presence of an external magnetic field which gives negative magnetic susceptibility and is governed by Curie's law at high temperatures (now called Landau diamagnetism and explains the de Haas – van Alphen effect which refers to the oscillation of the magnetic moment of a metal with increase in the applied static magnetic flux density); unified description of the second – order phase transitions (which was improved after about 25 years in 1960s); phenomenological theory for the investigation of quantum Fermi liquids; the Ginzburg–Landau theory of superconductivity; Landau damping of longitudinal space charge waves in plasma; the Landau pole in quantum electrodynamics which is the basic idea behind the renormalization technique; the two-component theory of neutrinos; the Landau–Hopf theory of turbulence in fluid flow; the stellar theory; study of metals at low temperatures; absorption of sound in solids; x – ray scattering by crystals; the problems of parity conservation and nuclear structure.

Landau's works on density matrices, Landau diamagnetism and theory of second – order phase transitions were carried out at the age of 19, 22 and 29 years, respectively. The first publication on the theory of He II appeared when he was just above 32.

15. **Subrahmanyan Chandrasekhar (1910 – 1995)**

India born American theoretical astrophysicist Chandrasekhar is remembered for his splendid contributions to the understanding developed through mathematical treatment of stellar structure, including the theory of white dwarf stars; stellar dynamics, together with the theory of stochastic processes and Brownian movement; the theory of radiative transfer, embracing the theory of stellar atmospheres; the quantum theory of the hydrogen anion; the theory of planetary atmospheres, including the theory of the illumination and the polarization of the sunlit sky; hydrodynamic and hydromagnetic stability, including the theory of the Rayleigh-Bénard convection; the stability of ellipsoidal figures of equilibrium; the general theory of relativity and relativistic astrophysics; the black holes and collision of gravitational waves. He also worked on problems in ballistics.

His initial celebrated work in astrophysics pertains to statistical mechanical study of the relativistic degenerate electron gas in a white dwarf showing that such a star explodes to become a very bright star known as supernova if its mass exceeds 1.44 times the mass of the sun (the so called Chandrasekhar limit). It is now established that the ultimate fate of a star is determined by its mass. Smaller stars become white dwarfs, while larger stars, after the supernova stage, end up as neutron stars or black holes.

He followed a very interesting style of pursuing research: he would prepare himself for a particular area of his liking, carry out exhaustive investigations on problems in this for few years and then write a monograph summarizing the major concepts in the field before shifting to another field and repeat the pattern.

Chandrasekhar published his first research paper on the Compton Scattering and the New Statistics at the age of 19 years and this was soon followed by his famous work on the Chandrasekhar limit. His complete work on stellar structure, the white dwarf stars and the initial contributions to the field of stellar dynamics appeared before he was 32 years old.

16. Richard Phillips Feynman (1918 – 1988)

One of the extraordinarily ingenious researcher and passionate teacher Feynman was an American theoretical physicist who is venerated not only for his innovative researches on variety of problems but also for the lucidly presented three – volume 'Lectures on Physics' for the undergraduate students, numerous books on different topics at higher level, simplified and charismatic presentation of difficult concepts in his lectures and the persistent sense of wit. His inspirational adage was "some essentially new physical ideas are needed".

His landmark research works are creation of modern version of quantum electrodynamics, principle of least action based path integral approach to quantum mechanics, graphic representation scheme for the complicated mathematical expressions governing the behavior of interacting particles containing radically original ideas to look at space – time (the Feynman diagrams), elegant atomic theory of a Bose liquid at low temperatures, circulation theorem and its application to describe the quantized vortex motion in a Bose fluid (particularly in liquid He II), parton model in particle physics, theory of weak interactions developed with Murray Gell-Mann which modified the Fermi theory taking care of parity violation, quantum chromodynamics, the variational perturbation theory and quantum gravity. He also worked on the Wheeler – Feynman absorber theory of electrodynamics. Feynman has been rightfully credited as the originator of the field of quantum computing and for introducing the concept of nanotechnology.

He was an active participant in the Manhattan project (where he and Bethe put forward the Bethe–Feynman formula for calculating the yield of a fission bomb) and the Rogers Commission that investigated the Space Shuttle Challenger disaster in 1986 (here, he played an important role to show that the failure

occurred due to malfunctioning of the O – ring at very low temperature).

Feynman was 21 when he published his first one - page note on the scattering of cosmic rays by the stars of a galaxy and a paper of about 4 pages on the forces in molecules (this constitutes the well - known Hellmann–Feynman theorem). The Bethe – Feynman formula was developed at the age of about 25 and the development of both the path integral technique in quantum mechanics and the quantum electrodynamics was completed by the age of 30 years.

17. **In Lieu of Epilogue**

Before closing the article, it may be mentioned that (i) the narrative could have been quite lengthy as numerous physicists who made marvelous contributions when they were in this age range have been left out, and (ii) the purpose of this write – up was to bring out the exceptional works done by the physicists when they were young adults and not at all to diminish the important role played by the people who made impressive contributions after crossing the age of 32 years. In fact, a good number of physicists have become immortal in the history of the subject because of their wonderful researches done in older age. For example, one of the greatest experimentalists Michael Faraday (1791 – 1867) introduced the concept of electric and magnetic fields and presented the laws of electromagnetic induction and of electrolysis when he was around 40 though he had demonstrated the principle of working of an electric motor at the age of 30. Similarly, Albert Abraham Michelson (1852 - 1931) was 35 years old when the famous Michelson – Morley experiment concluding the absence of any motion of the earth relative to the ether was carried out; of course, at the age of 30 he had determined reasonably precise value of the speed of light. Max Karl Ernst Ludwig Planck's (1858 – 1947) work introducing the concept of quantum in his theory of black body radiation and Erwin Rudolf Josef Alexander Schrödinger's important publications on wave mechanics formalism of quantum mechanics also appeared when they were around 40.

In addition, among the physicists included in this article, the number of theoretical physicists surpasses that of the experimentalists. The reason for this is that generally theoretical physics is pursued by the people with a philosophical mind who have zeal to speculate about the highest principles using their powerful intuition and mathematical prowess. This usually happens at the age of about 25 years when he has been well exposed to the existing ideas, theories and the mathematical techniques but his mind is agile enough to conceive and execute radical ideas overhauling the previous views. On the other hand, experimental work requires professional maturity, confidence and experience in designing new equipment for the planned work and expertise to execute it properly, which generally delays the contribution.

References

1. G. Gamow, Thirty Years that shook Physics: The Story of Quantum Theory, (Anchor Books, Doubleday & Company, New York, 1966).
2. L. I. Ponomarev, The Quantum Dice, (Mir Publishers, Moscow, 1988).
3. N. Mukunda, The World of Bohr and Dirac : Images of Twentieth Century Physics, (Wiley Eastern, New Delhi, 1993).
4. G. Venkataraman, Quantum Revolution I The Breakthrough, (Universities Press, Hyderabad, 1994).

5. G. Venkataraman, Quantum Revolution II QED : The Jewel of Physics, (Universities Press, Hyderabad, 1994).
6. G. Venkataraman, Chandrasekhar and His Limit, (Universities Press, Hyderabad, 1994).
7. R. Spangenburg and D. K. Moser, The History of Science from the Ancient Greeks to the Scientific Revolution, (Universities Press, Hyderabad, 1999).
8. R. Spangenburg and D. K. Moser, The History of Science in the Eighteenth Century, (Universities Press, Hyderabad, 1999).
9. R. Spangenburg and D. K. Moser, The History of Science in the Nineteenth Century, (Universities Press, Hyderabad, 1999).
10. R. Spangenburg and D. K. Moser, The History of Science from 1895 to 1945, (Universities Press, Hyderabad, 1999).
11. I. James, Remarkable Physicists, (Cambridge University Press, Cambridge, 2004).

Errata

Debnarayan Jana

Department of Physics
University of Calcutta
92 A P C Road, Kolkata- 700009, India.
djphy@caluniv.ac.in

Submitted on 08-10-2018

There are two mistakes in the article 02 published in Volume 34, Issue 1.

1. Page 3, equation (9) is to be read as

$$\frac{1}{\lambda} = \frac{1}{2\pi}\int \frac{dk}{k^2 + B_0} = \frac{1}{2\sqrt{B_0}} \qquad (1)$$

2. Page 7, equation (29) is to be modified as (the second term in the first equation)

$$E = \frac{\pi^2\hbar^2}{2ma^2} - \frac{\pi^2\hbar^4}{m^2a^3V_0}[1 + \cos(Ka)] \qquad (2)$$

with $J = \frac{\pi^2\hbar^4}{2m^2a^3V_0}$